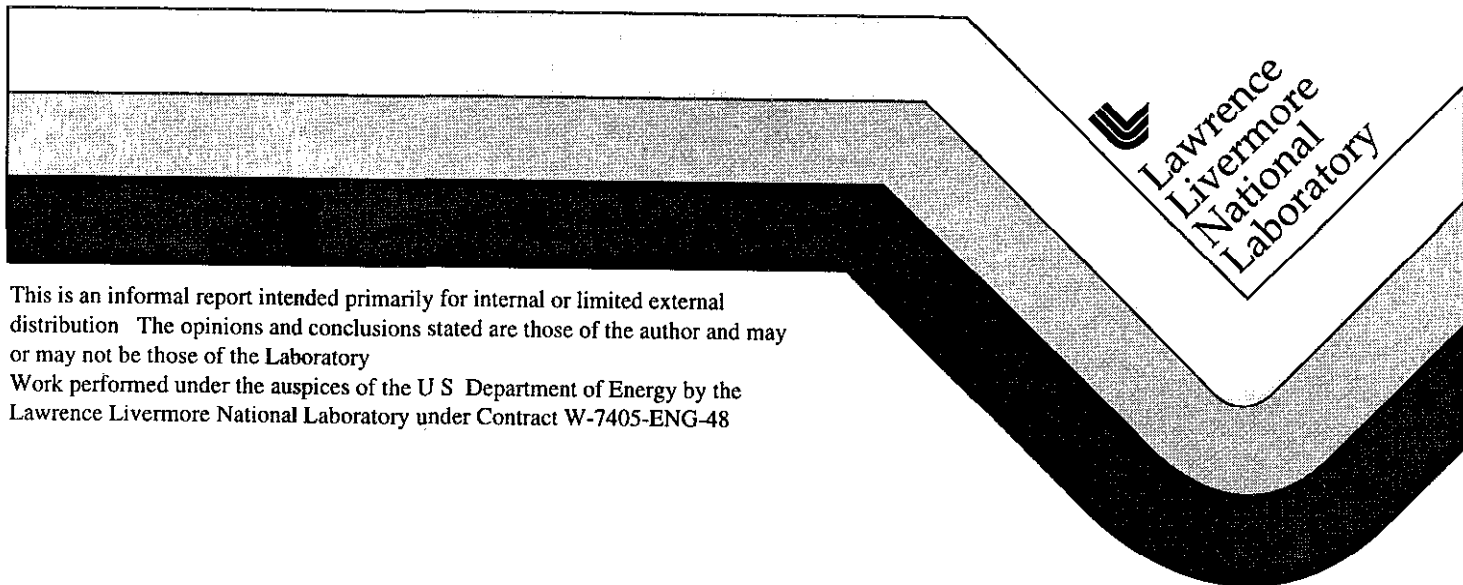


# CARNELIAN Containment Data Report

T. Stubbs  
R. Heinle

July 1998



## DISCLAIMER

This document was prepared as an account of work sponsored by an agency of the United States Government. Neither the United States Government nor the University of California nor any of their employees, makes any warranty, express or implied, or assumes any legal liability or responsibility for the accuracy, completeness, or usefulness of any information, apparatus, product, or process disclosed, or represents that its use would not infringe privately owned rights. Reference herein to any specific commercial products, process, or service by trade name, trademark, manufacturer, or otherwise, does not necessarily constitute or imply its endorsement, recommendation, or favoring by the United States Government or the University of California. The views and opinions of authors expressed herein do not necessarily state or reflect those of the United States Government or the University of California, and shall not be used for advertising or product endorsement purposes.

This report has been reproduced  
directly from the best available copy

Available to DOE and DOE contractors from the  
Office of Scientific and Technical Information  
P O Box 62, Oak Ridge, TN 37831  
Prices available from (615) 576-8401, FTS 626-8401

Available to the public from the  
National Technical Information Service  
U S Department of Commerce  
5285 Port Royal Road  
Springfield, VA 22161

CARNELIAN Instrumentation Summary

Instrumentation	Fielded on this Event	Data Return	Present in this Report
<u>Plug Placement</u>	yes	yes	yes <sup>(a)</sup>
<u>Radiation</u>	yes	yes	yes
<u>Pressure</u>			
Stemming	yes	yes	yes
Challenge	no	-	-
Cavity	no	-	-
Atmospheric	no	-	-
<u>Motion</u>			
Free Field	no	-	-
Surface	yes	yes	yes
Plug	yes	yes	yes
Stemming	no	-	-
Surface Casing	no	-	-
Emplacement Pipe	yes	yes	yes
<u>Hydroyield<sup>(b)</sup></u>	yes	yes	no
<u>Collapse<sup>(c)</sup></u>	yes	yes	yes
<u>Stress</u>	no	-	-
<u>Strain<sup>(d)</sup></u>	yes	yes	no
<u>Other Measurements<sup>(e)</sup></u>	yes	yes	yes

- (a) Description only
- (b) SLIFER or CORRTEX data, see reference 3
- (c) EXCOR or CLIPER in emplacement hole
- (d) Strain load on emplacement pipe, recorded in the stemming log<sup>(2)</sup>
- (e) Internal emplacement pipe temperature and pressure

Event Personnel

Containment Physics

B Hudson	LLNL
V Wheeler	LLNL
J Kalinowski	EG&G/AVO
T Stubbs	EG&G/AVO

Instrumentation

L Starrh	LLNL
A Bruns	EG&G/AVO
M Reed	EG&G/NVO
A Moeller	EG&G/NVO

## Contents

1	Event Description	
1 1	Site	1
1 2	Emplacement	1
1 3	Instrumentation	2
2	Stemming Performance	
2 1	Radiation and Pressure	9
2 2	Motion . . . . .	10
3	Collapse phenomena	
3 1	Motion . . . . .	38
3.2	Radiation and Pressure . . . . .	38
4	Measurements on the Emplacement Pipe	
4 1	Explosion-Induced Motion	57
4 2	Collapse-Induced Motion	58
4 3	Pressure, Temperature, and Radiation	58
	References	76

## 1. Event Description.

### 1.1 Site

The CARNELIAN event was detonated in hole U4af of the Nevada Test Site as indicated in figure 1.1. The CARNELIAN device had a depth-of-burial (DOB) of 208 m in the alluvium of Area 4, about 70 m above the Paleozoic formation and 330 m above the standing water level, as shown in the geologic cross-sections of figure 1.2<sup>(1)</sup> Figure 1.3 displays the local surface area showing nearby events. Stemming of the 2.44 m diameter emplacement hole followed the plan shown in figure 1.4. A log of the stemming operations was maintained by Holmes & Narver<sup>(2)</sup>

Detonation time was about 07:00 PDT on July 28, 1977, and collapse progressed to the surface at about 19 minutes after the detonation resulting in a crater having a "cookie-cutter" geometry (steep walls with a relatively flat bottom) with a mean radius of 32.2 m and a maximum depth of 10.5 m.

No radiation arrivals were detected above ground and the CARNELIAN containment was considered successful.

### 1.2. Emplacement

There were three stemming plugs above the CARNELIAN event, each composed of rigid two-part-epoxy (TPE). The first (bottom) was about 9.7 m thick and the second was 3.0 m thick. Thickness of the top plug TPE was 3.4 m, the bottom of which was 2.5 m above the bottom of the surface casing. This top plug was overlain with 1.7 m of foam cubes and overton sand which was further overlain with a 4.4 m thick layer of soft "coal-tar epoxy" to act as a gas seal. A drag ring system was mounted to the emplacement pipe at the position of the bottom rigid plug, coupling this plug to the geologic formation. The emplacement pipe in the regions of the top and intermediate plugs was coated with hydroseal to allow free motion of the pipe through these structures. Except for a thin layer of pea gravel about 10 m below the bottom plug, the plugs, and magnetite around the device, the hole was filled with LLL mix to about 2.7 m below the ground surface. See figure 1.4.

CARNELIAN included a mechanical PINEX experiment as part of the device diagnostics and, for this, the emplacement pipe was left open above the detector plate which was extracted to a receptacle above the ball valve closure on the top of the pipe. This receptacle was detached from the pipe shortly after the detonation and pulled to a location beyond the expected extent of the resulting crater. Below the detector plate, the pipe was sealed with a pressure plate in the region of the deepest rigid plug and a series of three pressure domes below the pressure plate.

### 1.3 Instrumentation

Figure 1 5 is a schematic layout of the instrumentation designed to monitor the containment performance of the CARNELIAN event.

Nine stations were fielded in the stemming to monitor pressure and radiation at elevations about 1 m above each of the three pressure domes and the detector plate, about 4 m on either side of the intermediate plug, about 8 m beneath the top plug, and midway between each of the three rigid plugs (two stations).

The internal gas pressure and temperature of the lower four sealed sections of the emplacement pipe were monitored just below the corresponding pressure dome or pressure plate defining the section. An additional station monitored pressure and radiation internal to the pipe near its top at a depth of about 19 m. Vertical motion (acceleration and velocity) of the emplacement pipe was monitored at each of the three pressure domes, at the location of the neutron detector plate, and near the top of the pipe below the ball valve. An additional motion station was fielded on the pipe about 4 m below the bottom pressure dome and the pinhole of the PINEX experiment. Internal gas pressure and temperature was also monitored at this station.

Standard LLNL vertical motion canisters, containing variable reluctance velocity and acceleration transducers, were employed in all three of the rigid stemming plugs, and in the ground surface, 15.24 m from SGZ. The recording trailer was instrumented for vertical and radial-horizontal acceleration.

Data from each of the above instruments were transmitted to the recording trailer by an analog system and recorded on magnetic tape.

Two CLIPER sensors, one attached to the instrumentation pendant, were fielded to monitor cavity collapse and chimney formation

One "D-cable" systems was fielded to monitor the stemming emplacement and was recorded post-shot to sense collapse

Strain (load) was monitored at a station on the emplacement pipe near its top These are noted in the stemming log<sup>(2)</sup>

Results of the hydrodynamic yield measurements are reported elsewhere<sup>(3)</sup>

A history of the fielding operations of the instrumentation is outlined in reference 4 Further details of the instrumentation are given in reference 5

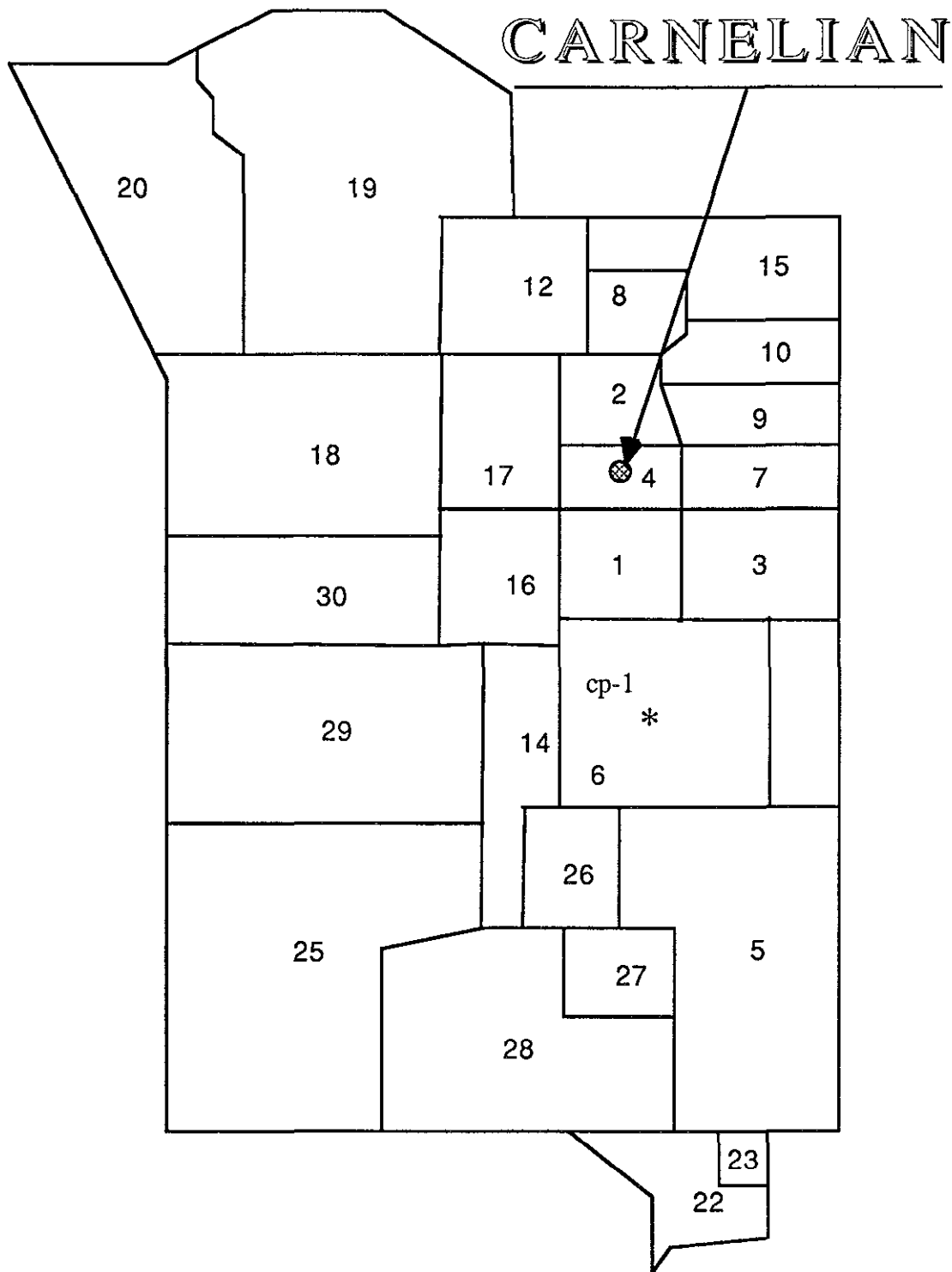


Figure 1 1 Map of the Nevada Test Site indicating the location of hole U4af

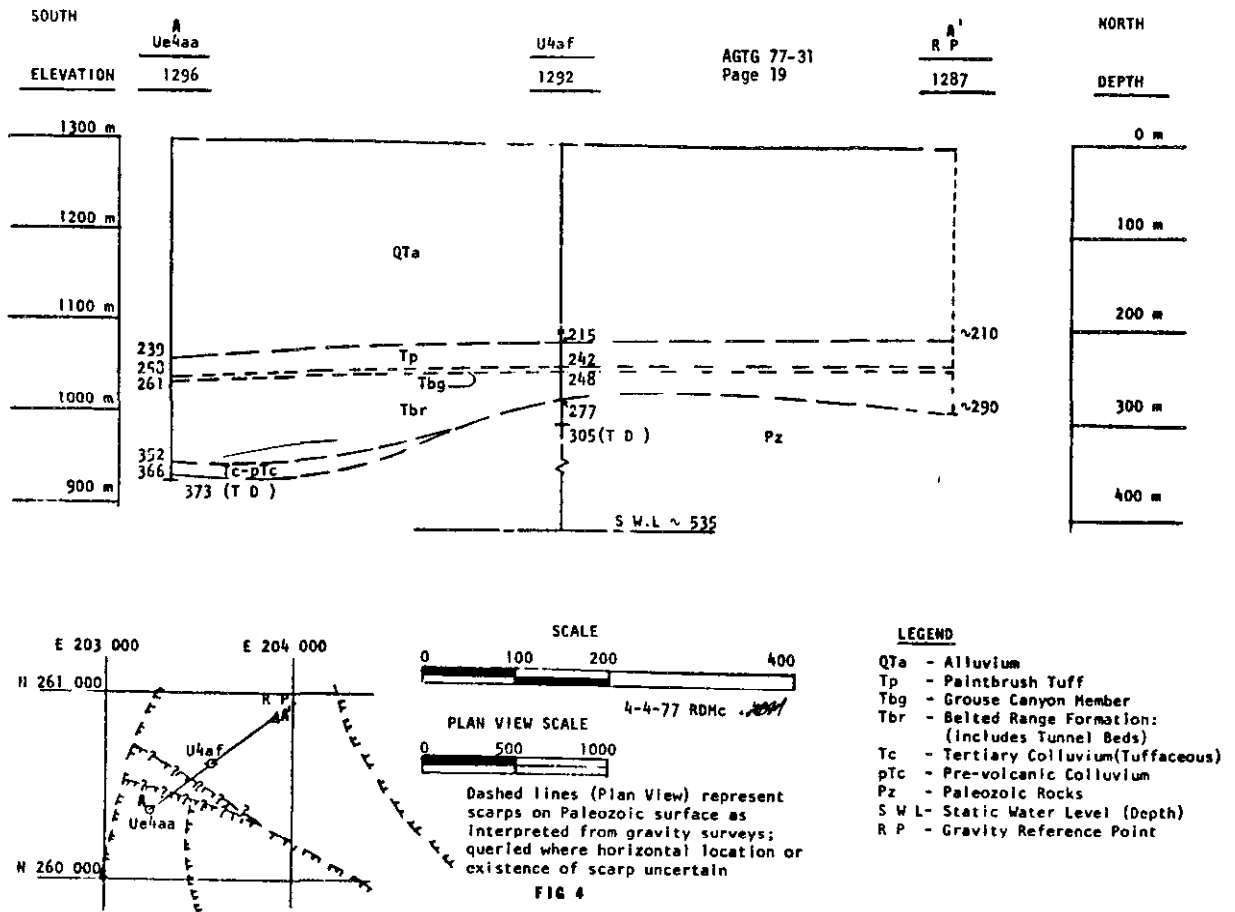


Figure 1.2 Southwest-Northeast geologic cross section through hole U4af

# LOCATION MAP OF U4af

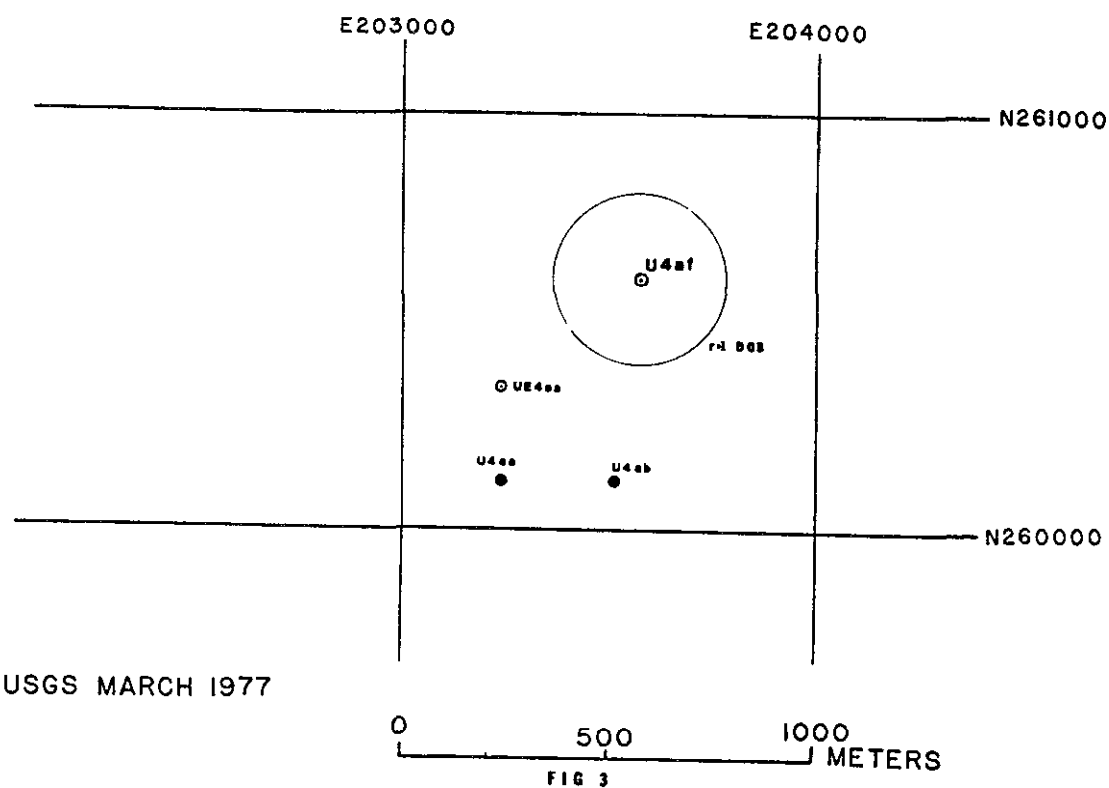


Figure 1.3 Ground surface in region of Hole U4af showing nearby event sites.

# U4AF "AS BUILT"

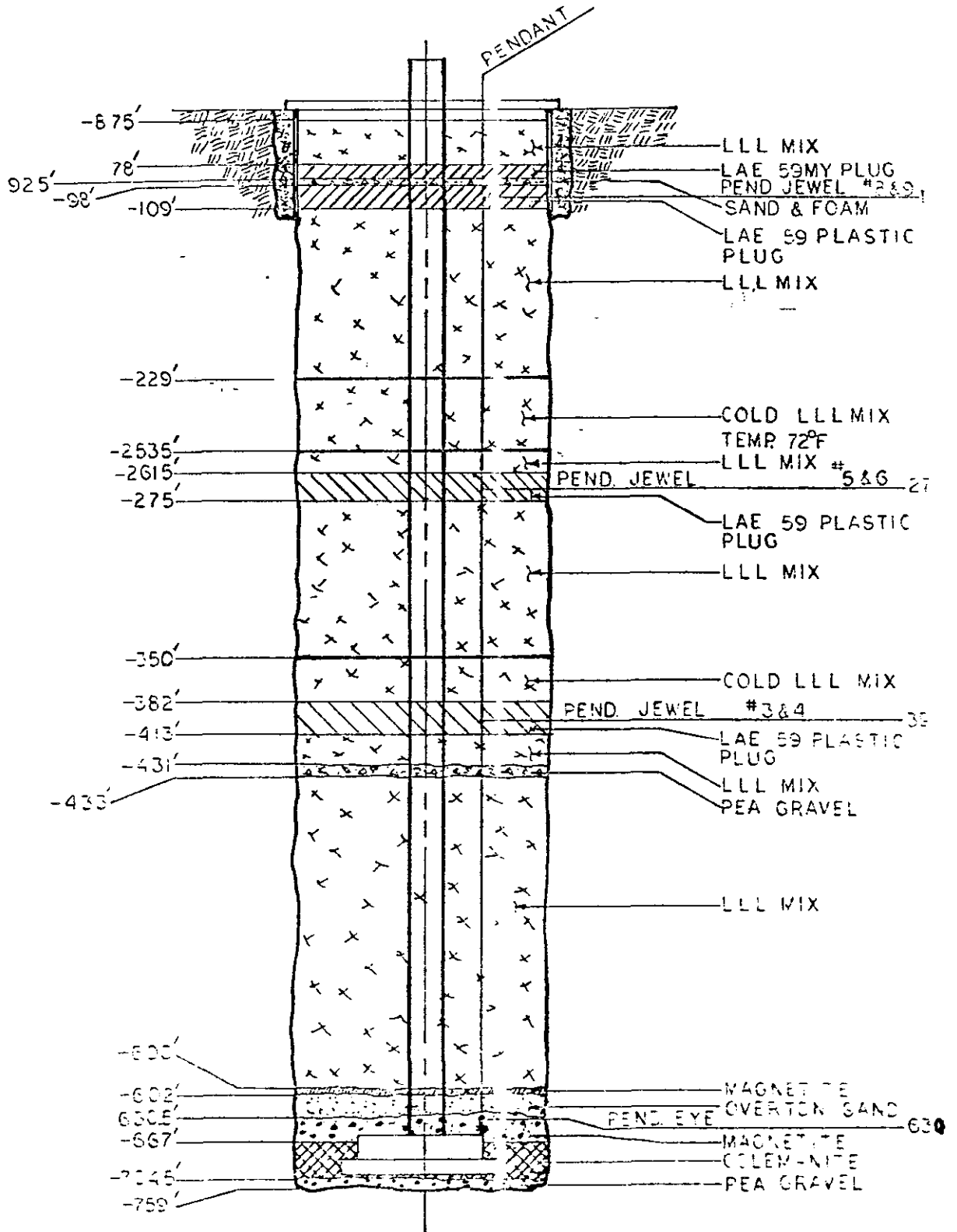


Figure 1 4 As-built stemming plan for the event CARNELIAN in Hole U4af



## 2. Stemming Performance

### 2.1 Radiation and Pressure

Stemming pressure and radiation stations were fielded on the CARNELIAN event at nine locations as indicated in figure 1 5. The pressure and radiation wave forms from about 50 s before detonation until 1200 s after (or as long as the station lasts, whichever is shorter), recorded at all stemming stations, are shown in figures 2.1-2 9. The first 20 to 30 s of pressure and radiation are also shown, for greater definition, in figures 2 10 - 2 17. It is common for the radiation channels to have a brief period when the signal is forced to zero beginning at zero time. However, at all stations (except 33 and the one immediately above the formation coupling plug, 35) there appears to be a brief period of radiation channel saturation which may be due to shine from the emplacement pipe.

Figure 2.1 shows a prompt arrival of both pressure and radiation in the stemming at the elevation of the deepest pressure dome (station 32). Signals from this station were lost at about 100 ms. The early radiation is likely the "shine" from the (open) emplacement pipe while the pressure history suggests a slight increase until loss. At the second pressure dome, the radiation and pressure histories initially both show a jump which then monotonically decay (figures 2 2 and 2.10). However, about 40 s after detonation, there is a radiation arrival followed by several additional arrivals without corresponding changes pressure.

Again, at station 34 (the elevation of the third pressure dome, see figures 2 3 and 2 11) there is both a prompt radiation arrival and a pressure jump with a monotonic decay. A second radiation arrival occurs at about 60 s and may be a further continuation of cavity gas migration up the stemming but without driving pressure. The early portion of the radiation seen at both stations 33 and 34 is likely due to pipe "shine" while the pressure histories can be accounted for by compression.

Pressure histories from all stations above station 34 can be explained as the result of stemming or ground motion. With the exception of stations 35 and 39 (figures 2 12 and 2 16), all stations above the formation coupling plug may have shown brief effects of shine before they were temporarily discharged by the EMP.

## 2.2 Motion

Explosion-induced histories of the motion measured in the stemming and on the ground surface during the CARNELIAN event are shown in figures 2 18–2 23. Characteristics of the associated motion and transducers are given in tables 2.1–2 3.

The drag ring system on the emplacement pipe may have induced motion that interfered with the ground motion signal at station 21 at early times (figure 2.18).

Early time acceleration induced from the emplacement pipe was also observed at station 22 (figure 2 19). Since the pipe was "greased" with hydroseal in the region of this plug the magnitude of the acceleration induced from the pipe motion is larger than expected. Its integral is almost negligible, however.

The emplacement pipe was also coated with hydroseal in the region of the top TPE plug and the pipe-induced motion at this station was strongly mitigated (figure 2 20, station 23). The explosion-induced motion in the stemming structures and on the ground surface (figure 2 21, station 61) was otherwise unremarkable.

Motion of the recording trailer (station 71) is displayed in figures 2 21 and 2 23 and the first 1.5 seconds of the vertical, horizontal-radial displacement trajectory of the recording trailer is displayed in figure 2 24.

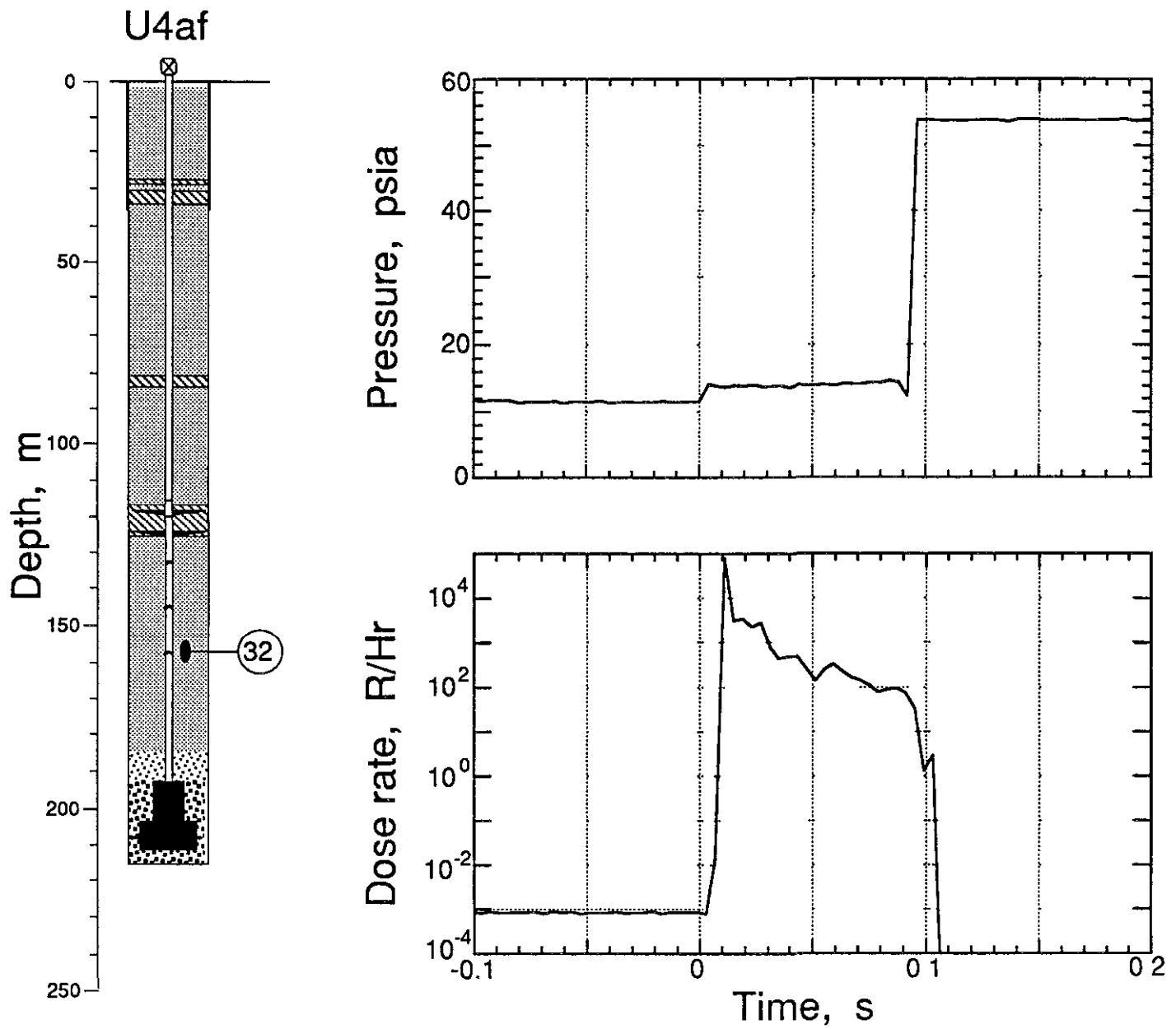


Figure 2.1 Pressure and radiation as monitored in the coarse stemming at an elevation of 0.9 m above that of the deepest pressure dome (station 32 at 157.3 m depth)

U4af

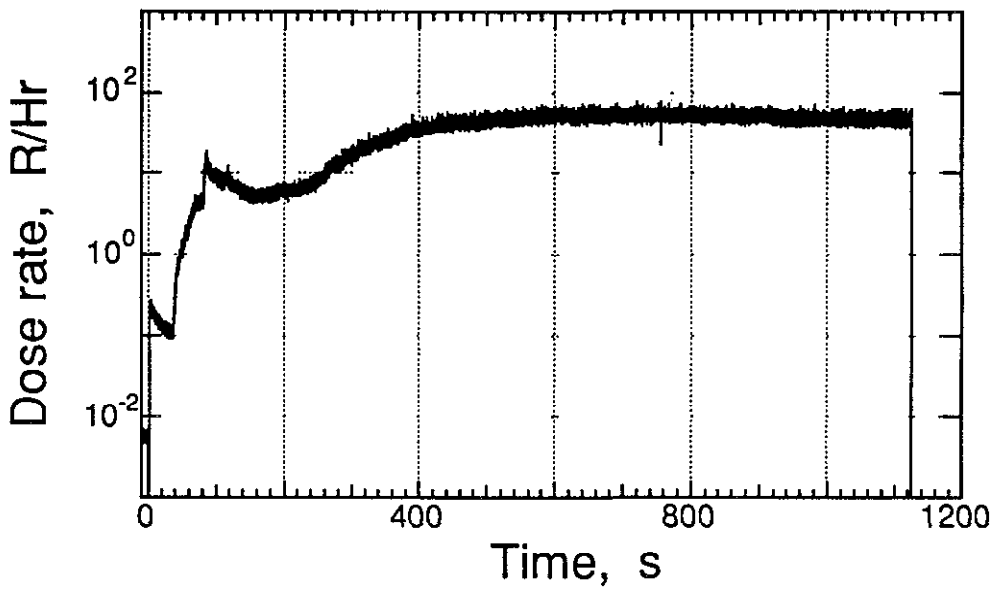
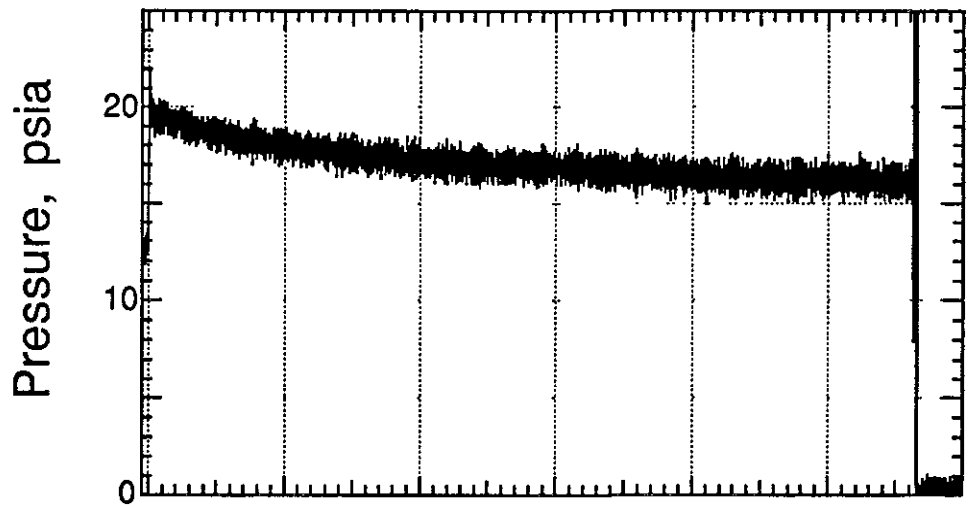
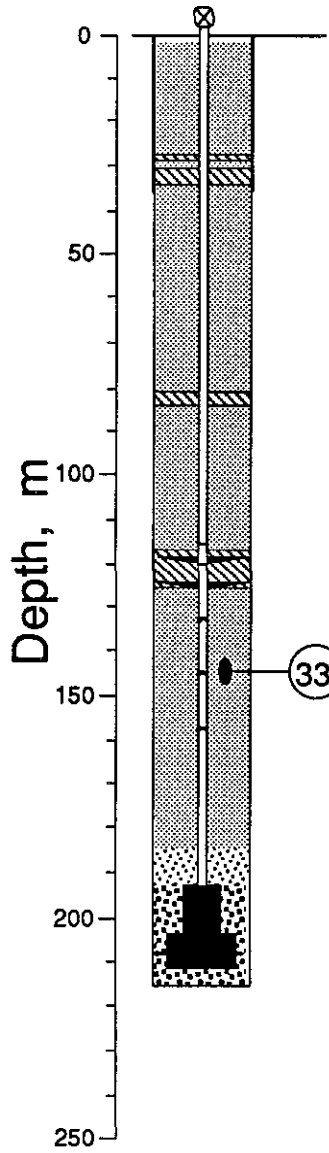


Figure 2 2 Pressure and radiation measured in the fines stemming at an elevation of 0.6 m above that of the mid pressure dome (station 33 at 144.8 m depth)

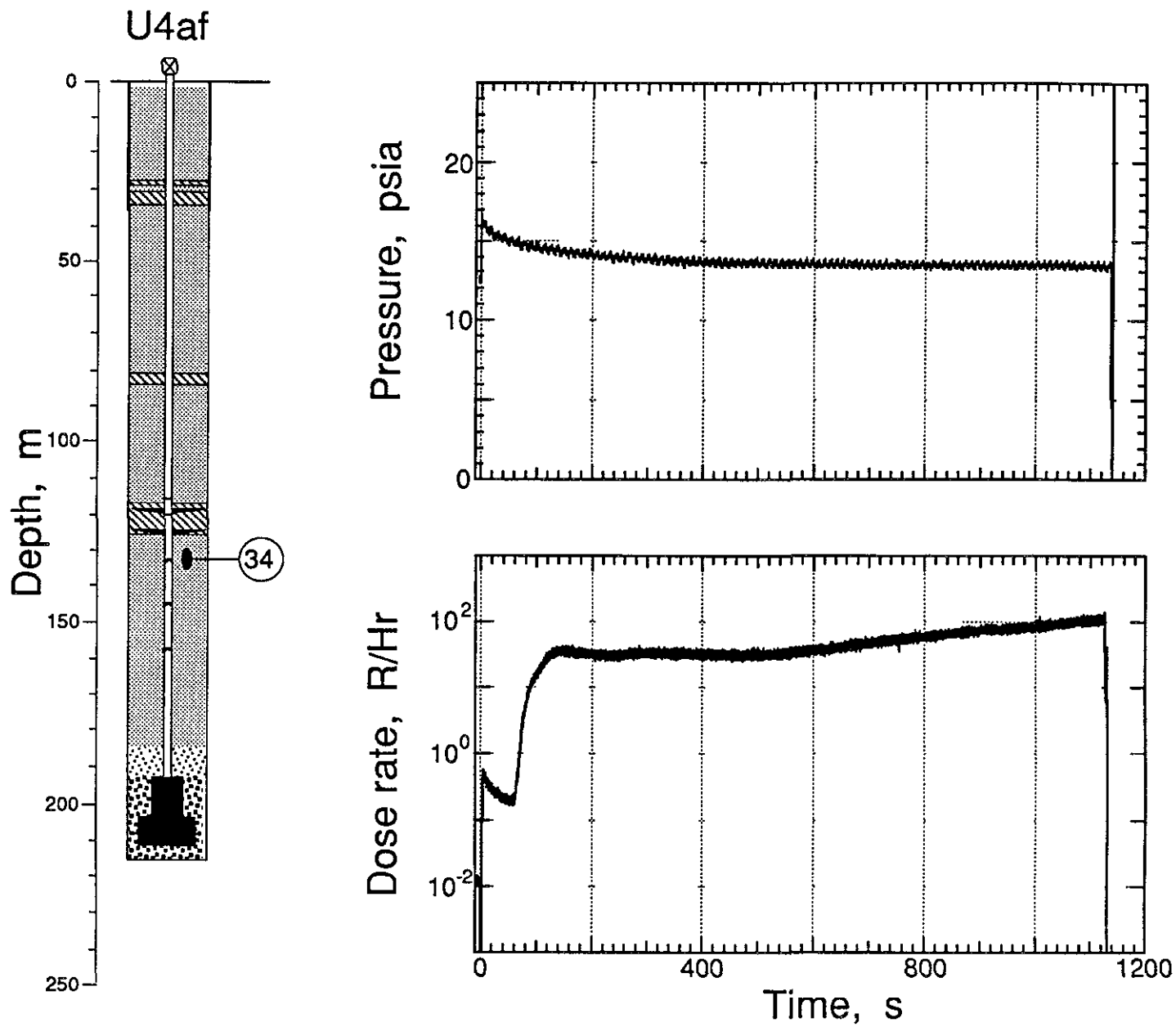


Figure 2 3 Pressure and radiation measured in the coarse stemming at an elevation of 0.7 m above that of the third pressure dome (station 34 at 132.3 m depth)

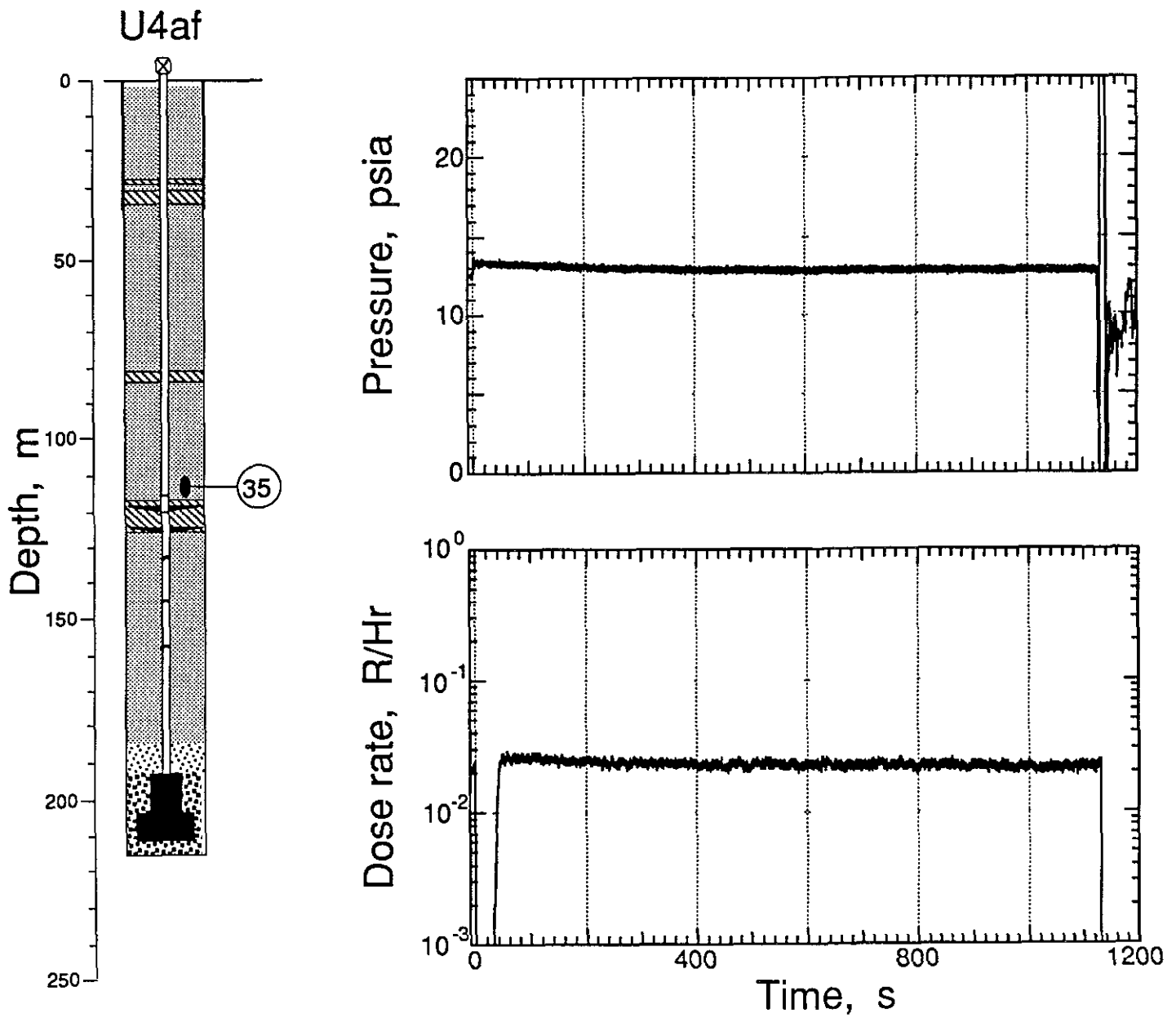


Figure 2.4 Pressure and radiation measured in the stemming above the formation coupling plug and 2.4 m above the elevation of the detector plate (station 35 at 112.8 m depth)

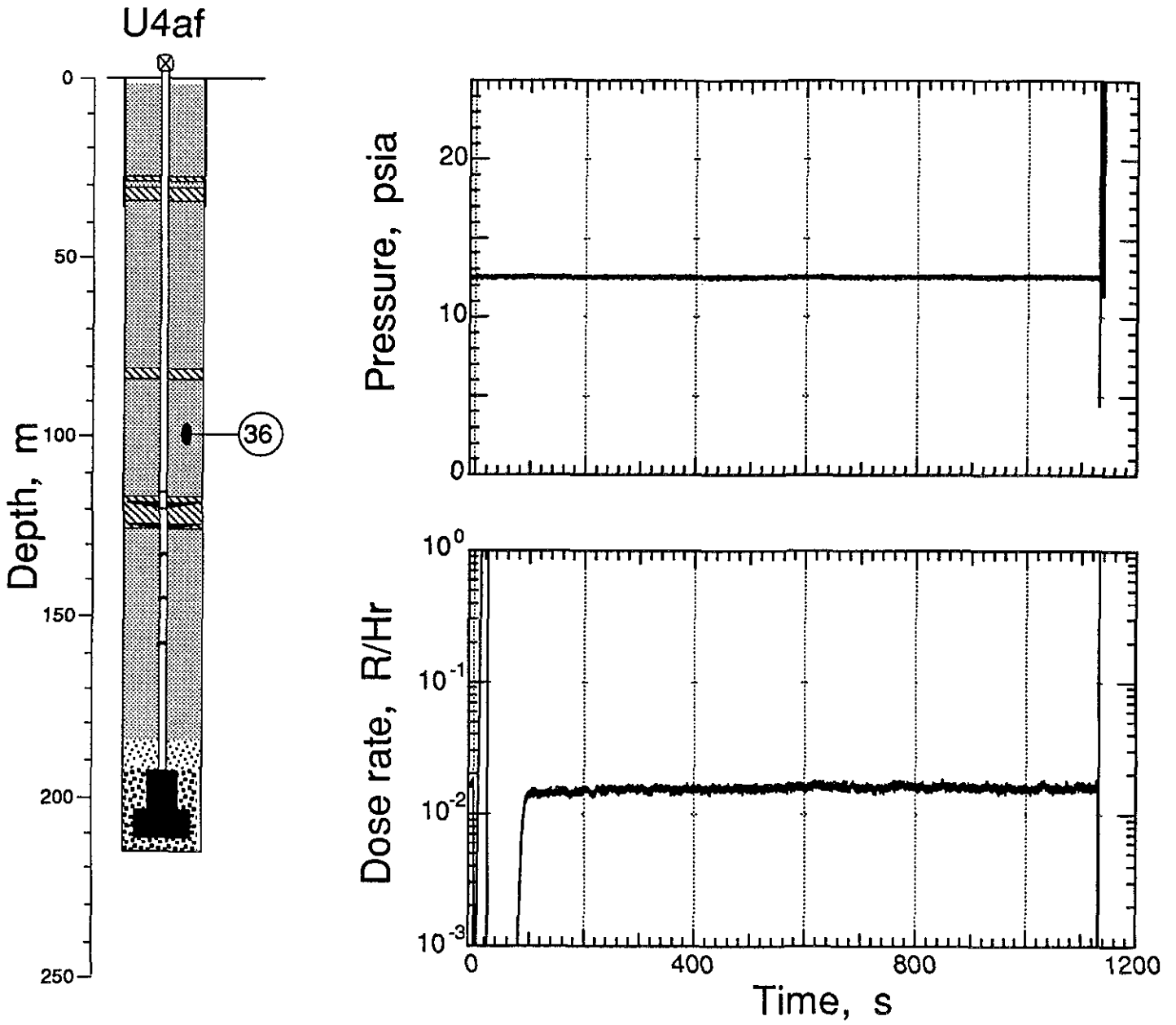


Figure 2.5 Pressure and radiation measured in the stemming mid way between the formation coupling plug and the intermediate rigid plug (station 36 at 99.1 m depth)

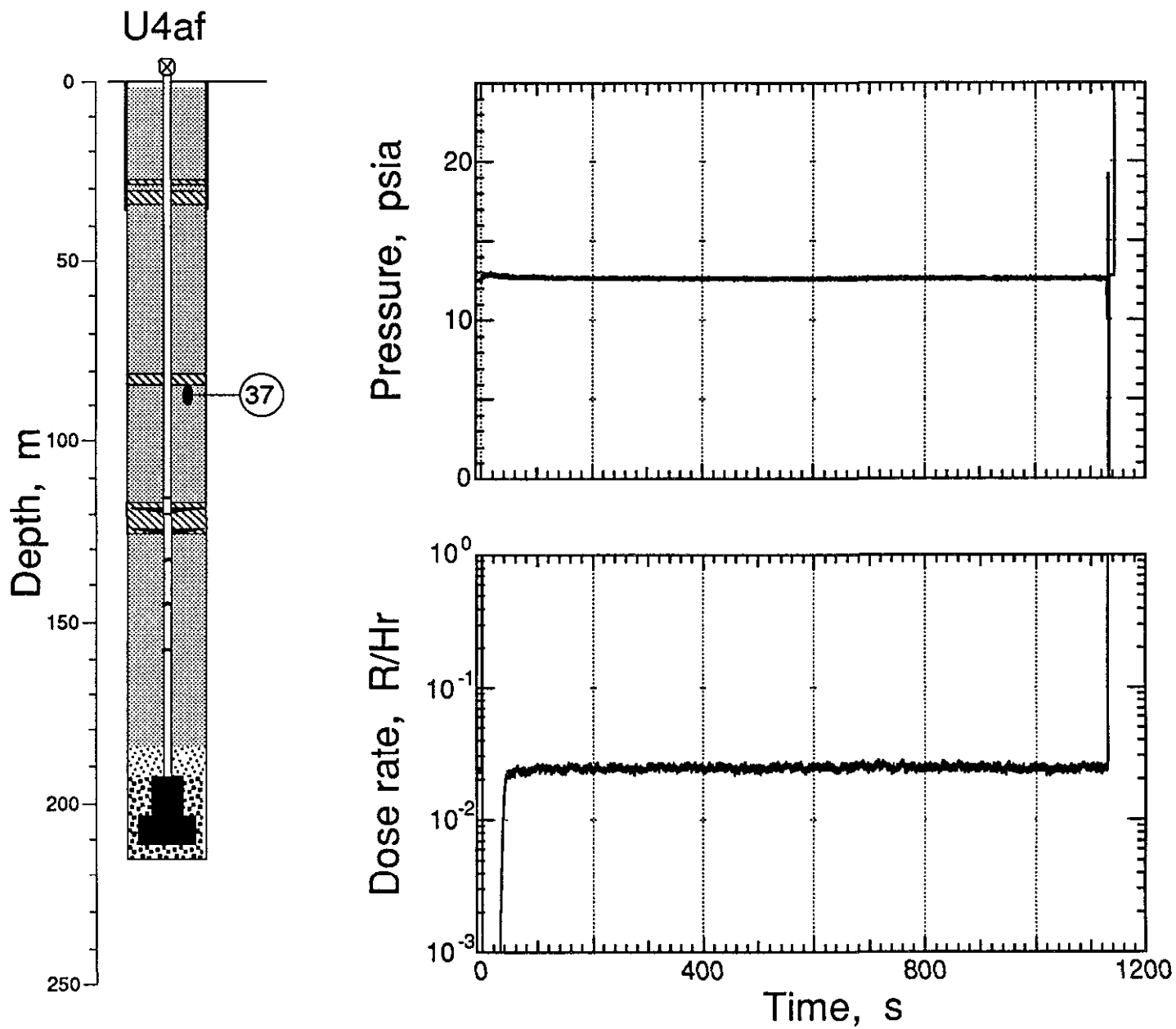


Figure 2 6 Pressure and radiation measured in the stemming beneath the intermediate rigid plug (station 37 at 86.9 m depth)

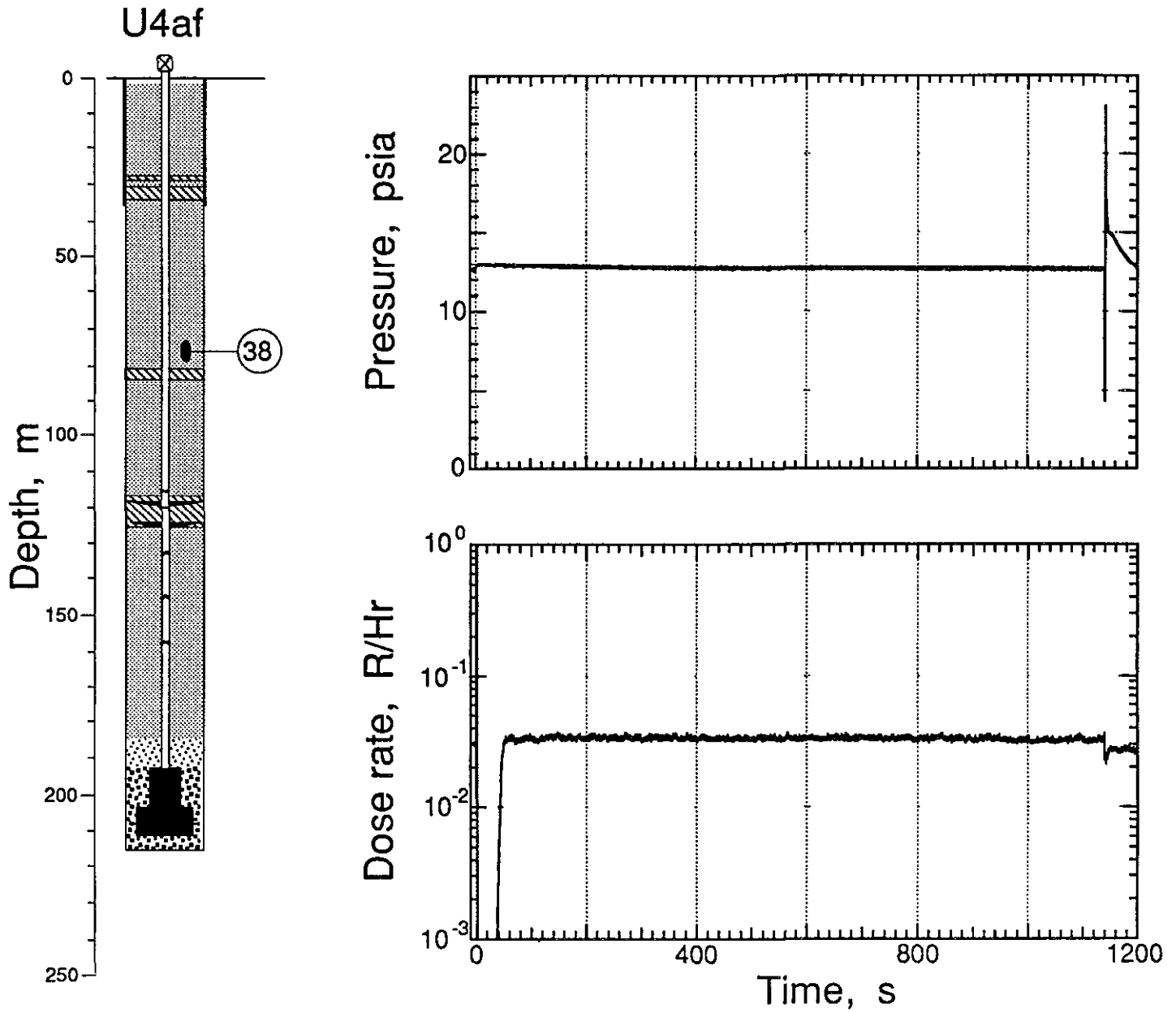


Figure 2.7 Pressure and radiation measured in the stemming above the intermediate rigid plug (station 38 at 76.2 m depth)

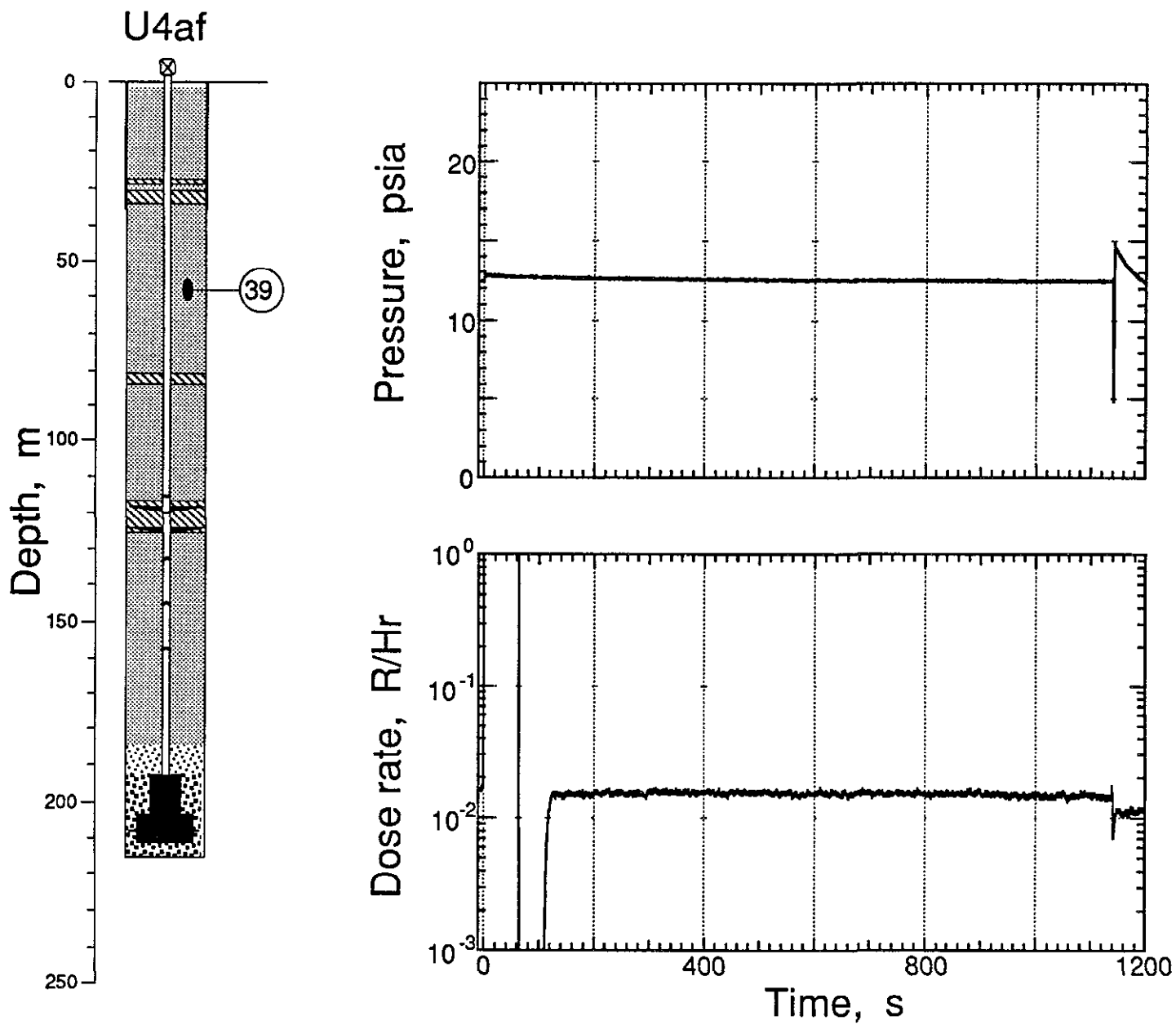


Figure 2 8 Pressure and radiation measured in the stemming mid way between the intermediate and top plugs (station 39 at 57 9 m depth)

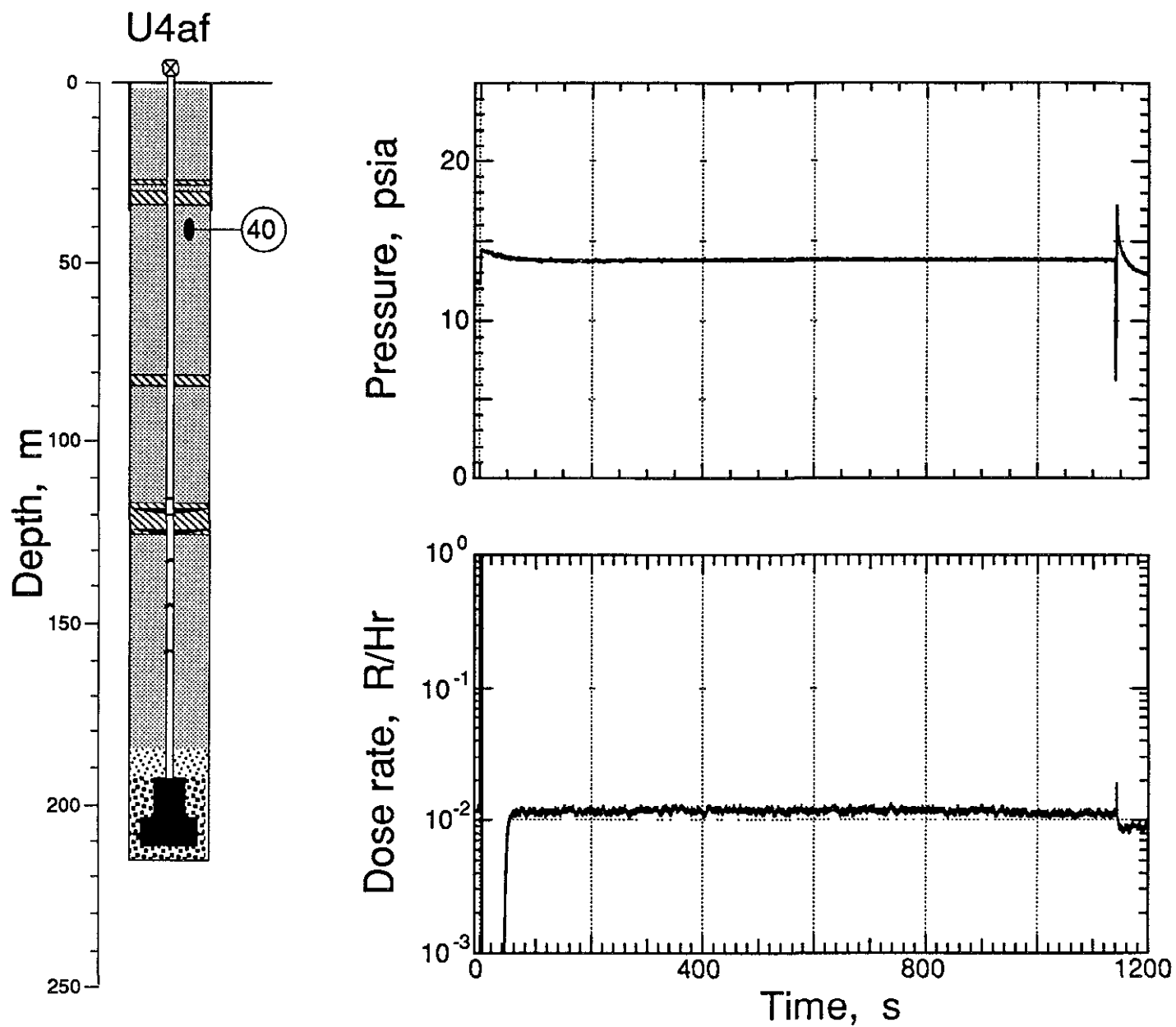


Figure 2 9 Pressure and radiation measured in the stemming beneath the top plug (station 40 at 41.1 m depth)

U4af

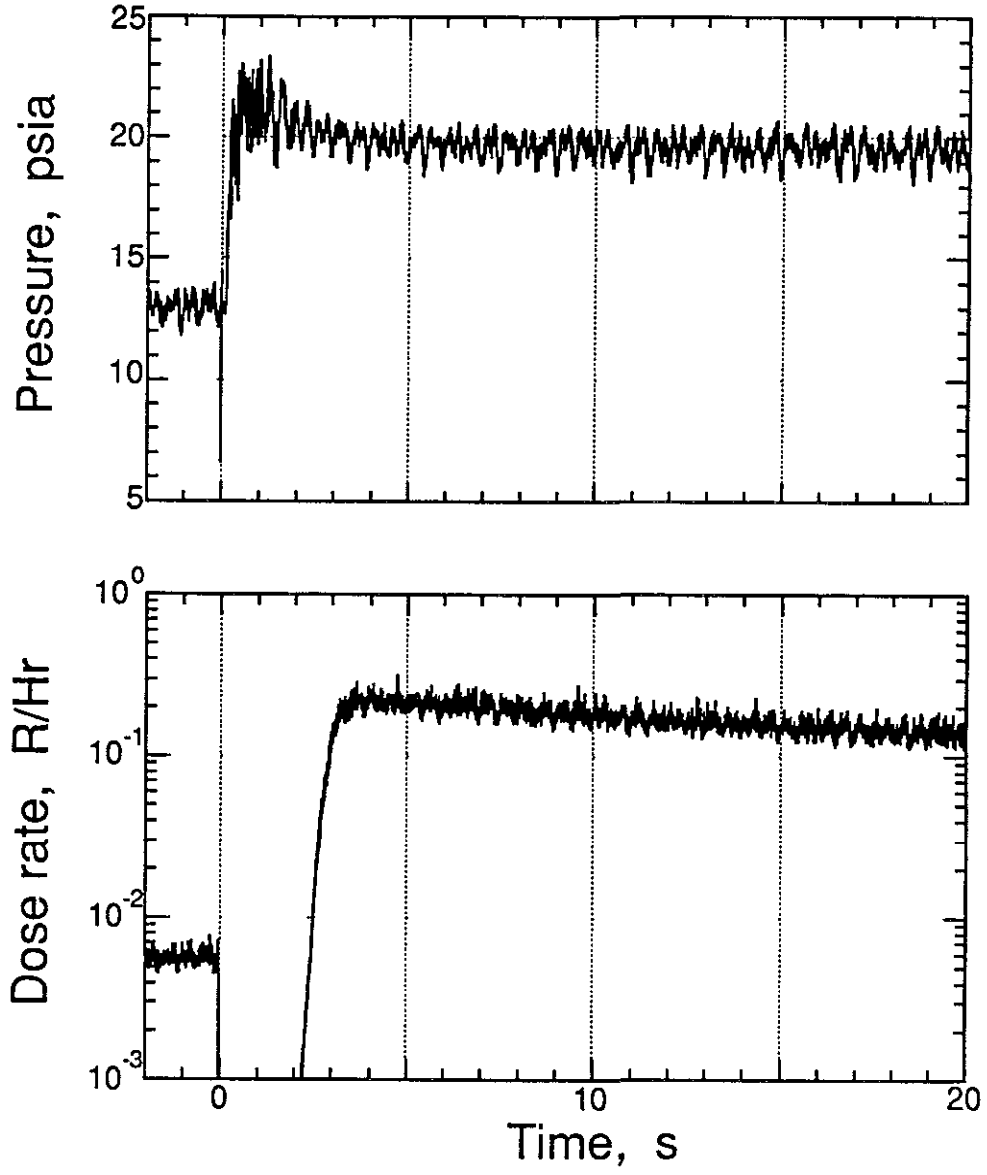
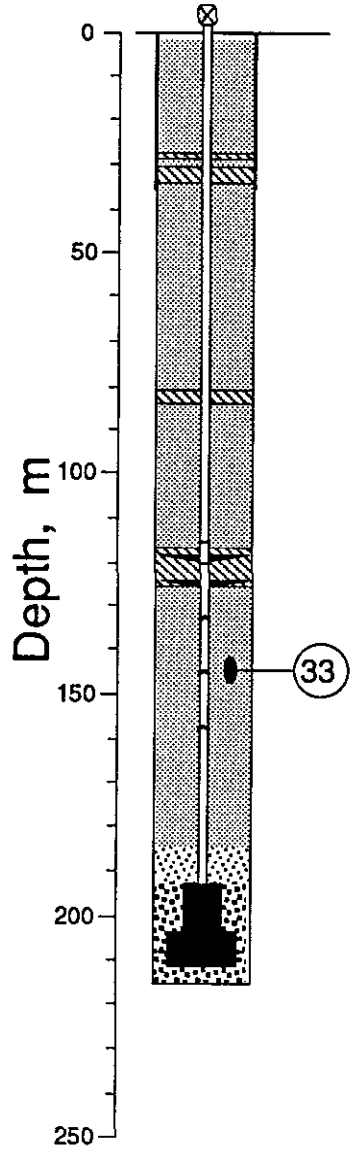


Figure 2 10 Early-time pressure and radiation measured in the fines stemming at an elevation of 0.6 m above that of the mid pressure dome (station 33 at 144.8 m depth). The usual "blanking" at zero time of radiation signal precludes information for the first few seconds.

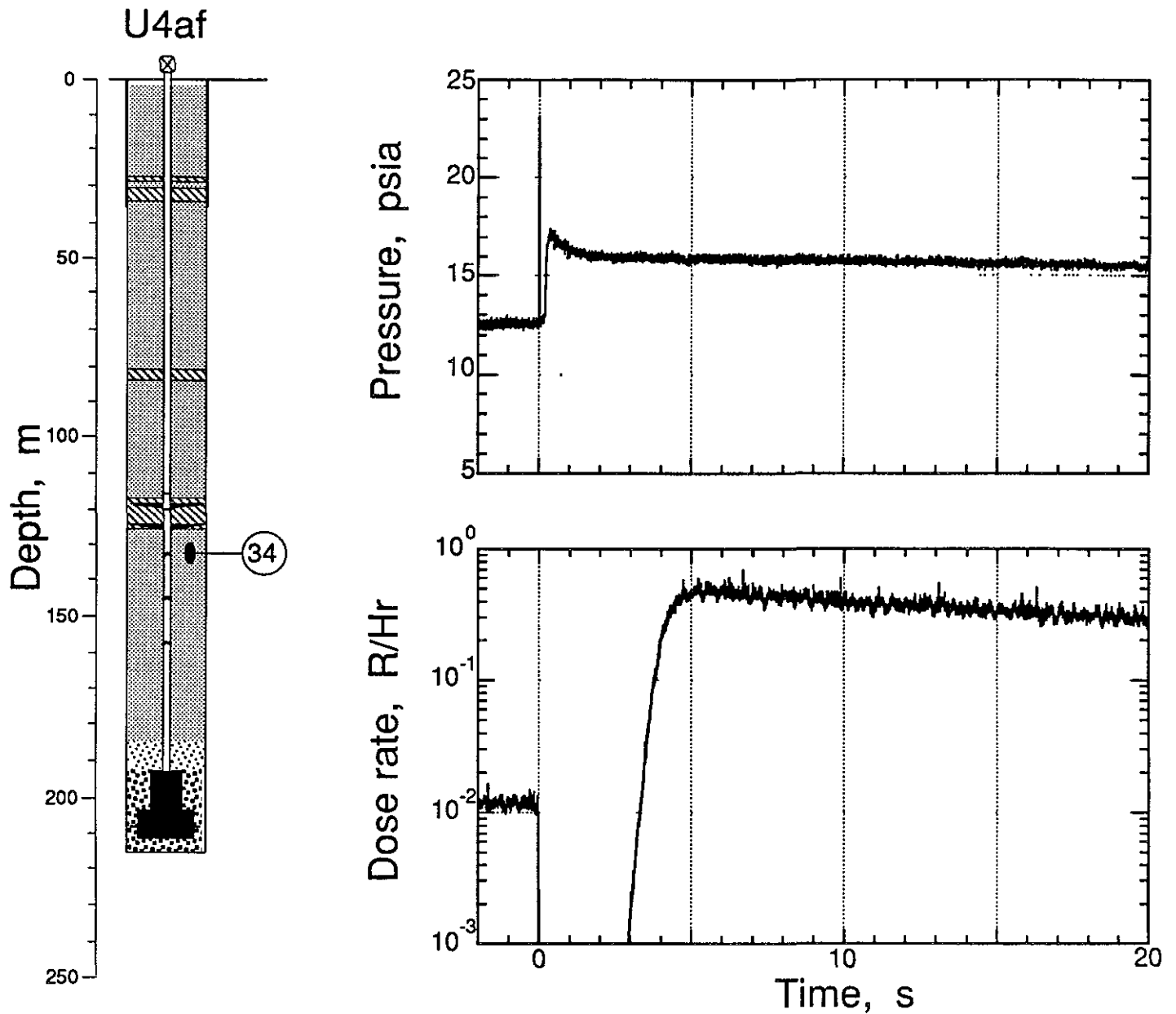


Figure 2 11 Early-time pressure and radiation measured in the coarse stemming at an elevation of 0.7 m above that of the third pressure dome (station 34 at 132.3 m depth). The usual "blanking" at zero time of radiation signal precludes information for the first few seconds.

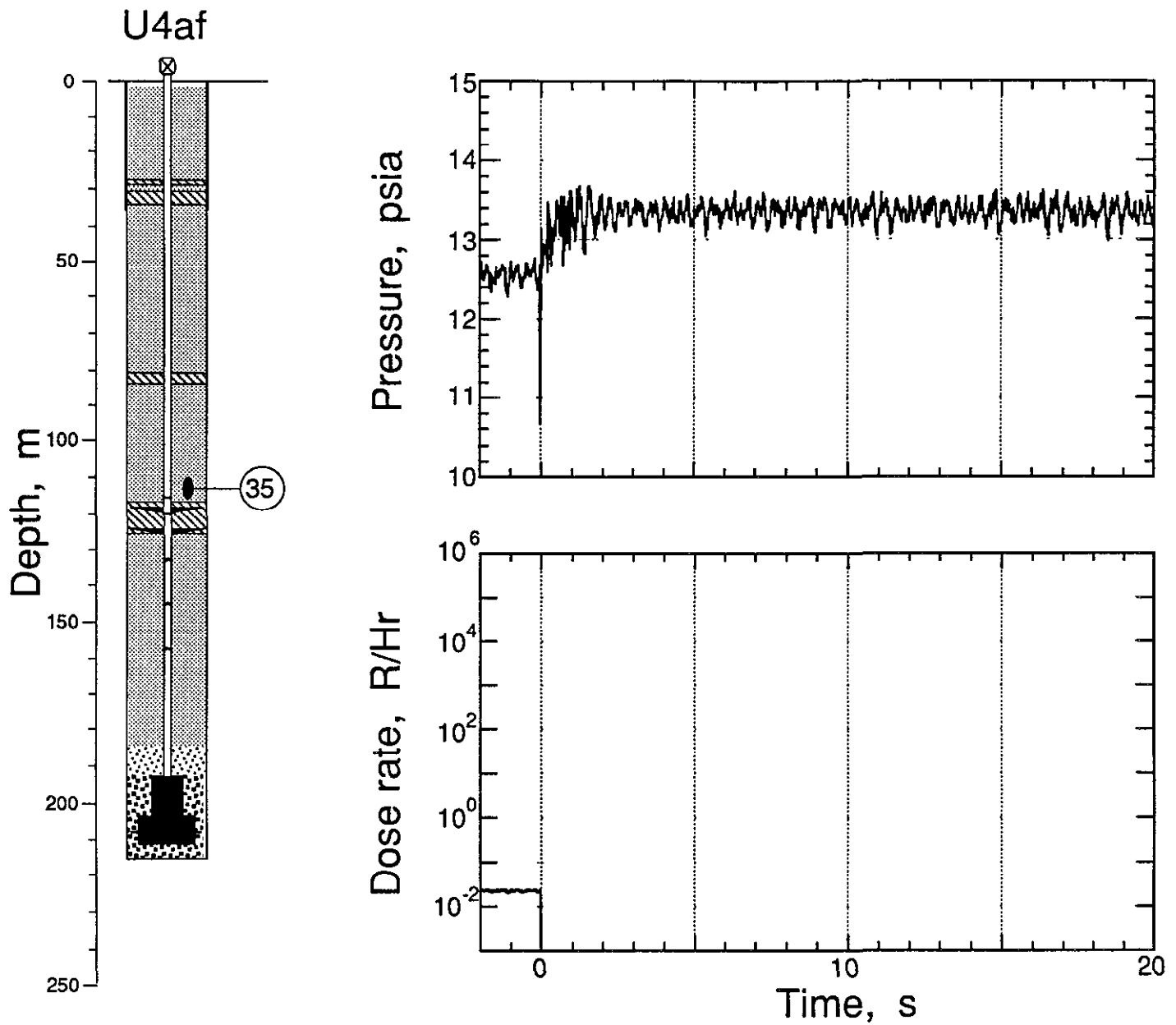


Figure 2 12 Early-time pressure and radiation measured in the stemming above the formation coupling plug and 2.4 m above the elevation of the detector plate (station 35 at 112.8 m depth). The usual "blanking" at zero time of radiation signal precludes information for more than 60 seconds.

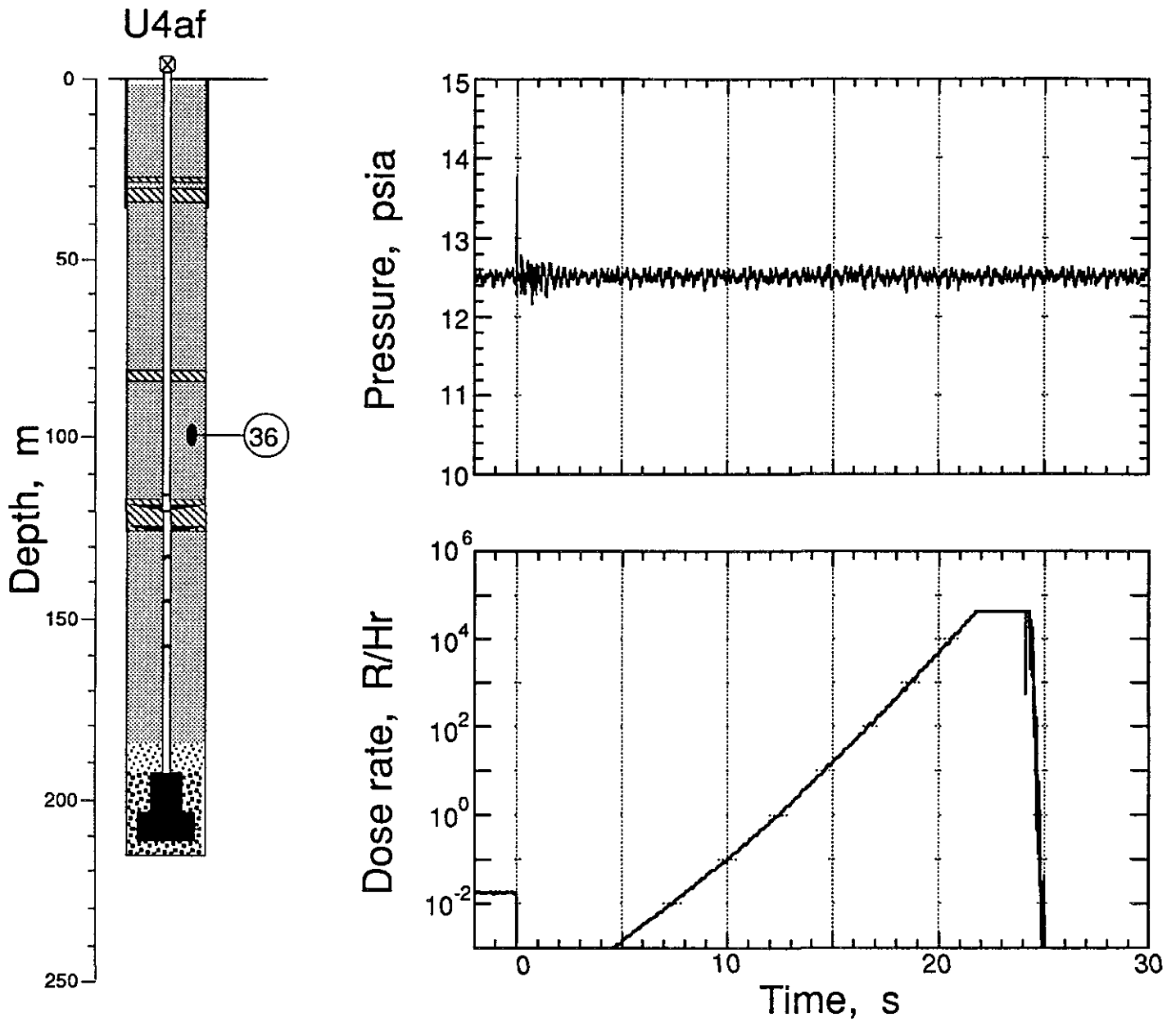


Figure 2 13 Early-time pressure and radiation measured in the stemming mid way between the formation coupling plug and the intermediate rigid plug (station 36 at 99.1 m depth). The usual "blanking" at zero time of radiation signal precludes information more than 80 seconds except for a period of brief channel saturation which may be shine from the emplacement pipe.

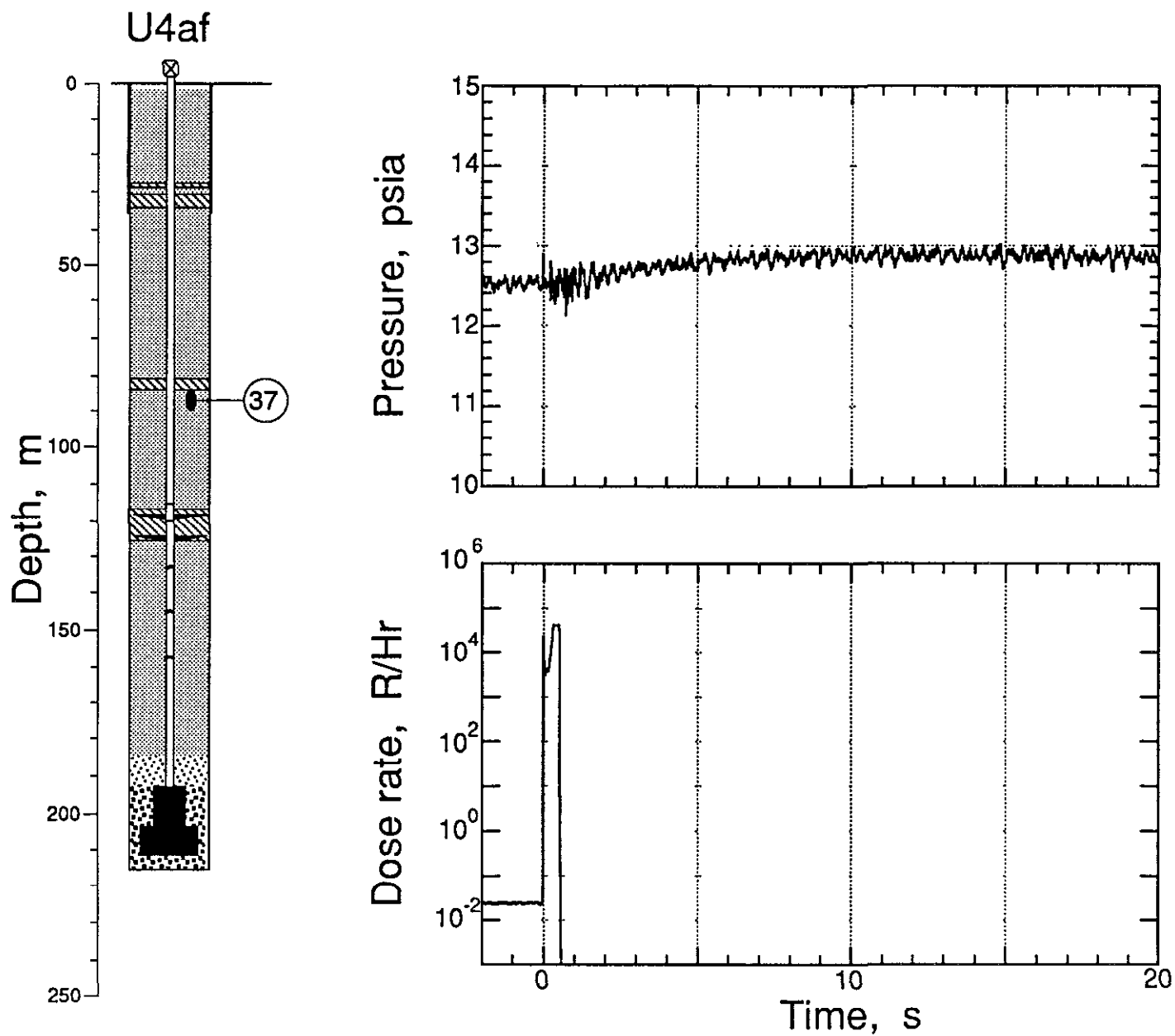


Figure 2 14 Early-time pressure and radiation measured in the stemming beneath the intermediate rigid plug (station 37 at 86.9 m depth). The usual "blanking" at zero time of radiation signal precludes information more than 30 seconds except for a period of brief channel saturation which may be shine from the emplacement pipe.

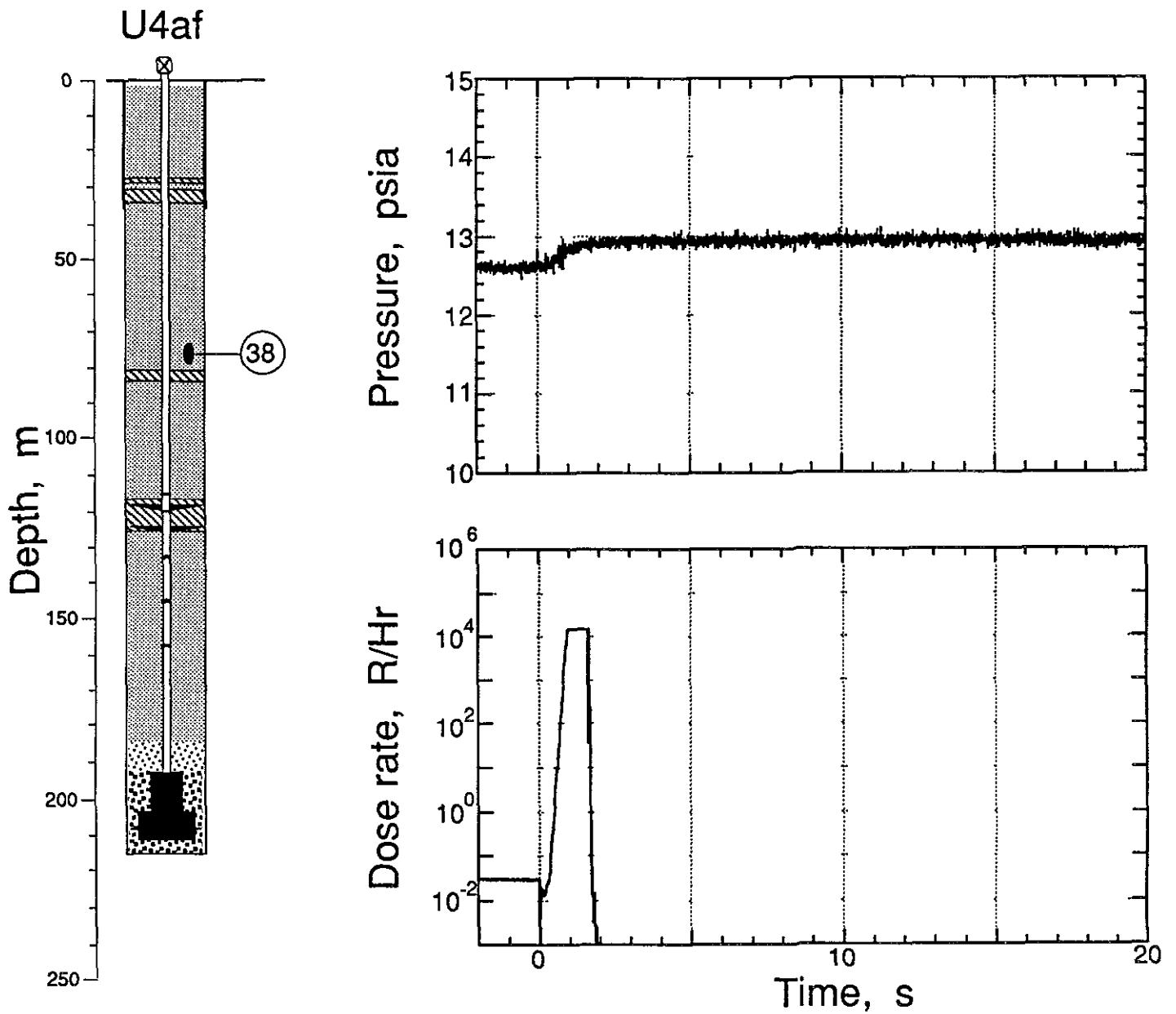


Figure 2 15 Early-time pressure and radiation measured in the stemming above the intermediate rigid plug (station 38 at 76.2 m depth). The usual "blanking" at zero time of radiation signal precludes information more than 40 seconds except for a period of brief channel saturation which may be shine from the emplacement pipe.

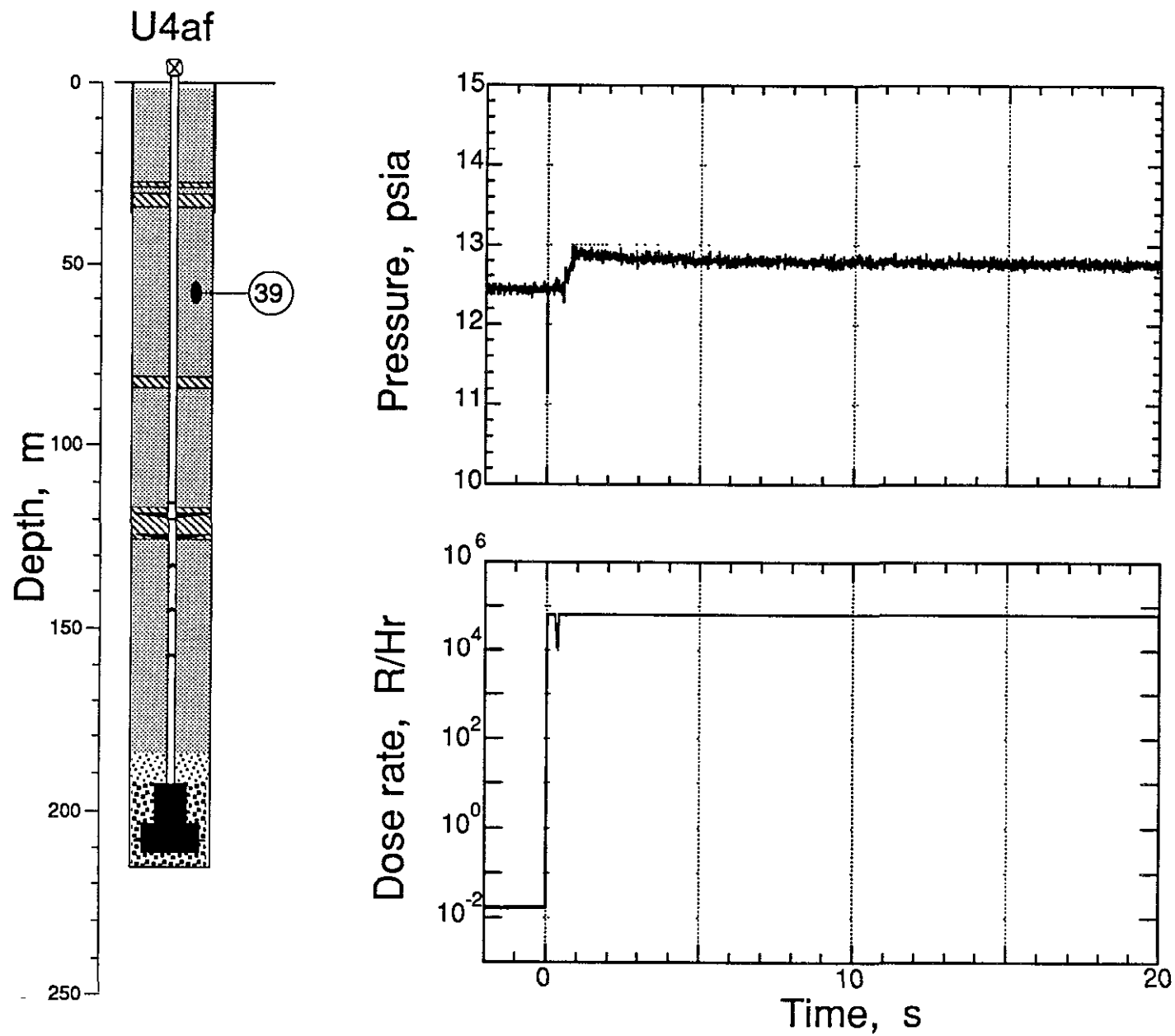


Figure 2 16 Early-time pressure and radiation measured in the stemming mid way between the intermediate and top plugs (station 39 at 57.9 m depth). The signal on the radiation channel is unlikely to be shine from the emplacement pipe

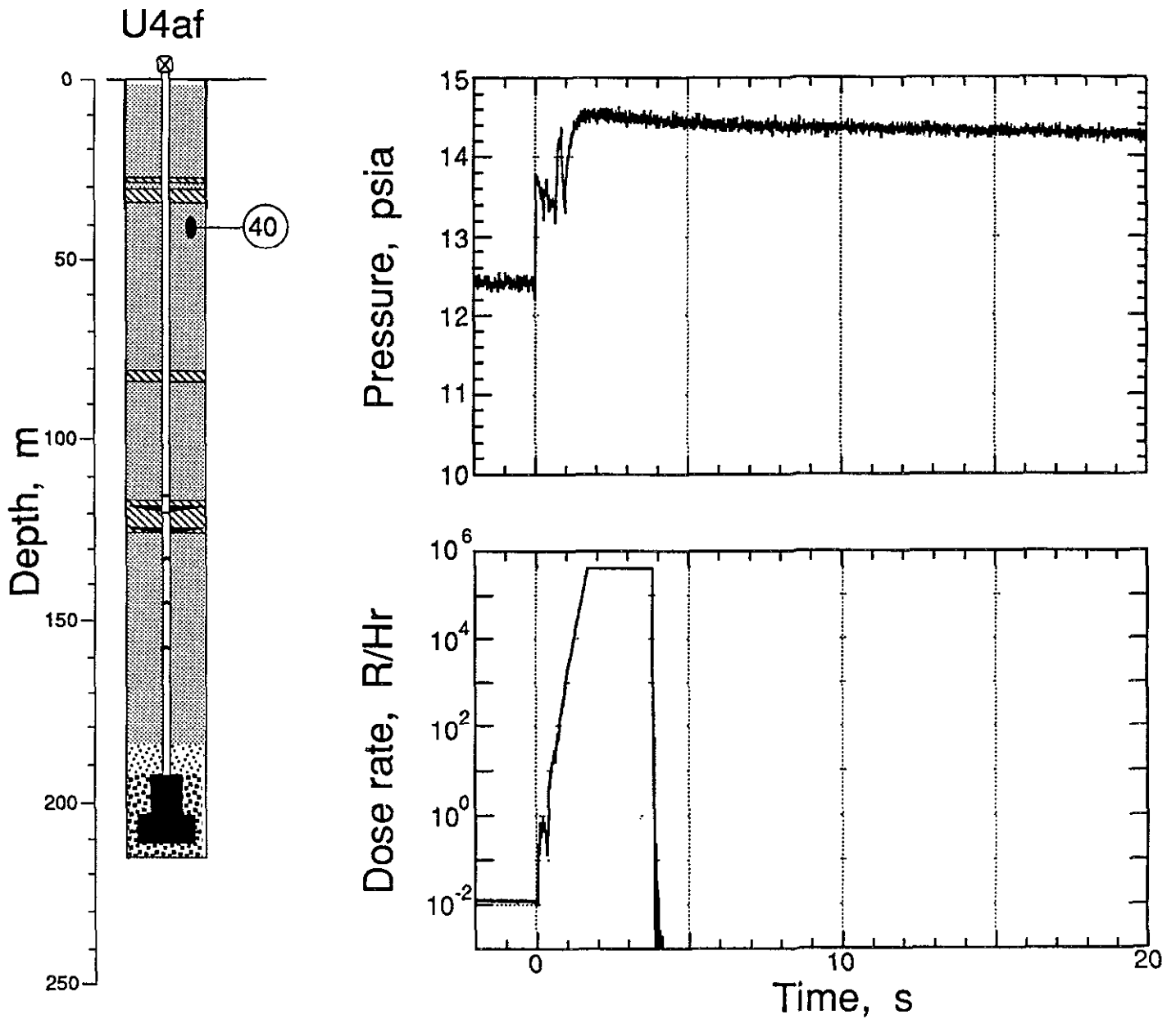


Figure 2 17 Early-time pressure and radiation measured in the stemming beneath the top plug (station 40 at 41.1 m depth) The usual "blanking" at zero time of radiation signal precludes information more than 40 seconds except for a period of brief channel saturation which may be shine from the emplacement pipe

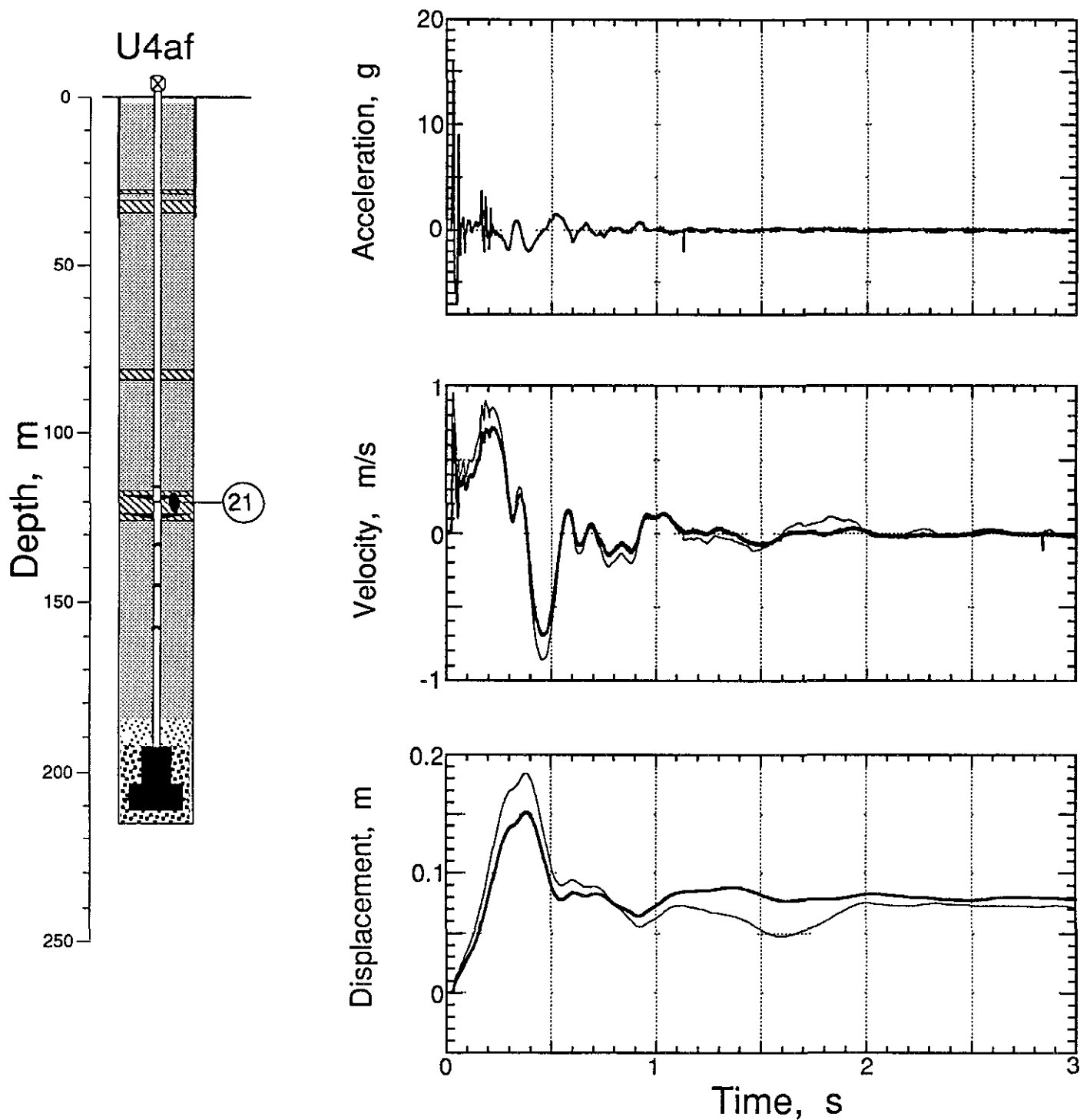


Figure 2 18 Explosion-induced vertical motion of the bottom rigid plug (station 21, at a depth of 120.5 m). The acceleration at early time shows strong motion induced by the emplacement pipe and the drag rings. When there is more than one trace in a plot, the lighter is derived from the accelerometer.

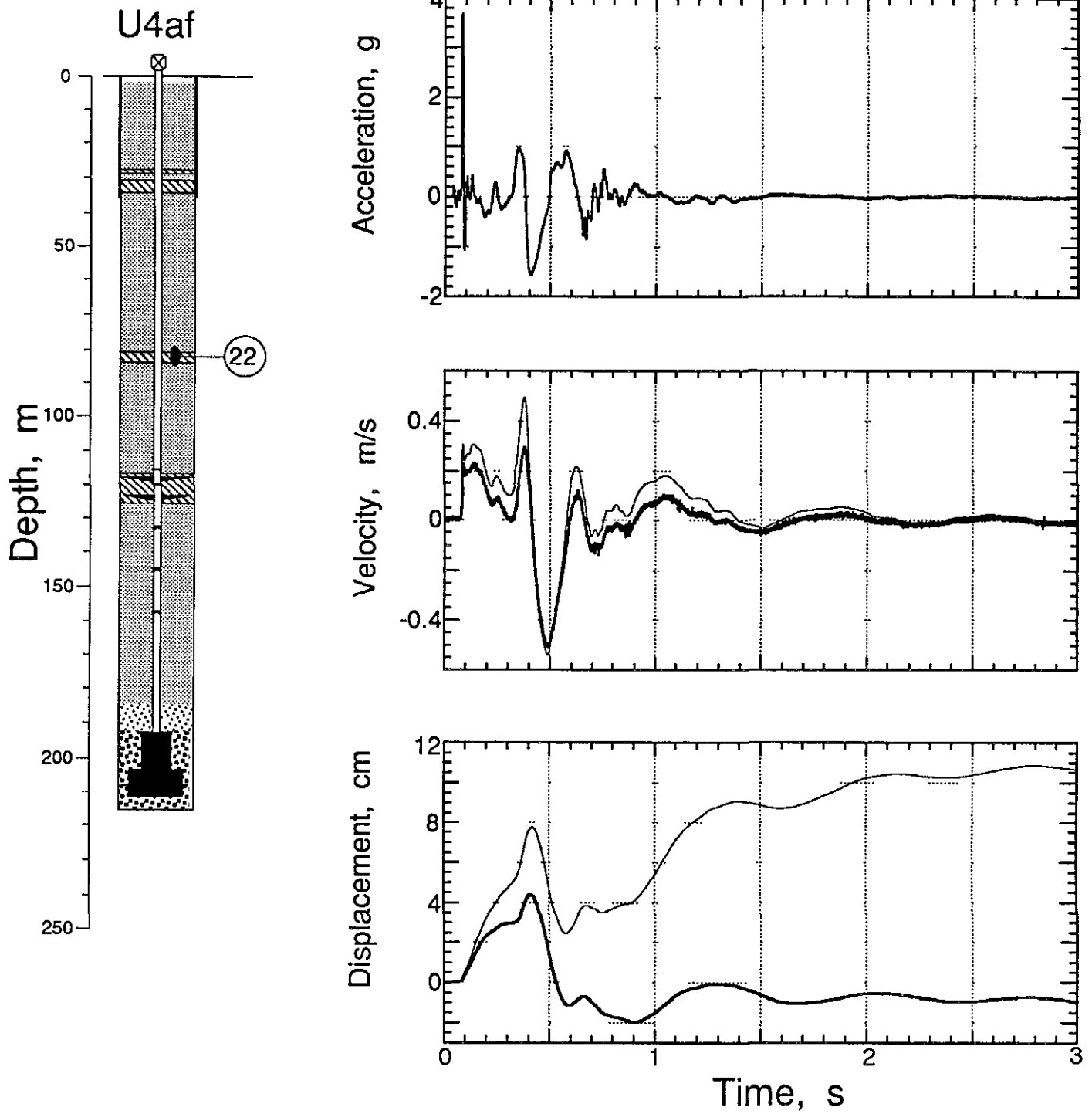


Figure 2 19 Explosion-induced vertical motion of the intermediate rigid plug (station 22, at a depth 82.3 m) When there is more than one trace in a plot, the lighter is derived from the acclerometer

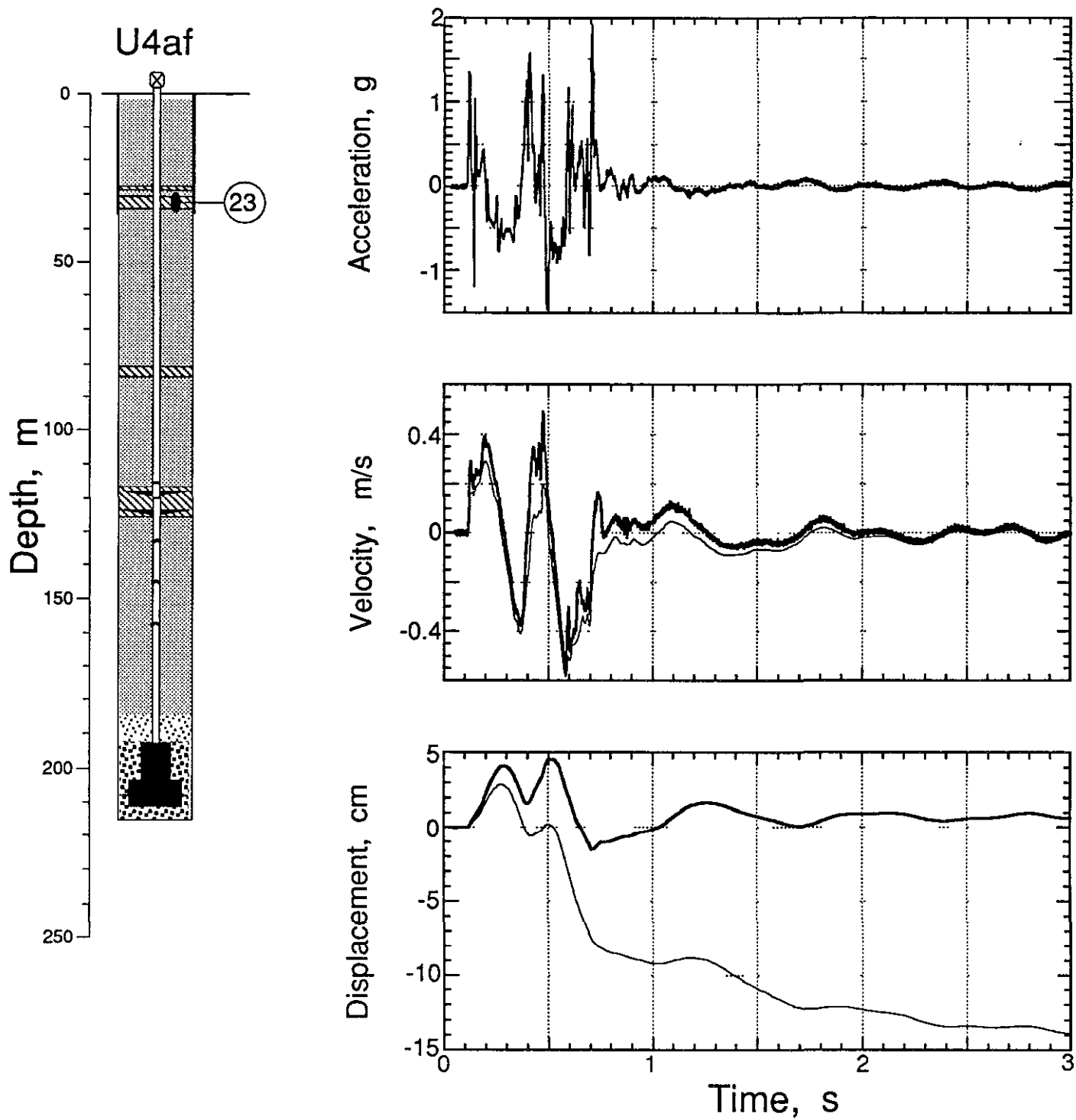


Figure 2.20 Explosion-induced vertical motion of the top rigid plug (station 23, at a depth of 32.3 m). When there is more than one trace in a plot, the lighter is derived from the accelerometer. When there is more than one trace in a plot, the lighter is derived from the accelerometer.

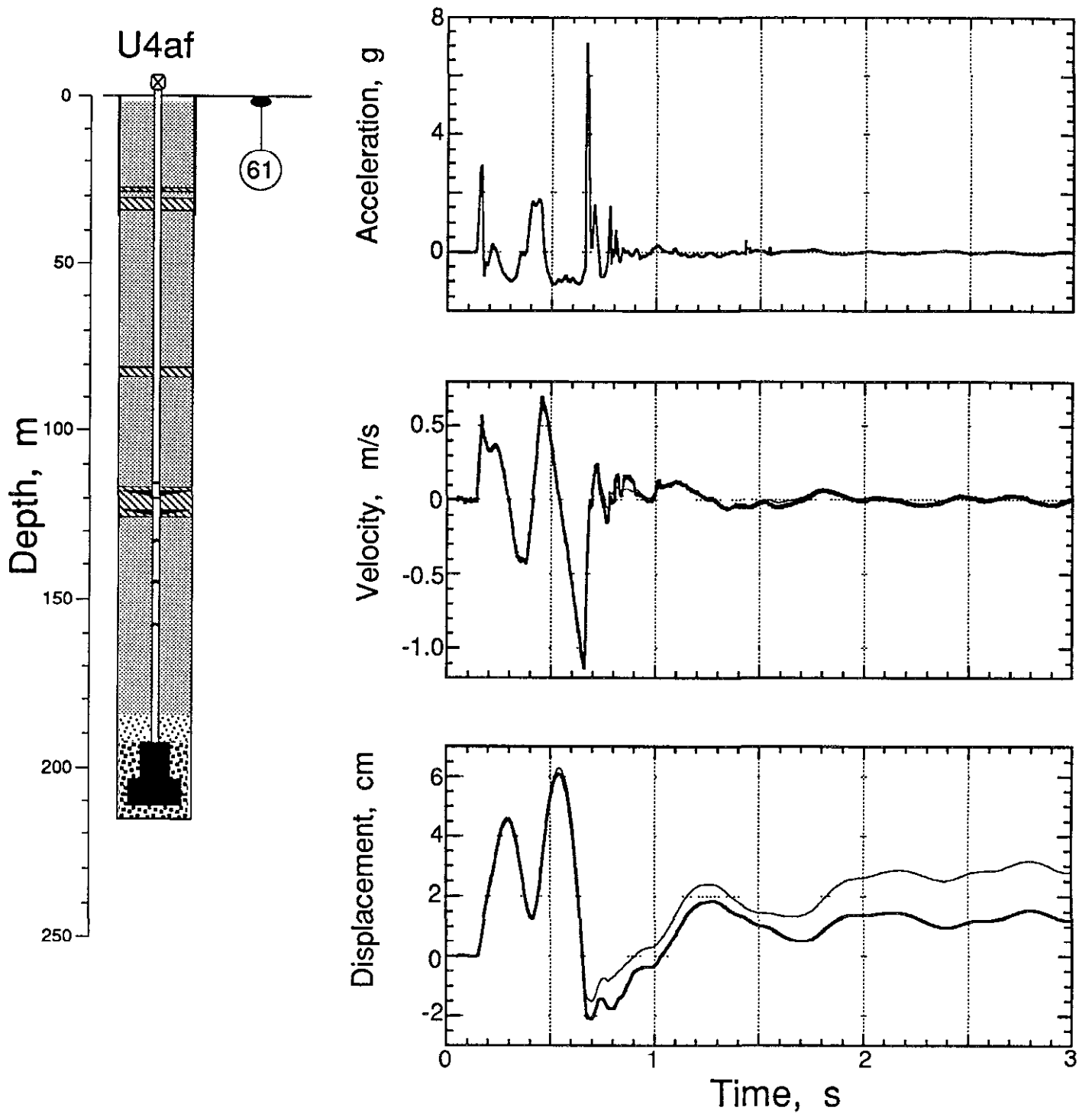


Figure 2 21 Explosion-induced vertical motion of the ground surface at a depth of 0 9 m and horizontal range of 15 24 m (station 61 )

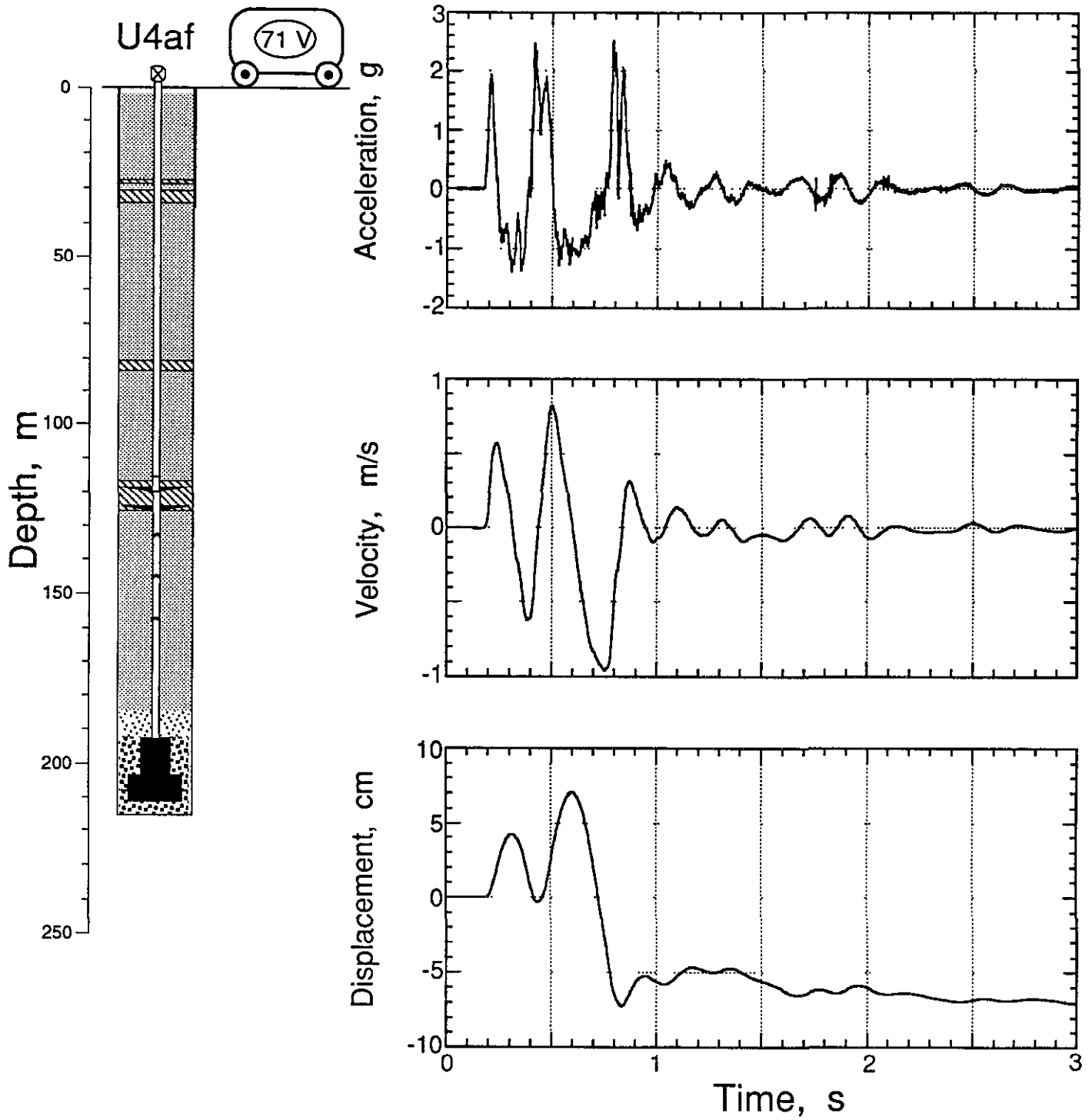


Figure 2 22 Explosion-induced vertical motion of the recording trailer (station 71)

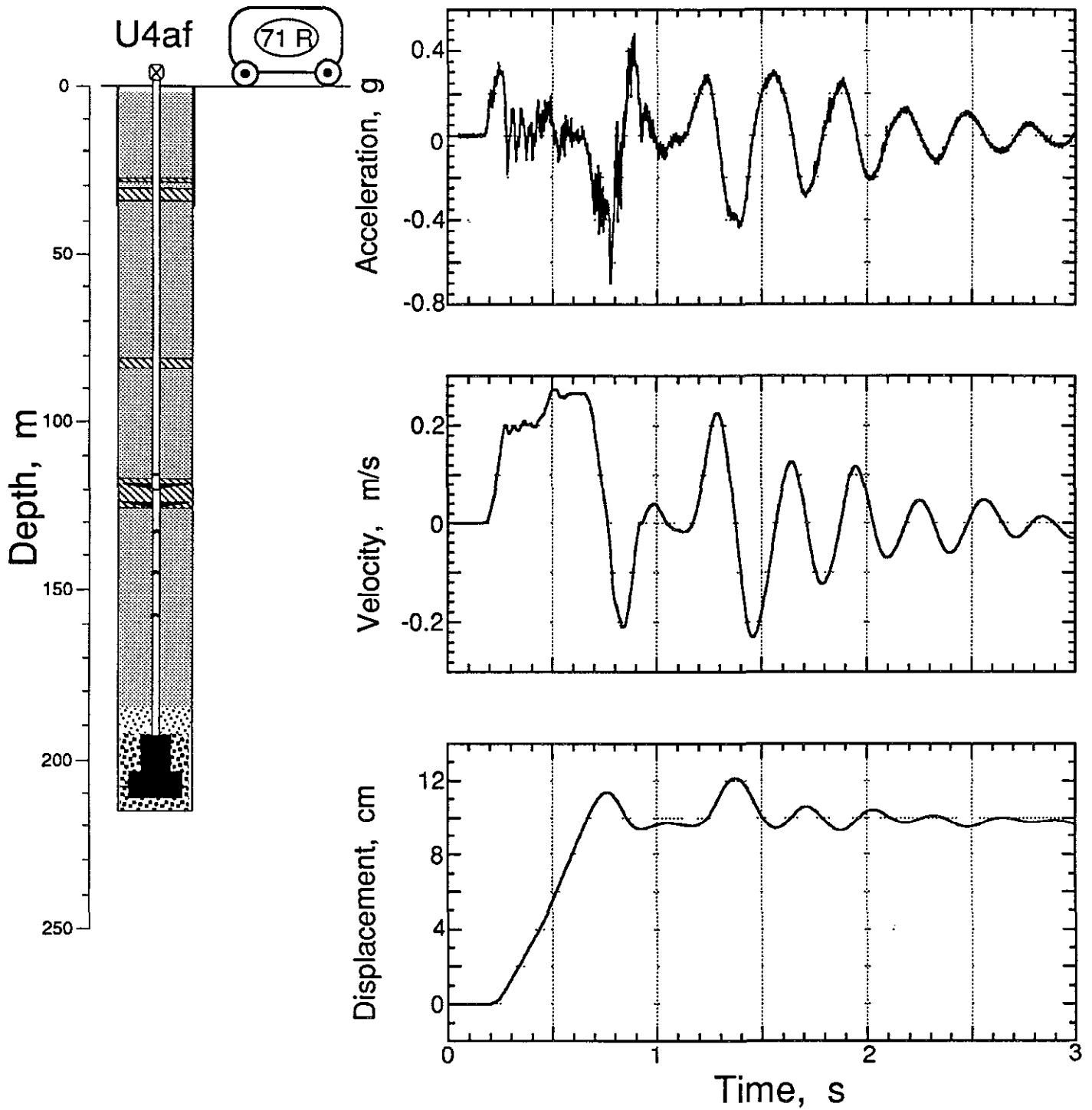


Figure 2 23 Explosion-induced horizontal-radial motion of the recording trailer (station 71)

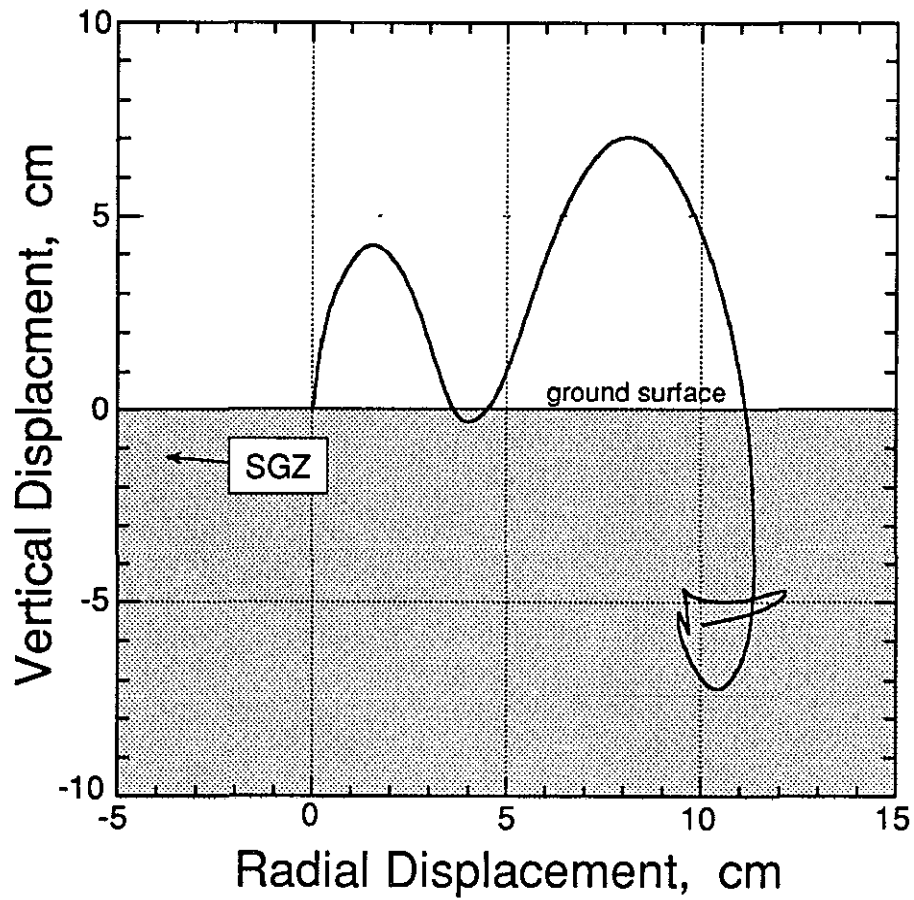


Figure 2 24 Displacement trajectory in the vertical-radial plane of the recording trailer during the first 1 5 s of motion

**Table 2.1 Summary of Containment-Related Motion**

Gauge	Slant Range (m)	Arrival Time (ms)	Acceleration Peak (g)	Velocity Peak (m/s)	Displacement Peak (cm)	Displacement Residual (m)
2av	47.3	10.8	500(a), 2000	15(a)	25(a)	(b)
2uv		11.0	-	18(a)	20(a)	(b)
3av	50.0	11.5	480(a), 620	18(a)	(b)	(b)
3uv		11.8	-	15.5(a)	21(c)	(b)
5av	62.5	14.3	360(a), 300	14.5(a), 40.8	19(a), >220	(b)
5uv		14.1	-	13(a), 35	16(a), >130	(b)
7av	75.0	17.2	265(a), 150	8.5(a), 4.5	8.5(a), 27	21
7uv		17.0	-	7.7(a), 4.2	7.0(a), 27	21
9av	92.7	21	9.5(a), (d)	0.73(a), 0.58	14.3	20
9uv		25	-	0.73(a), 0.67	14.6	7
11av	208.5	131	1.9, 2.5	0.39	3.6	-8
11uv		130	-	0.35	3.3	-9
21av	87.4	21	15.8(a)	0.95(a), 0.95	18.5	7
21uv		21	-	0.74(a), 0.71	15.0	8
22av	125.0	35, 73	3.7	0.50	7.8	10.5
22uv		75	-	0.30	4.4	-1
23av	175.0	107	1.34	0.29	2.9	-14
23uv		110	-	0.39	4.1	0.4
61av	207.3	138	2.9, 7.0(e)	0.48	4.6	3
61uv		142	-	0.57	4.6	1.3
71av	231.5(f)	176	1.92, 2.5(e)	0.57	4.2	-7
71ar		175	0.35, 0.46(e)	0.27	11.3	10

- (a) Pipe-induced motion
- (b) Channel lost prior to attaining this
- (c) Approximate
- (d) Very indistinct
- (e) Slap-down
- (f) In recording trailer, range is approximate

**Table 2.2 Containment-Related Accelerometer Characteristics**

<u>Gauge</u>	<u>Natural Frequency (Hz)</u>	<u>Damping Ratio</u>	<u>System Range (g's)</u>
2av	1500	0.65	2000
3av	1430	0.65	2000
5av	1700	0.65	2000
7av	1500	0.65	1000
9av	1600	0.65	400
11av	710	0.65	100
21av	320	0.60	15
22av	350	0.60	15
23av	340	0.65	15
61av	345	0.55	25
71av	230	0.75	10
71ar	255	0.65	10

**Table 2.3 Containment-Related Velocimeter Characteristics**

<b>Gauge</b>	<b>Natural Frequency (Hz)</b>	<b>Time to 0.5 Amplitude (s)</b>	<b>Calibration Temperature (°F)</b>	<b>Operate Temperature (°F)</b>	<b>System Range (fps)</b>
2uv	3 70	130	74 9	84 2	600
3uv	3 85	97	75 2	84 9	500
5uv	4 00	56	74 1	87 2	240
7uv	3.85	34 5	74.5	86 4	200
9uv	3.75	16	74 9	79 4	60
11uv	3 03	19 7	74.8	68 1	50
21uv	2.78	22.5	75.0	118 8	36
22uv	3 13	18 4	74 9	101 4	36
23uv	3 23	18 5	74.6	116 6	36
61uv	2 63	38	74 8	68 1	36

### 3 Collapse phenomena

#### 3.1 Motion

Collapse-induced histories of the stemming and ground surface motion measured on the CARNELIAN event are shown in figures 3 1-3 5 All stations in and above the top plug survived collapse which reached the ground surface about 1141 s after detonation (figure 3 4) Both motion channels of station 61 were driven beyond the system limits by the slap-down at collapse, damaging the velocimeter To bring the integral of the acceleration (velocity) to the zero base line at late time, the accelerometer data were augmented by about 8 g's during the single, short period that the signal was "band-edged" (The integral of the unaltered accelerometer data indicated that the velocity was offset below zero by about 50 cm/s at late time )

The plug and ground surface collapse motion data (Figures 3 1 - 3 4) show an upward progression of the collapse process occurring from about 1135 to 1140 s. Collapse motion of station 11 near the top of the emplacement pipe (figure 3 5) begins shortly before 1136 s, the time of the drop of the formation coupling plug (station 21 ) and a major second drop begins at about 1138 s, the time the intermediate plug (station 22) fell Since there seems to have been little change in displacement of the emplacement pipe at the time the ground surface fell (stations 23 and 61, around 1141 s) and only a small acceleration signal from the "slap-down" of station 23, the top plug may have moved around the emplacement pipe leaving it protruding above its initial position relative to the surface casing A visual comparison of the displacements in figures 3 5 and 3.3 suggests that the pipe relative protrusion is about 1 m.

#### 3.2 Radiation and Pressure

Pressure and radiation histories recorded during the collapse activity are shown in figures 3 6 - 3 13 All stations except 32 (which was lost before collapse) show a drop in pressure characteristic of a stemming fall at collapse Progression of the collapse is indicated by the composite plot of pressure histories of figure 3 14 Also included are the displacement histories of the stemming plugs and the ground surface during the collapse epoch

The D-cable (station 93) indicated an immediate change of character (within the first two seconds after detonation) at a depth corresponding to just below of the intermediate rigid plug. The cable TDR signal remained constant until about 1131 s and then indicated a character change to a depth corresponding to near the bottom of the surface casing at about 1138 s. This history is also shown in figure 3.14.

A change in radiation corresponding in time to the decrease in pressure is seen at stations 33, 34, 38, 39, and 40 (figures 3.6, 3.7, 3.11, 3.12 and 3.13). The reduction in the dose rate at stations 33 and 34 may be explainable as due to an increase in the shielding afforded by the falling stemming. All stations above the intermediate plug survived until recording was terminated and the pressure and radiation histories from these three stations for almost 6000 s following collapse are shown in figures 3.15 - 3.17. A slight change (decrease) in radiation level corresponding to the change in pressure from collapse was seen at all three stations. A slight, brief increase in the radiation level, prior to the permanent decrease, was seen at station 40 (figure 3.13). Since the final permanent level for all three stations is less than the original source chip level, this may have been caused by a slight movement of the source chip with respect to the detector occasioned by the collapse.

CLIPER information is not available

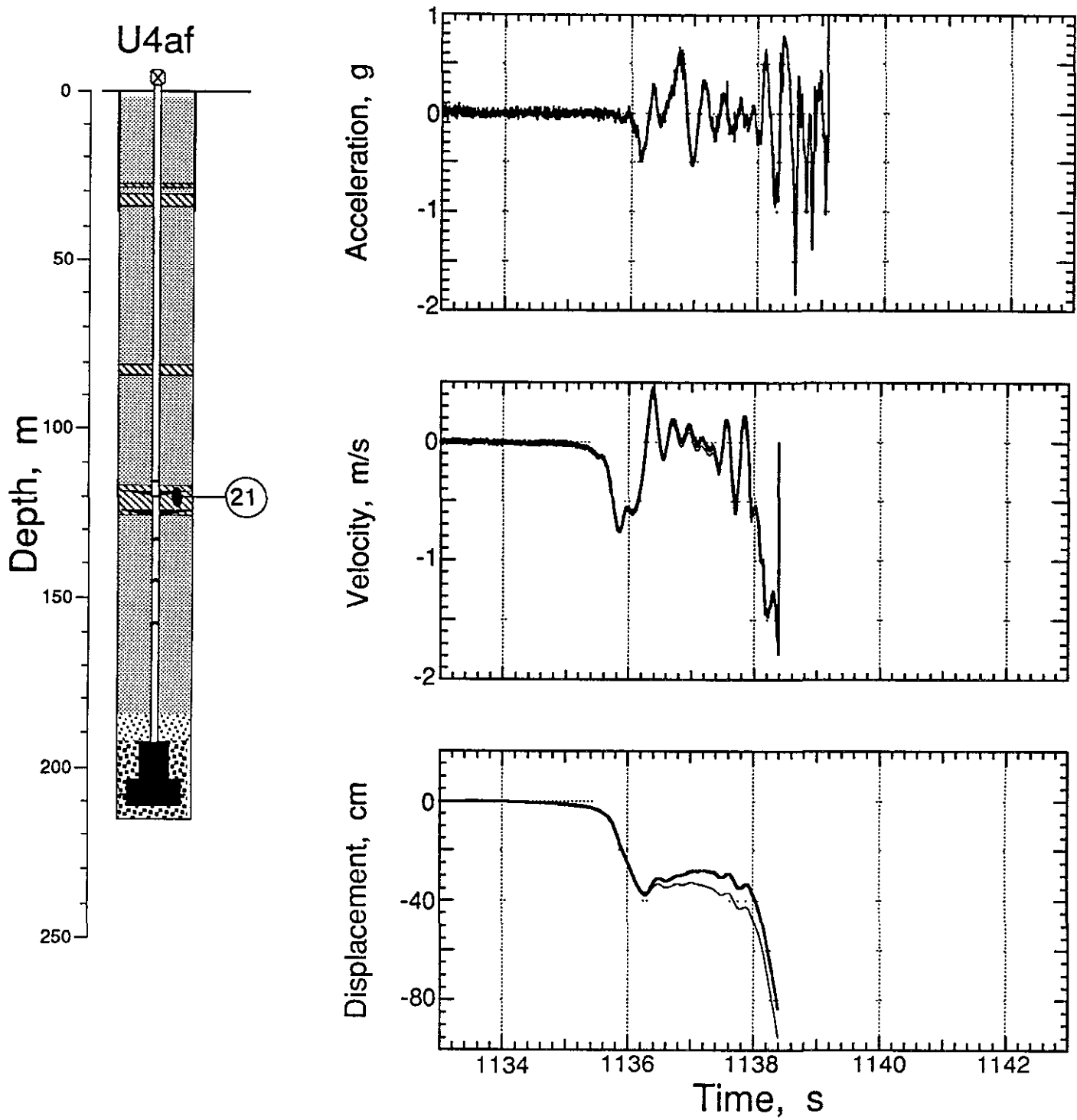


Figure 3 1 Collapse-induced vertical motion of the bottom rigid plug (station 21, at a depth of 120.5 m) When there is more than one trace in a plot, the lighter is derived from the accelerometer.

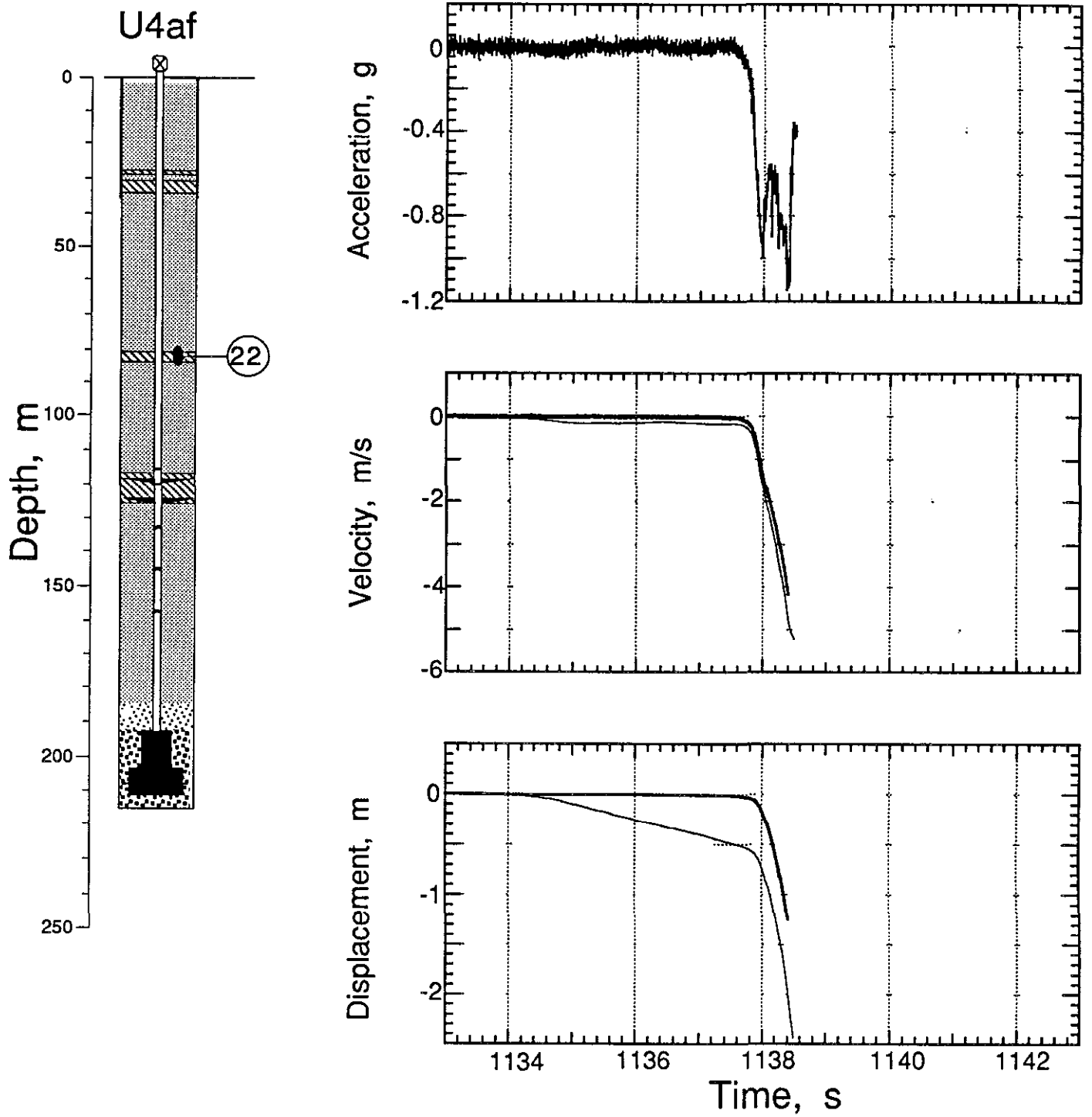


Figure 3 2 Collapse-induced vertical motion of the top rigid plug (station 22, at a depth of 82.3 m). When there is more than one trace in a plot, the lighter is derived from the accelerometer.

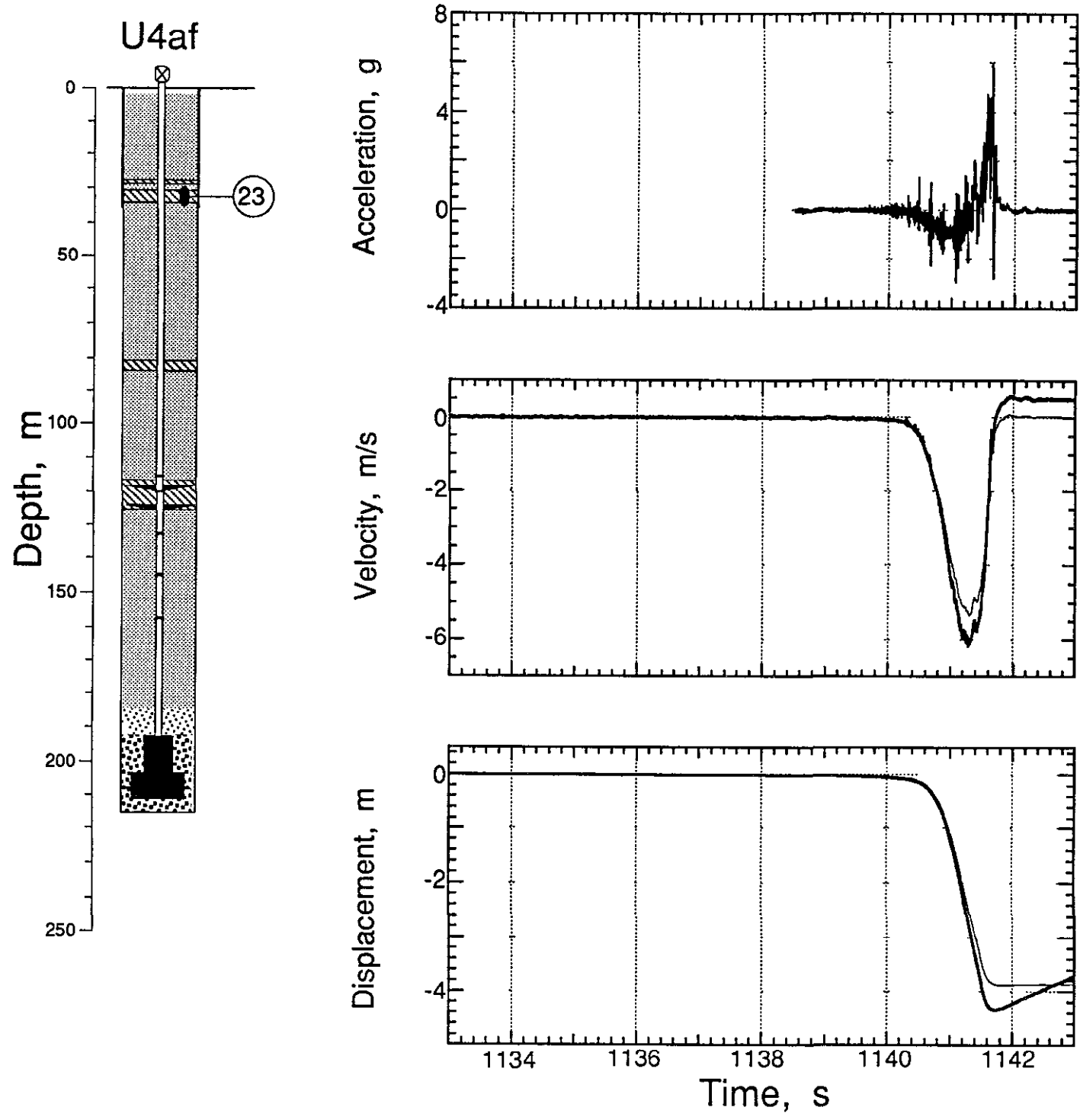


Figure 3.3 Collapse-induced vertical motion of the top plug (station 23, at a depth of 32.3 m)  
 When there is more than one trace in a plot, the lighter is derived from the accelerometer

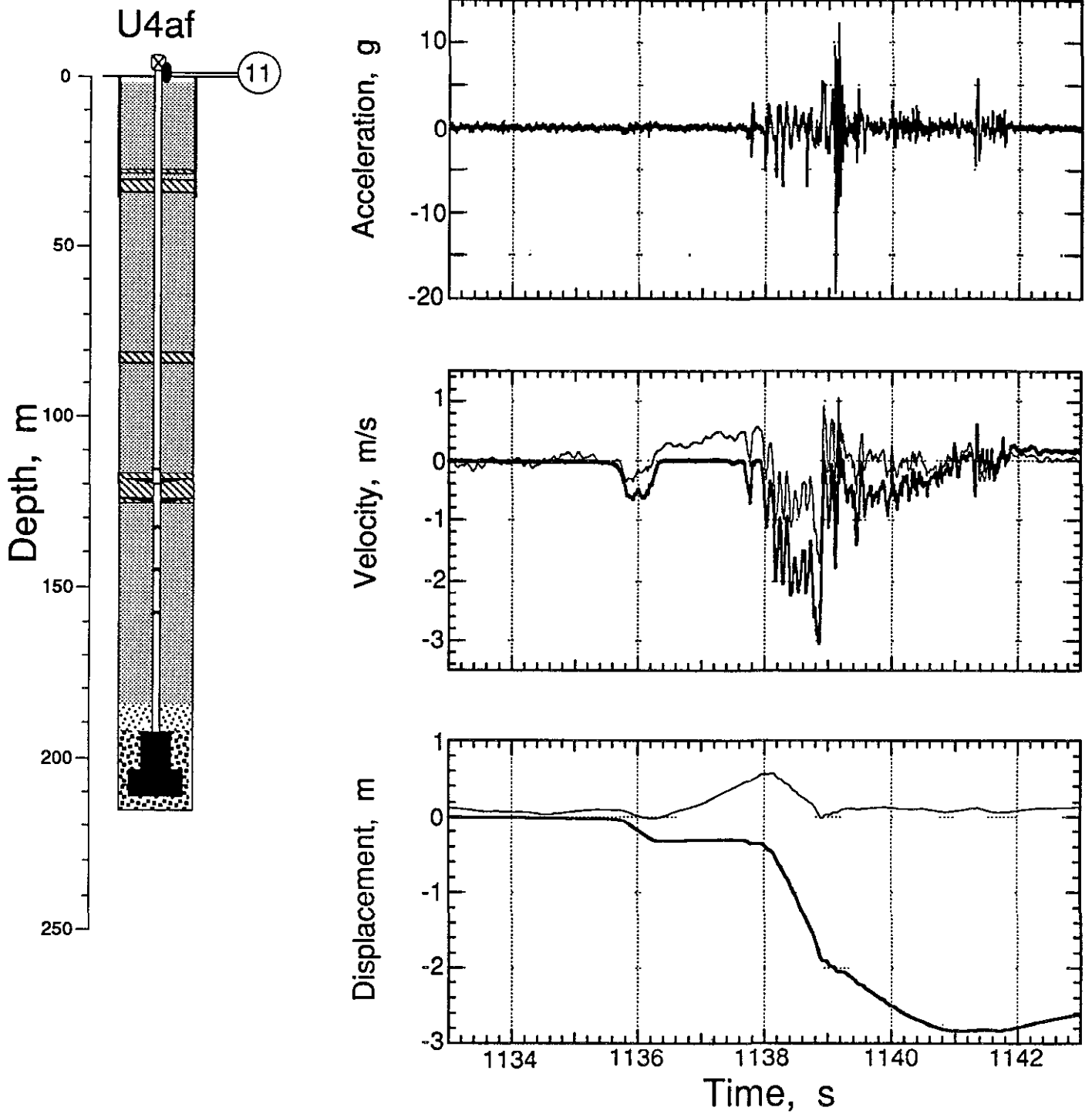


Figure 3 4 Collapse-induced vertical motion of the emplacement pipe (station 11, on the pipe 1 9 m above ground level but below the ball valve). When there is more than one trace in a plot, the lighter is derived from the accelerometer

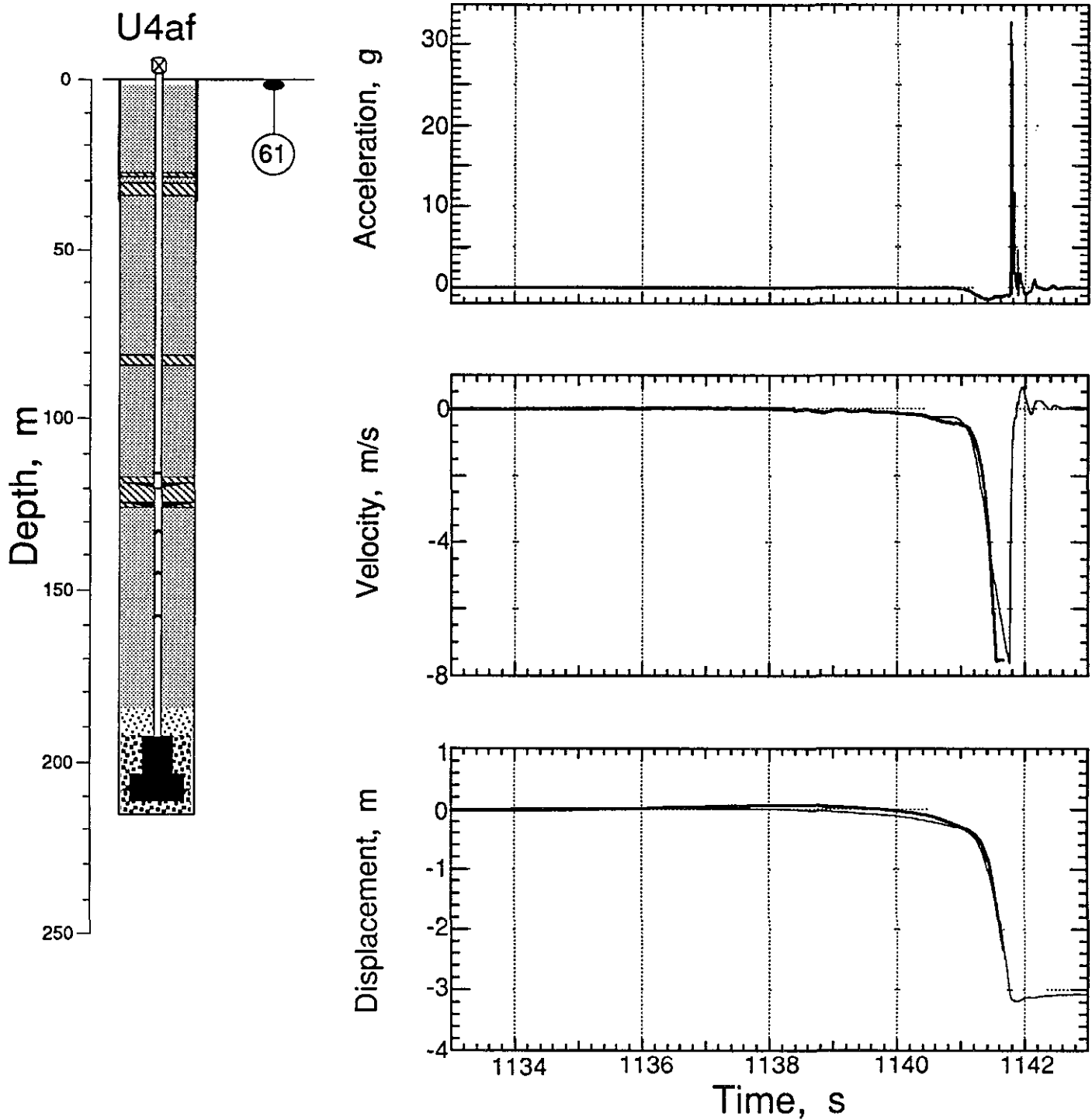


Figure 3.5 Collapse-induced vertical motion of the ground surface at a depth of 0.9 m and horizontal range of 15.24 m (station 61). When there is more than one trace in a plot, the lighter is derived from the accelerometer.

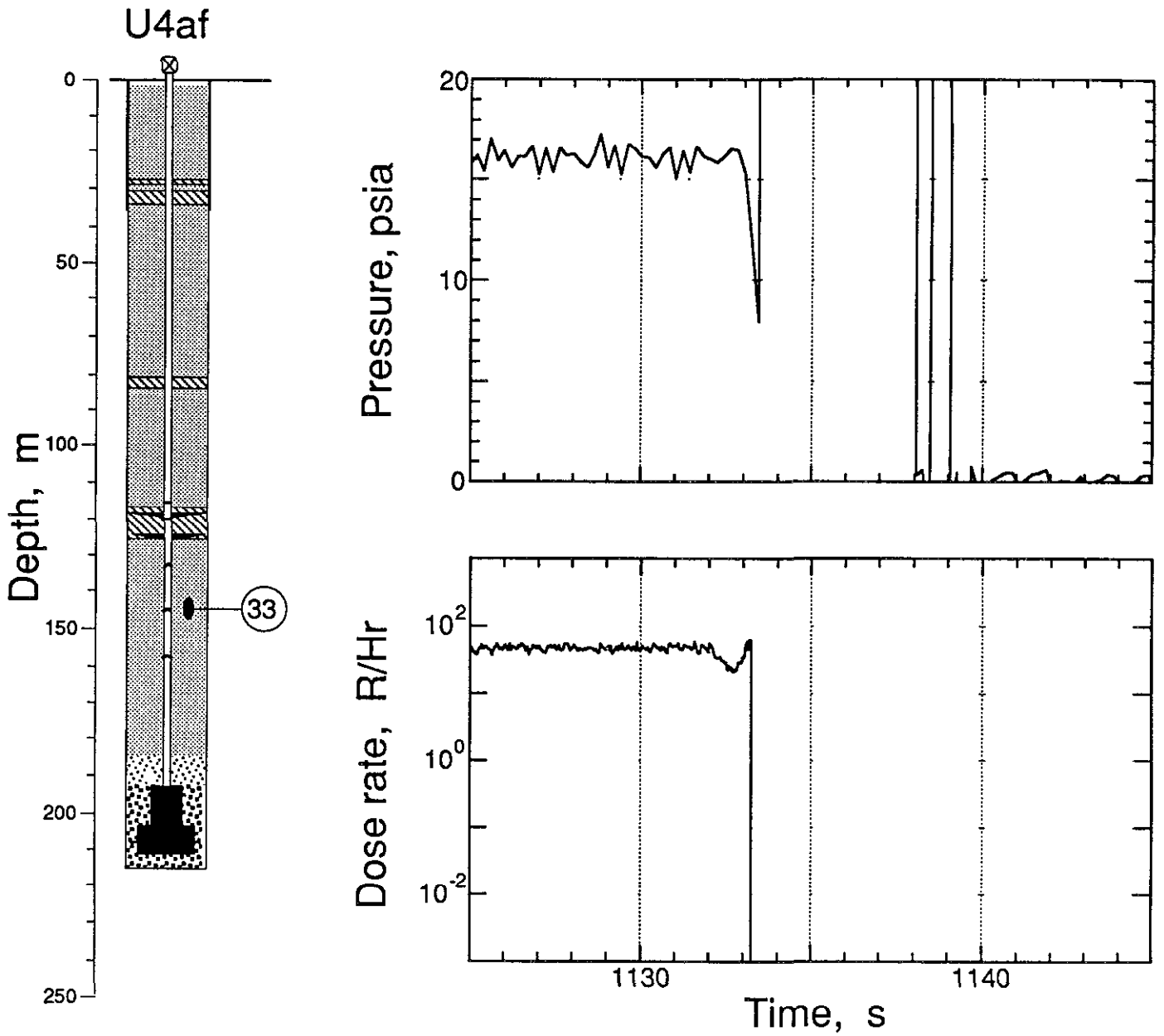


Figure 3.6 Collapse epoch pressure and radiation measured in the stemming at an elevation slightly above the second pressure dome (station 33 at 144.8 m depth)

U4af

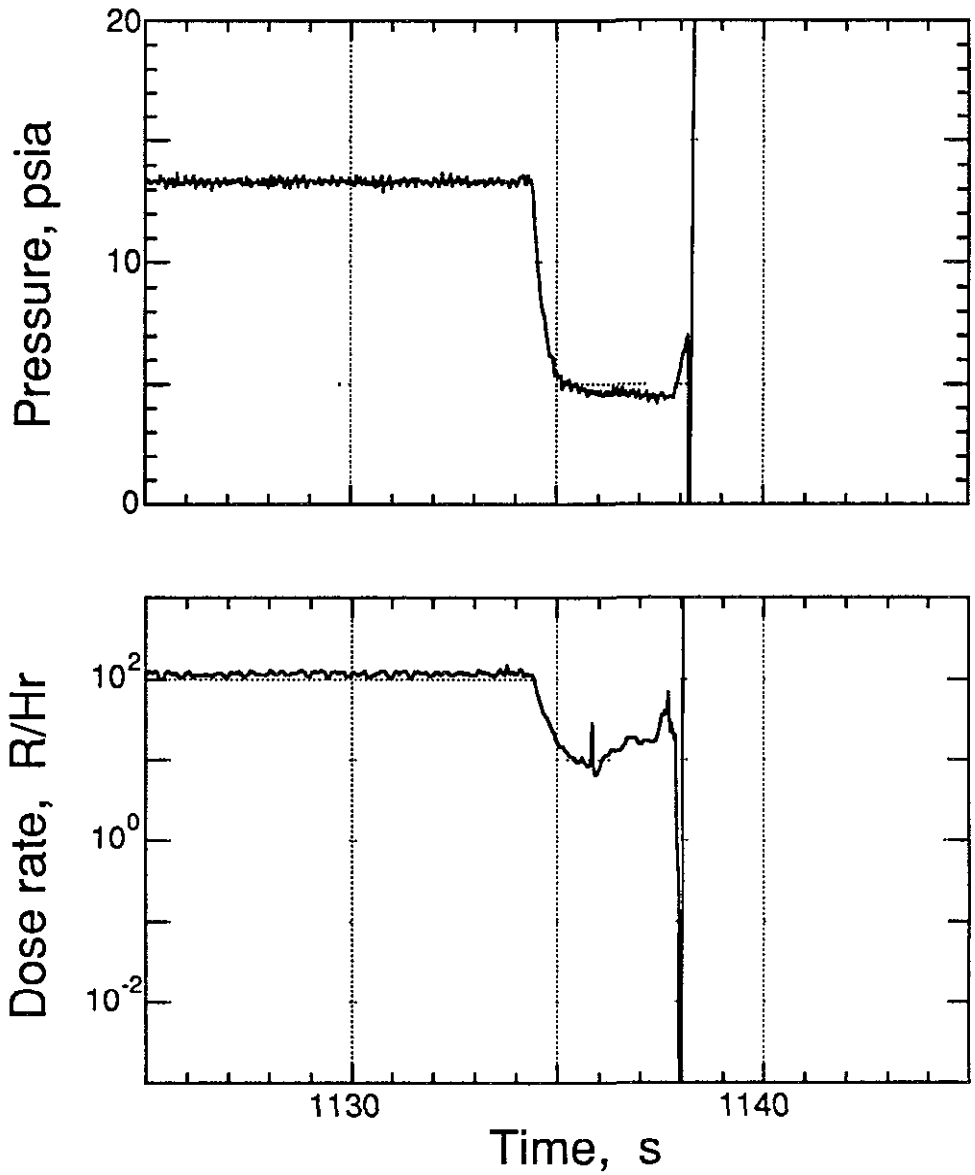
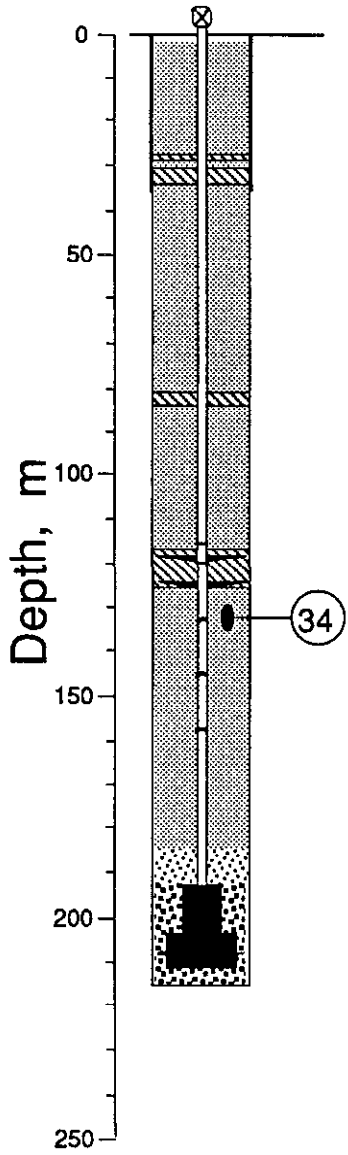


Figure 3 7 Collapse epoch pressure and radiation measured in the stemming at an elevation slightly above the third pressure dome (station 34 at 132.3 m depth)

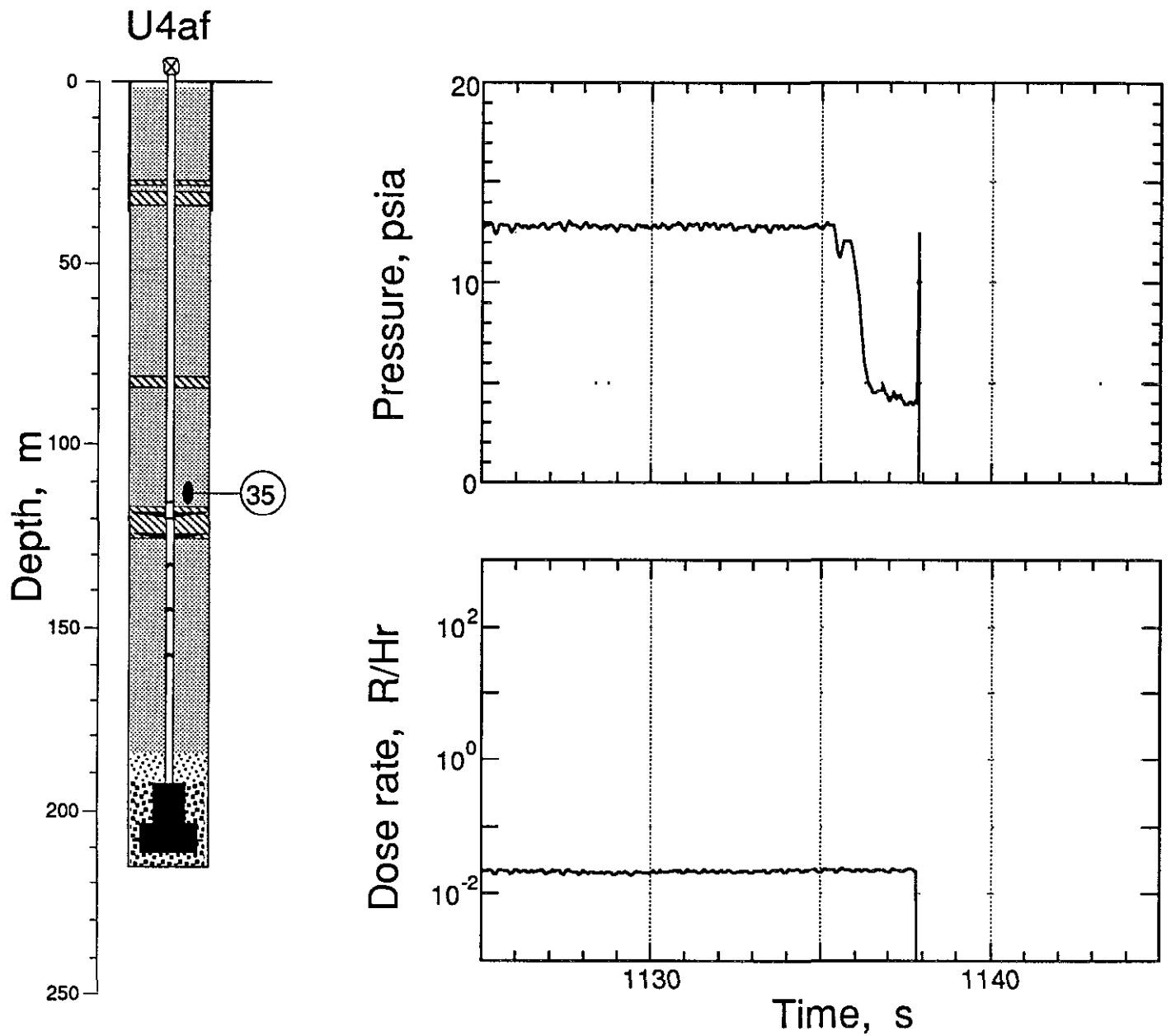


Figure 3.8 Collapse epoch pressure and radiation measured in the stemming above the formation coupling plug and the elevation of the detector plate (station 35 at 112.8 m depth)

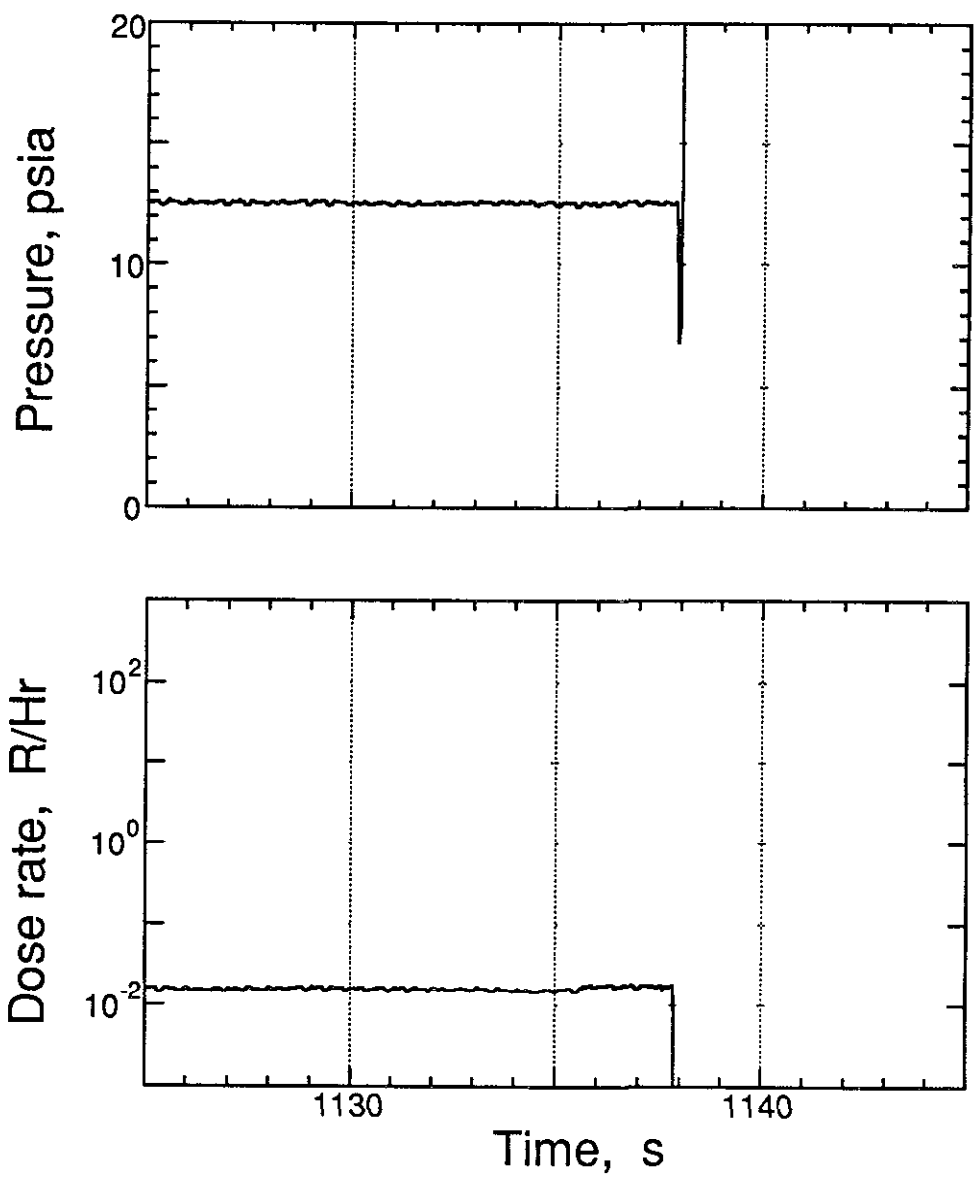
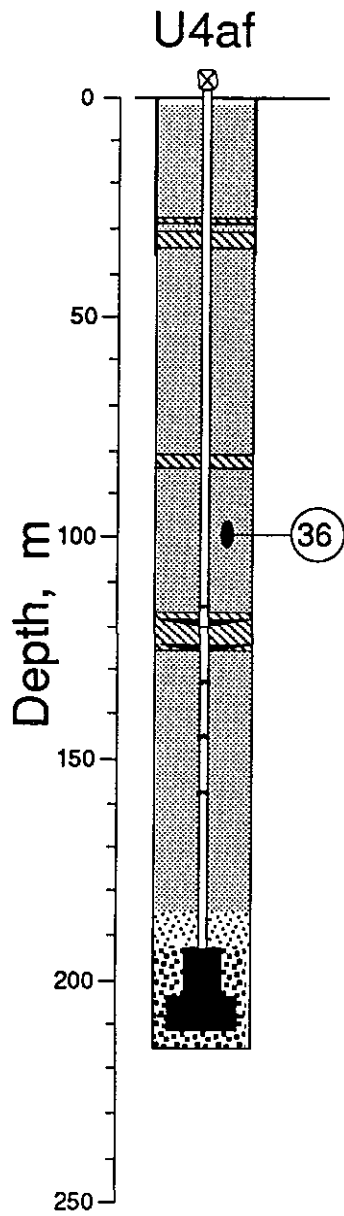


Figure 3 9 Collapse epoch pressure and radiation measured in the stemming midway between the formation coupling plug and the intermediate plug (station 36 at 99.1 m depth)

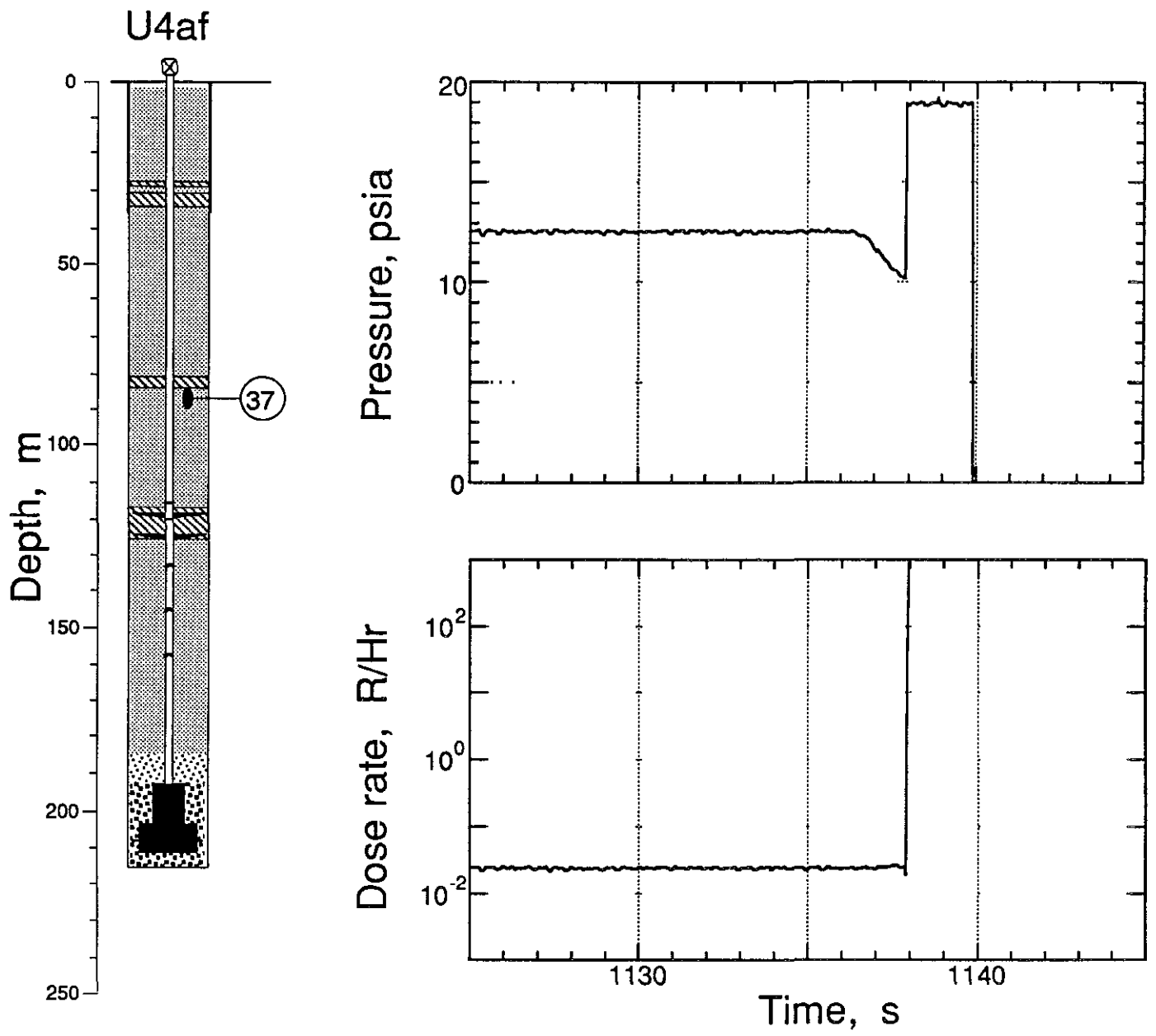


Figure 3 10 Collapse epoch pressure and radiation measured in the stemming beneath the intermediate plug (station 37 at 86 9 m depth)

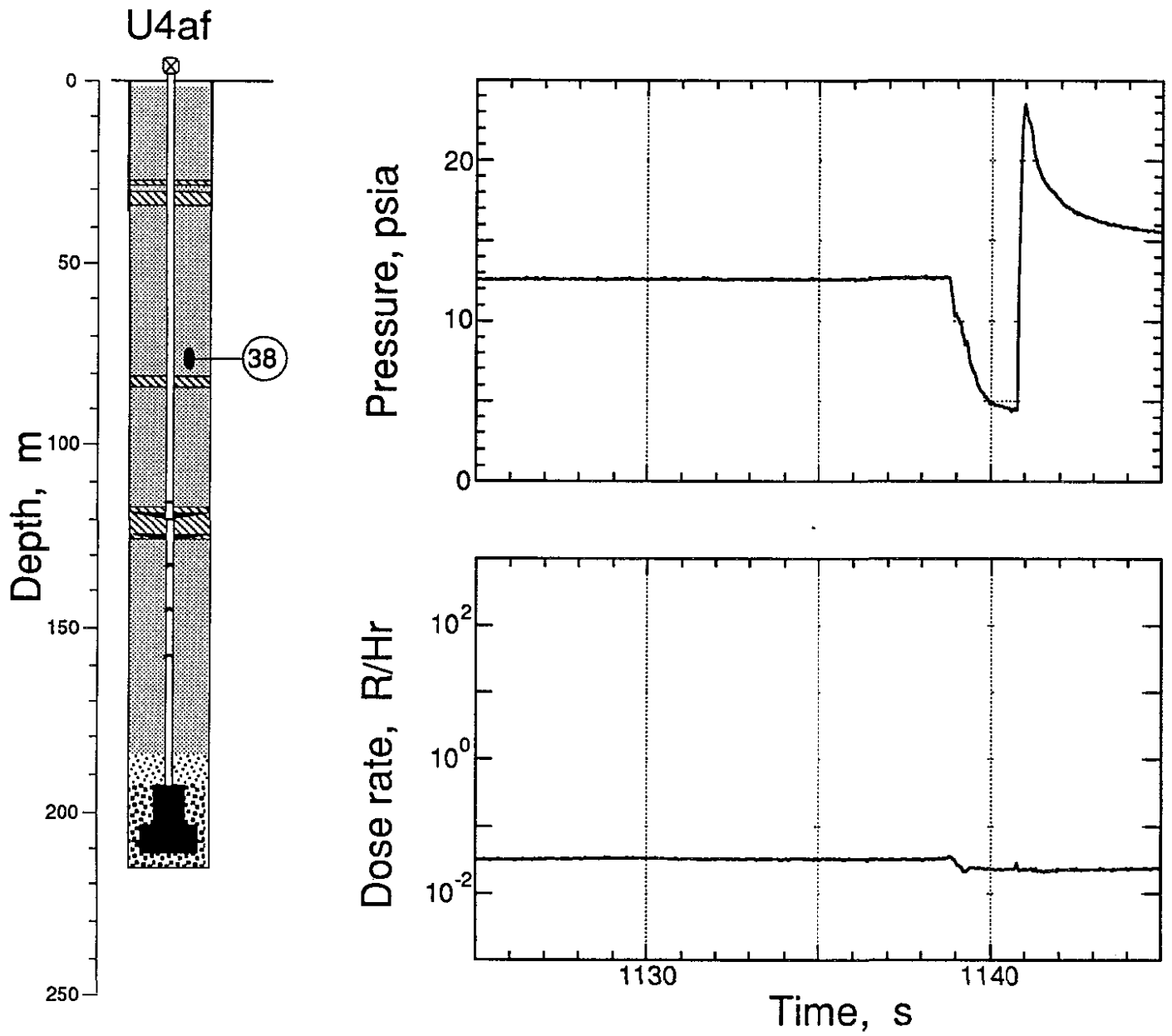


Figure 3 11 Collapse epoch pressure and radiation measured in the stemming above the intermediate plug (station 38 at 76.2 m depth)

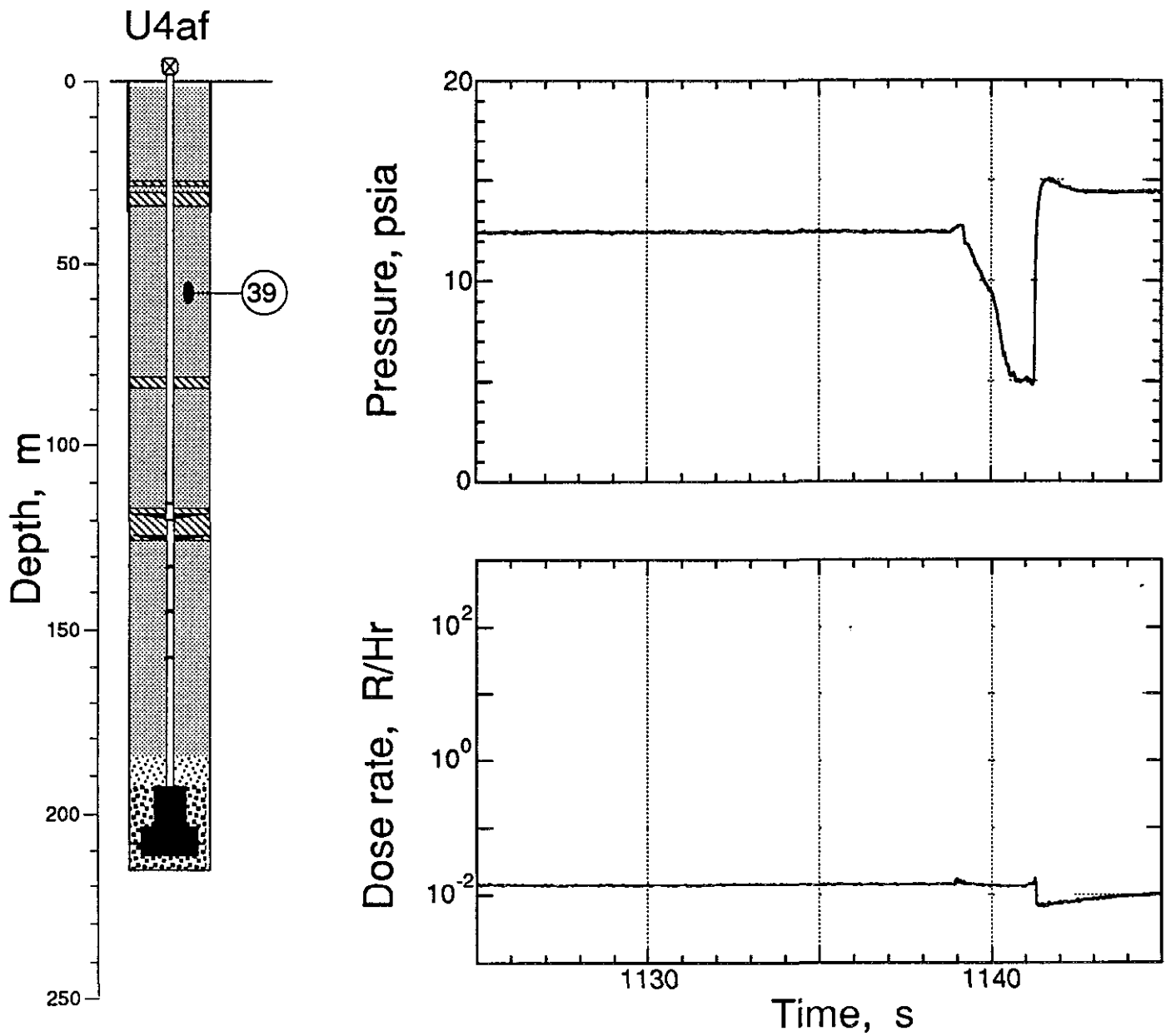


Figure 3.12 Collapse epoch pressure and radiation measured in the stemming midway between the intermediate and top plugs (station 39 at 57.9 m depth)

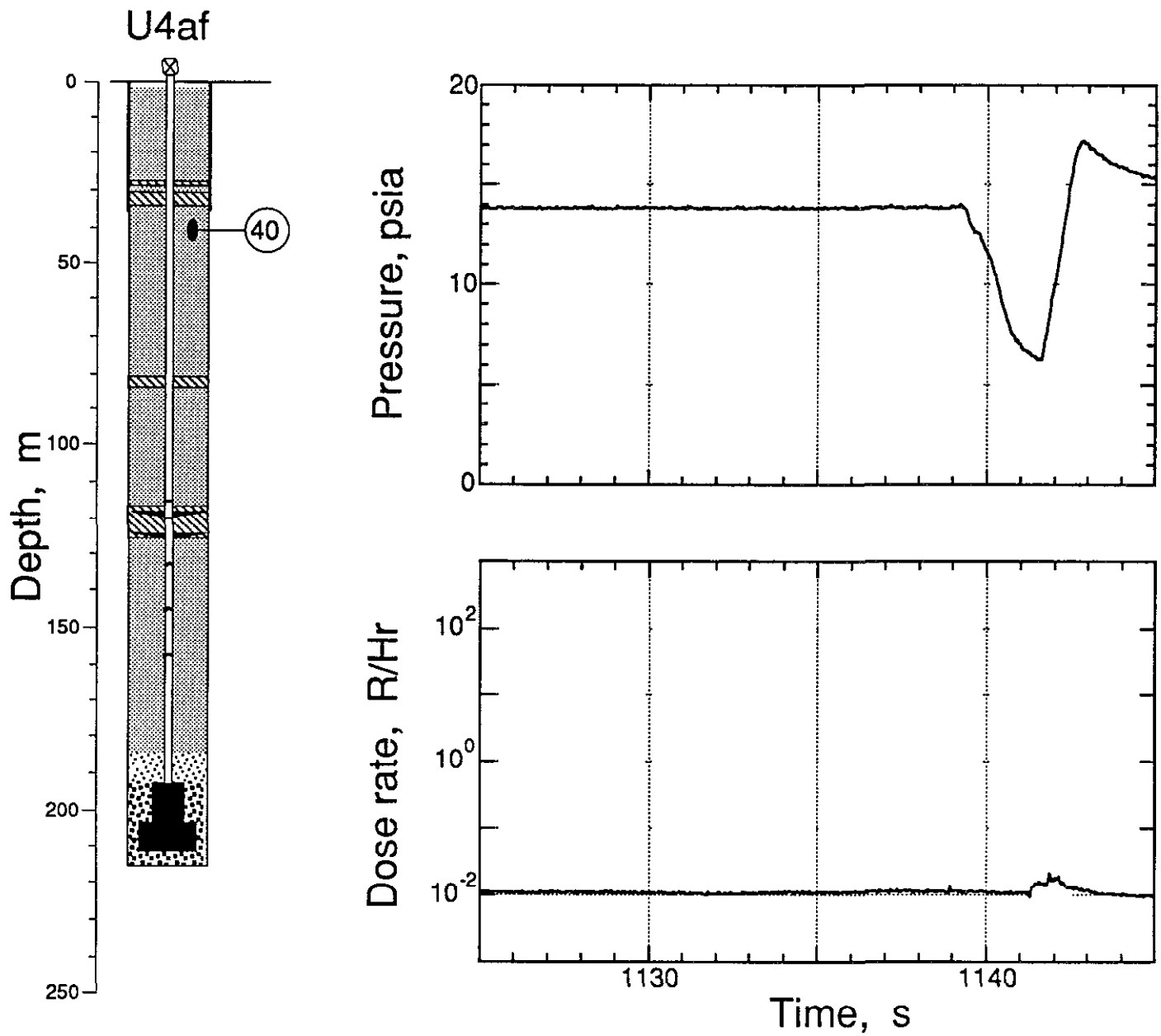


Figure 3 13 Collapse epoch pressure and radiation measured in the stemming beneath the top plug (station 40 at 41.1 m depth)

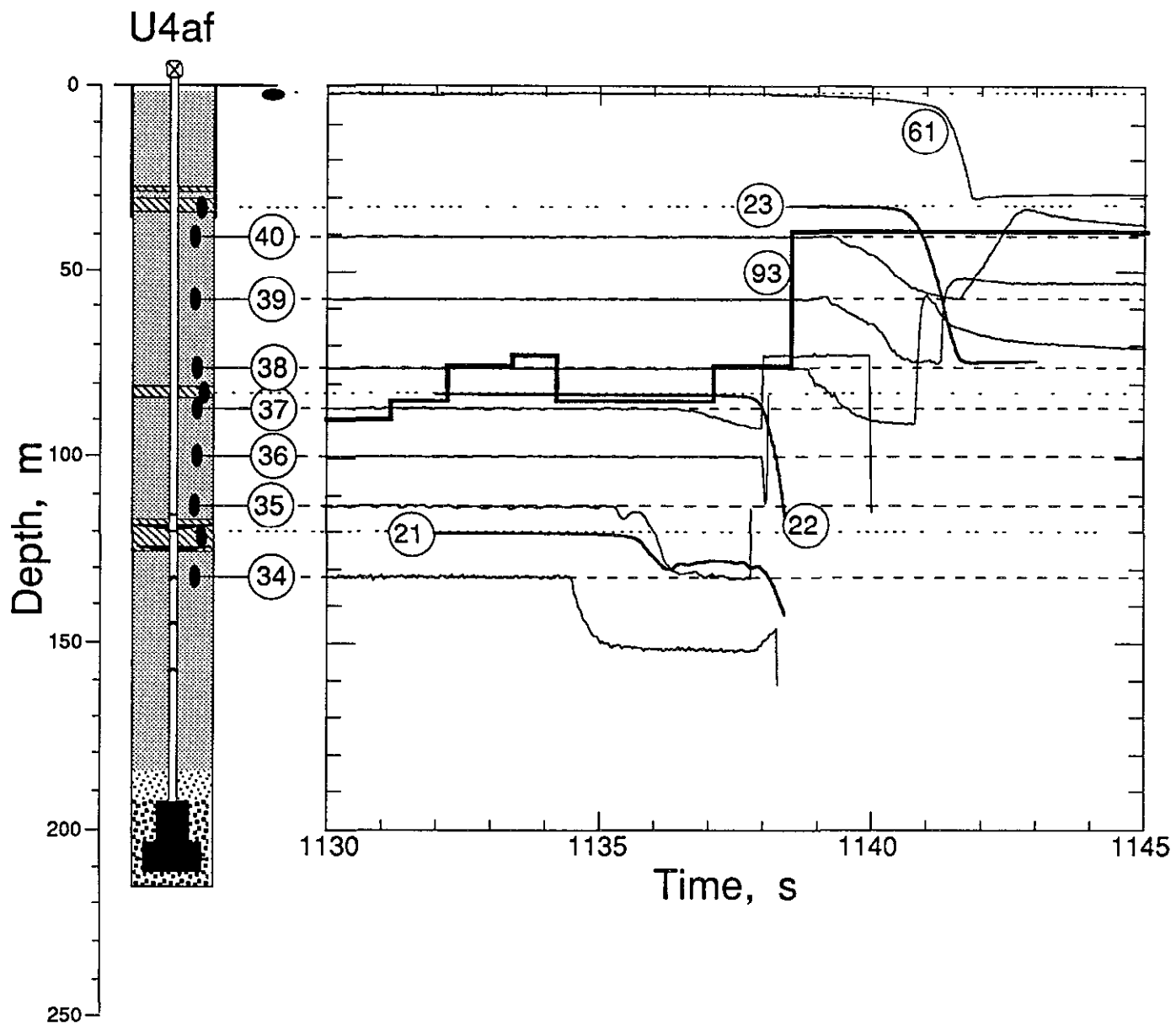


Figure 3 14 Progression of collapse is indicated by the displacement traces of stations 21, 22, 23, and 61. Also shown are the pressure histories of stations 34 - 40 during the collapse epoch. A best representative of the D-cable information is shown by the heavy trace of station 93.

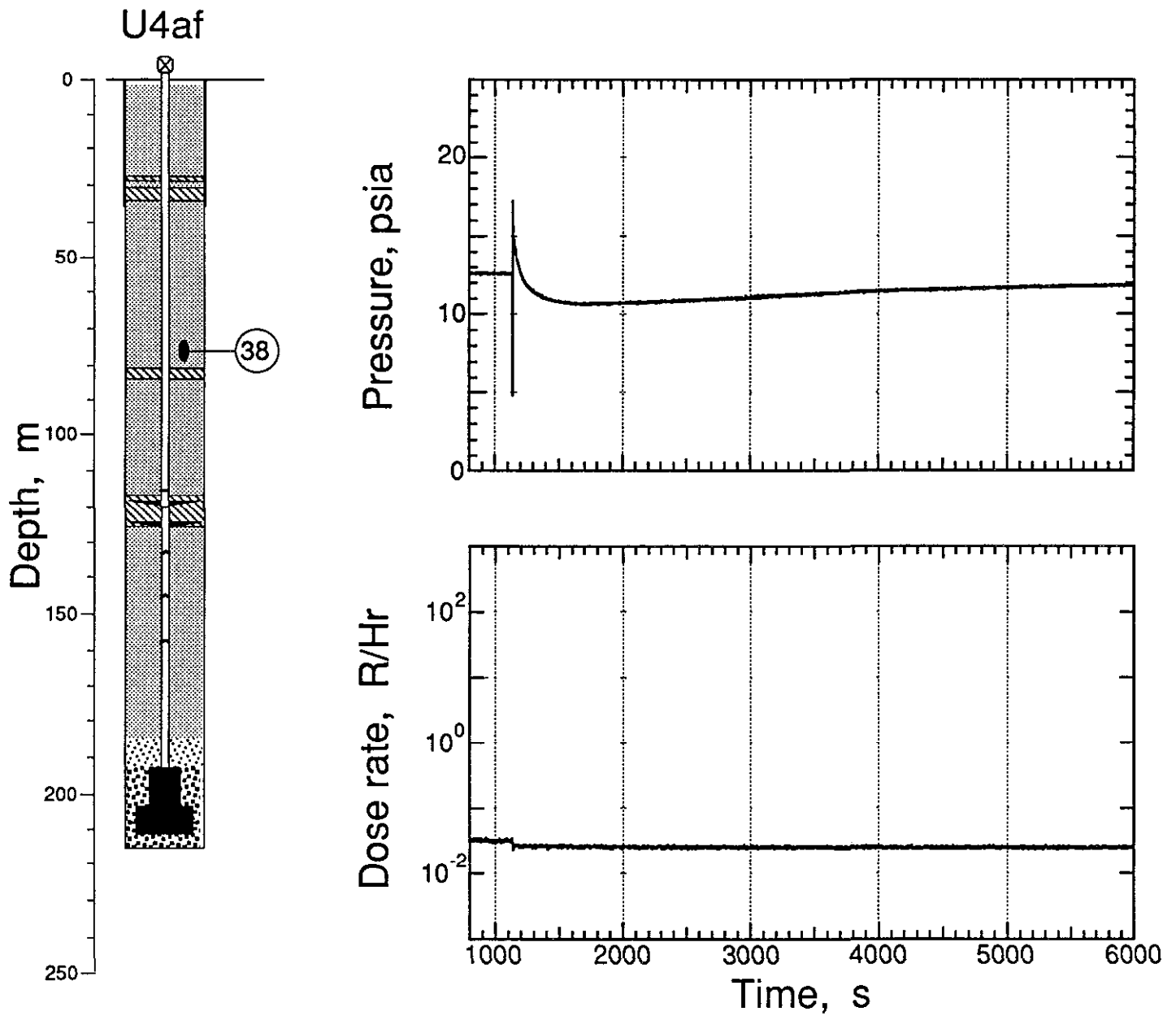


Figure 3 15 Long-time record including the collapse epoch of the pressure and radiation history in the stemming above the intermediate plug (station 38 at 76.2 m depth)

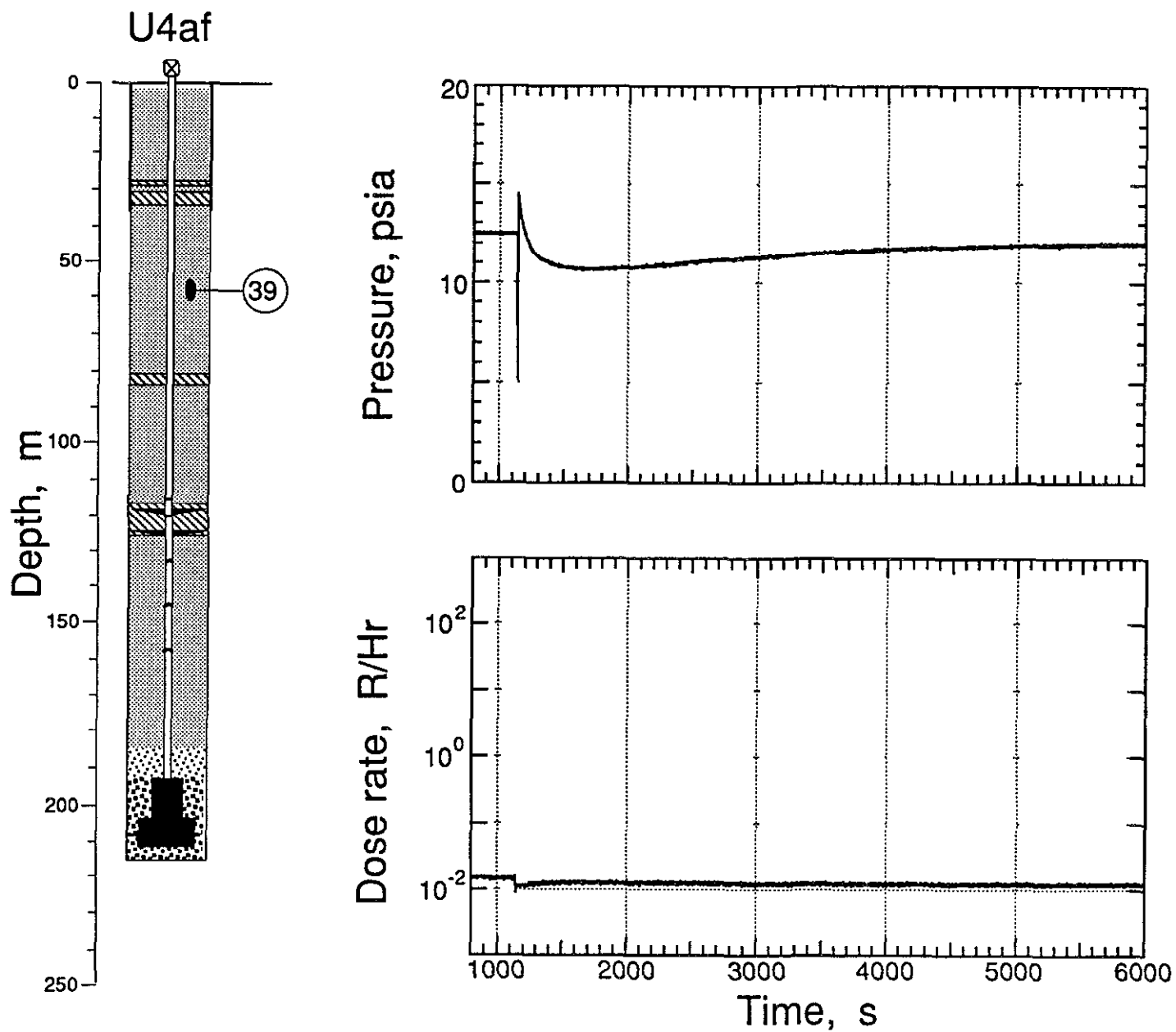


Figure 3 16 Long-time record including the collapse epoch of the pressure and radiation history in the stemming midway between the intermediate and top plugs (station 39 at 57.9 m depth)

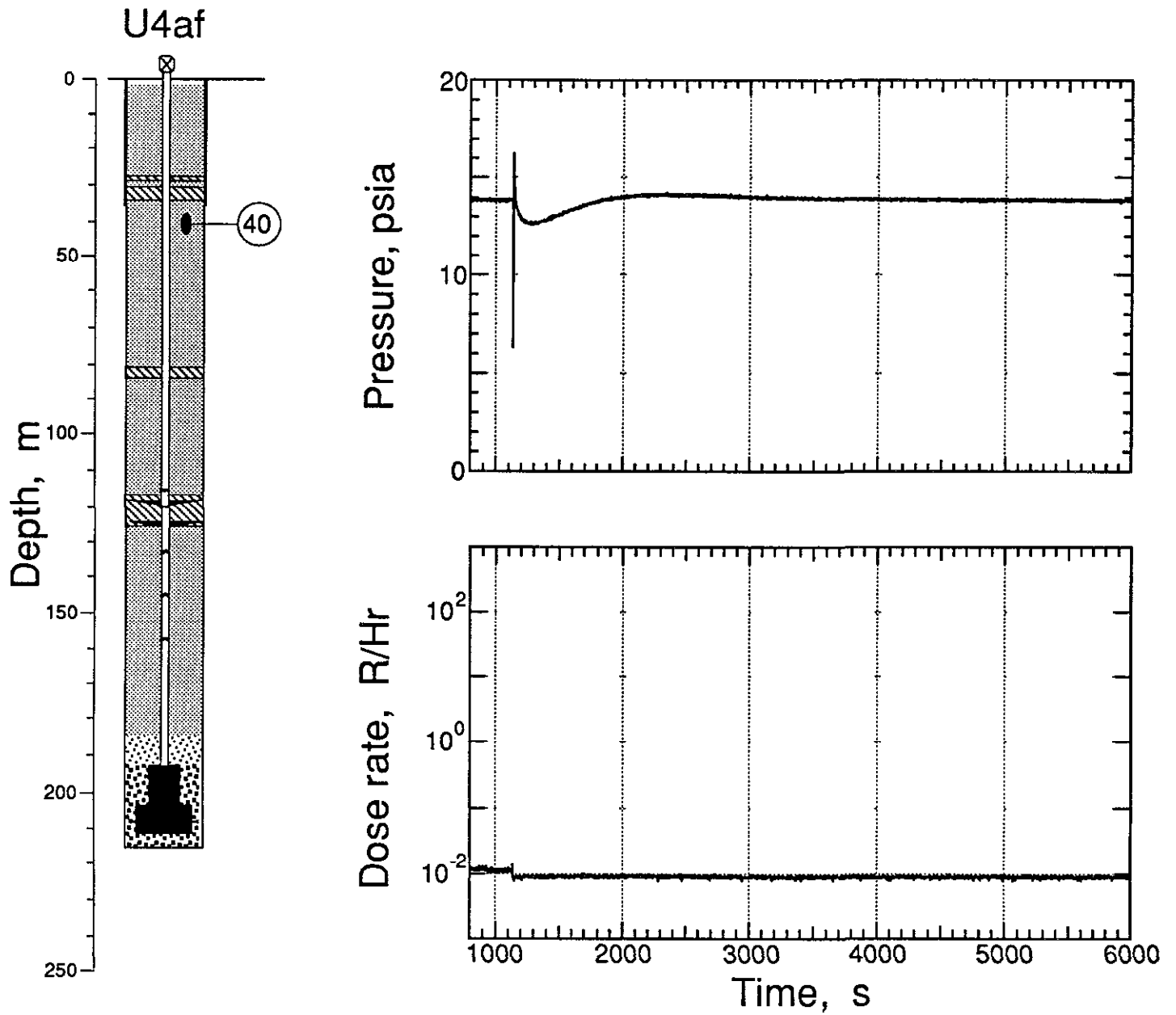


Figure 3 17 Long-time record including the collapse epoch of the pressure and radiation history in the stemming beneath the top plug (station 40 at 41.1 m depth)

## 4 Measurements on the Emplacement Pipe

### 4.1 Explosion-Induced Motion

Vertical motion of the emplacement pipe was monitored at six elevations on the emplacement pipe. Stations were fielded 2.4 m below the location of the pinhole (station 2) and at each of the three pressure domes (stations 3, 5, and 7). The detector plate (station 9) just above the formation coupling plug and the top section of the pipe near the ball valve (station 11) were also instrumented for vertical motion. Histories obtained at these locations are shown in figures 4.1-4.6. Peak motion values and transducer characteristics are given in tables 3.1-3.3.

Just below the pin hole (station 2, figure 4.1) and 2.7 m higher at the pressure dome (station 3, figure 4.2), all signals were lost at about 100 ms. At station 5, at the second pressure dome (figure 4.3), the signal from the accelerometer was lost at about 138 ms and from the velocimeter at about 127 ms. All other station signals survived until collapse (figures 4.4 - 4.6).

To insure that the line-of-sight for the neutron PINEX experiment remained open during emplacement, the pipe was supported from the top by break-away beams. The motion of the top of the pipe (station 11, figure 4.6) included "noise" contributions from the break-away beams between 200 and 300 ms and around 450 ms. Note that station 23, in the top plug (figure 2.20) shows little or no permanent displacement.

Motion of station 9, on the pipe at the elevation of the detector plate closely matches the motion of station 21, in the plug, as shown in the upper plot of figure 4.7 wherein the two displacement histories are overlain for the first 1.5 s. This indicates that the drag rings force the motion of the upper portion of the pipe to be nearly the same as that of the formation coupling plug. Also included in the upper plot of figure 4.7 is the displacement history of the emplacement pipe at station 7, 17.7 m below station 9 and 4.3 m below the formation coupling plug. The average strain history of the pipe between stations 7 and 9 (the difference in the displacement histories of stations 9 and 7 divided by their separation) is shown in the lower plot of figure 4.7.

## 4.2 Collapse-Induced Motion

Collapse-induced motion of the emplacement pipe is shown in figures 4.8 - 4.10. For completeness, the motion at station 11 is shown in figure 4.10 as well as figure 3.4. A composite plot of all of the displacement histories obtained from the emplacement pipe during the collapse along with the same data obtained from the formation coupling plug and the intermediate stemming plug is displayed in figure 4.11. Collapse reached the formation coupling plug at 1136 s at which time the plug and the emplacement pipe fall as a unit by about 0.3 m. There is no indication of motion at the higher plug stations until 1138 s when the intermediate plug begins to fall, taking the emplacement pipe with it. Shortly after 1140 s the top plug began to move, as seen in figure 3.3, but registered only a slight slap-down signal on the accelerometer of station 11 (figure 4.3) at about 1141.4 s. This suggests that the hydroseal applied to the pipe in the region of the top plug allowed the plug to move easily on the pipe.

## 4.3 Pressure, Temperature, and Radiation

Four sections of the emplacement pipe were sealed either by pressure domes or a pressure plate intended to retard and retain the gas pressure generated by the device. About 5 m above the pressure plate was a recoverable neutron detector which was drawn up through the pipe beyond the ball valve which was then closed shortly after the shot. Each of the four deepest sealed sections was internally monitored for pressure and temperature and the resulting data are shown in figures 4.12-4.16.

Station 2 (figure 4.12), below the pin hole, detected gas flow in the pipe. An initial pressure peak of 20 bar occurred at 1 s with an ultimate peak of about 120 bar at about 80 s. A temperature rise of 100 °C at around 120 ms was observed to begin at about 30 ms and a second arrival of temperature beginning at about 30 s rose to a stable level of about 185 °C at around 150 s.

The second sealed section of the emplacement pipe was monitored at station 4, 3.3 m below the second pressure dome (station 4, figure 4.13). The short-time inserts suggest that both temperature and pressure were unchanged until about 130 ms at which time both took an abrupt jump, the pressure to about 100 bar and the temperature to a saturation value of around 1300 °C. This behavior and that at later time suggest that both channels may have been damaged at 130 ms, the approximate time that motion station 5, on the second pressure dome was lost (figure 4.3). Since the driving pressure and temperature below the first pressure dome were both less than the levels in the inserts of figure 4.13 it is unlikely the data of station 4 are valid.

No significant temperature change was noted in the region between the second and third pressure domes (figure 4.14, station 6) although a slight pressure change was detected at early times (before 3 s). This reading was probably generated in the transducer, as suggested by the record at later times.

No significant temperature or pressure change was observed in the pipe section topped by the pressure plate (station 8, figure 4.15). It may be concluded that the cavity gasses were held below the pressure plate and possibly the third pressure dome.

Figure 4.16 displays the internal pressure and radiation measured in the recovery section of the emplacement pipe a depth of 18.6 m. No significant change in pressure or radiation was detected prior to collapse, when the station signals were lost.

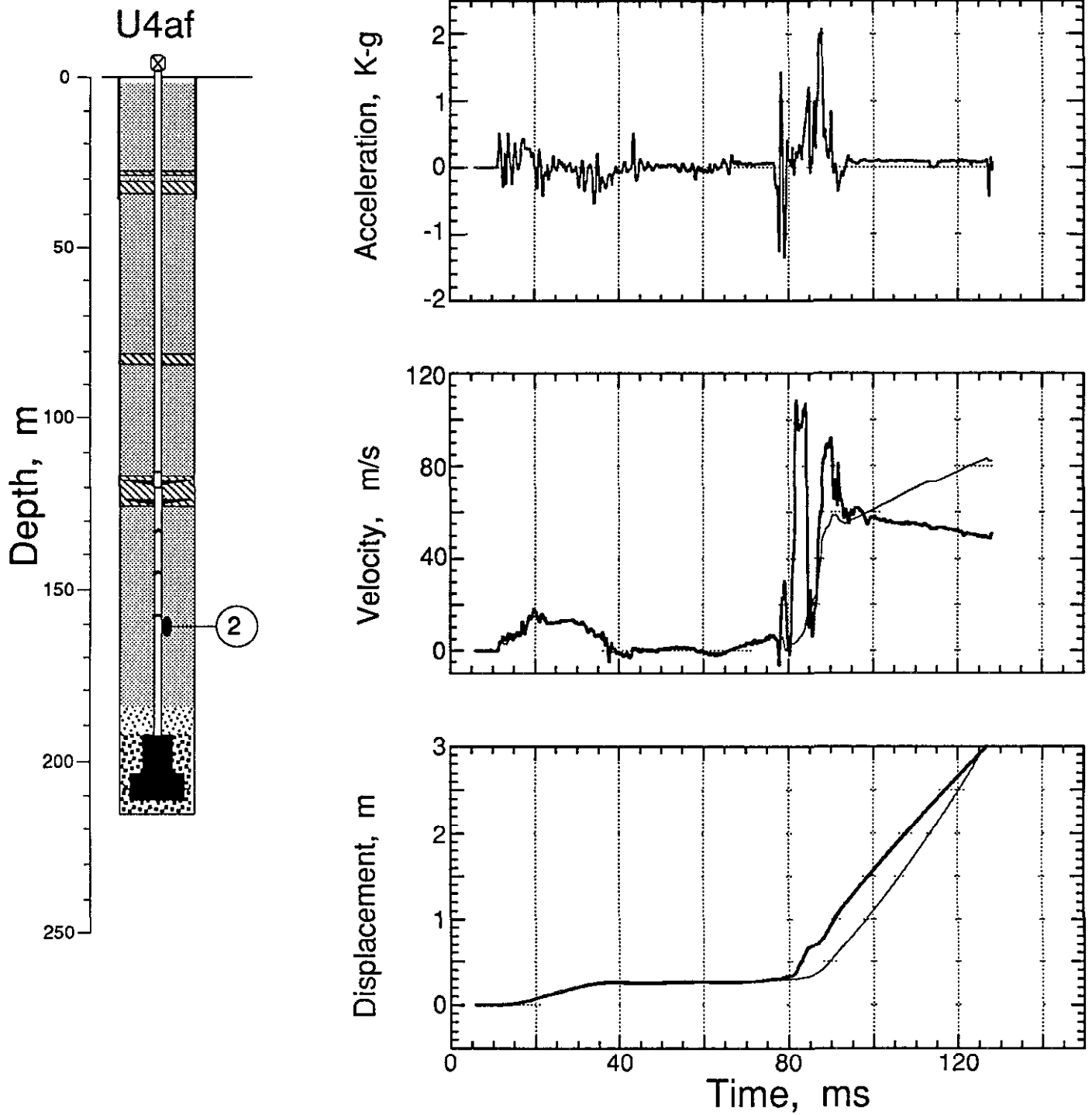


Figure 4.1 Explosion-induced vertical motion recorded on the emplacement pipe 2.4 m below the elevation of the pinhole (station 2 at a depth of 160.6 m). When there is more than one trace in a plot, the lighter is derived from the accelerometer.

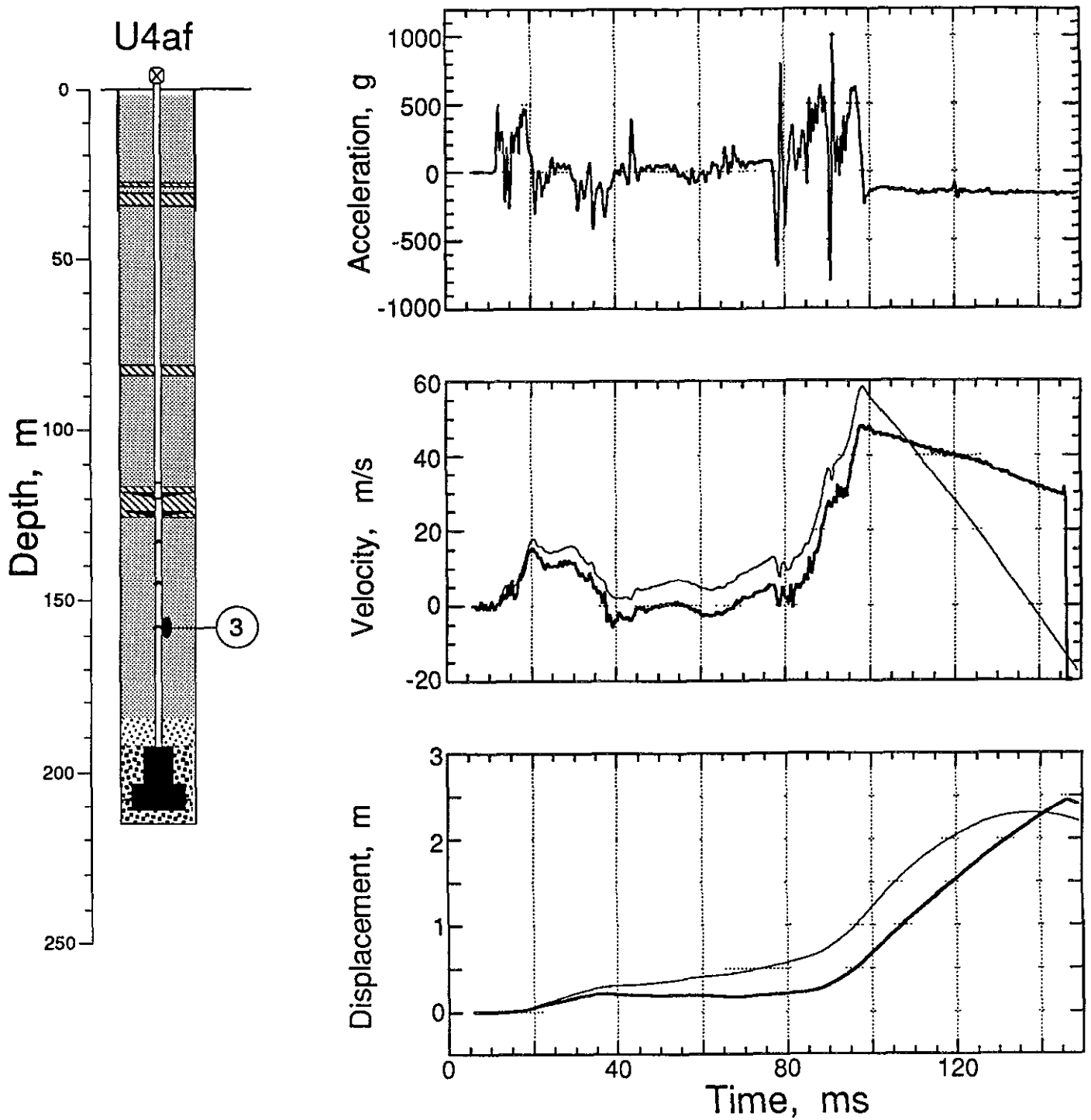


Figure 4.2 Explosion-induced vertical motion recorded on the emplacement pipe at the first pressure dome (station 3 at a depth of 157 m). When there is more than one trace in a plot, the lighter is derived from the accelerometer.

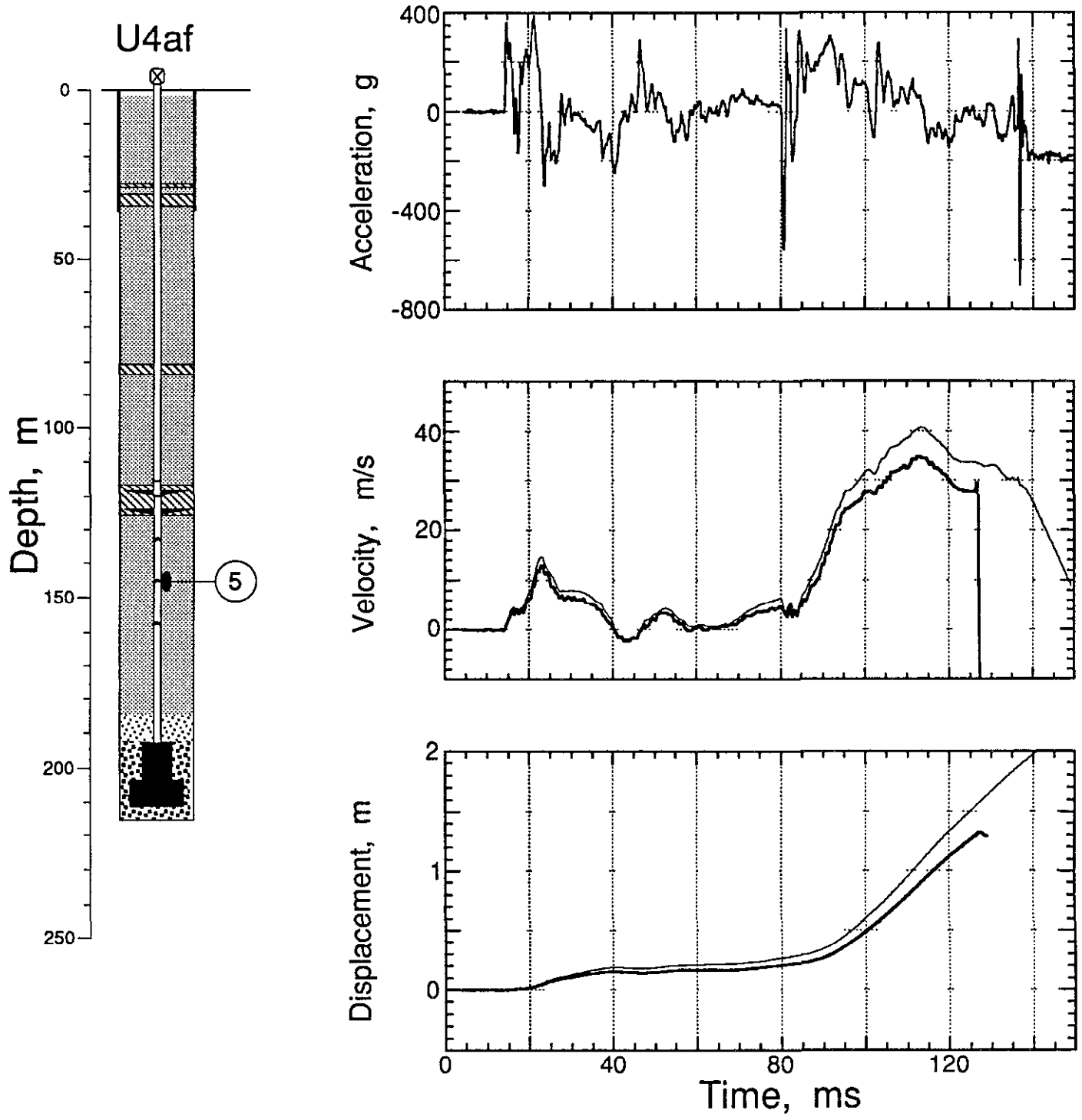


Figure 4.3 Explosion-induced vertical motion recorded on the emplacement pipe at the second pressure dome (station 5 at a depth of 145.4 m). When there is more than one trace in a plot, the lighter is derived from the accelerometer.

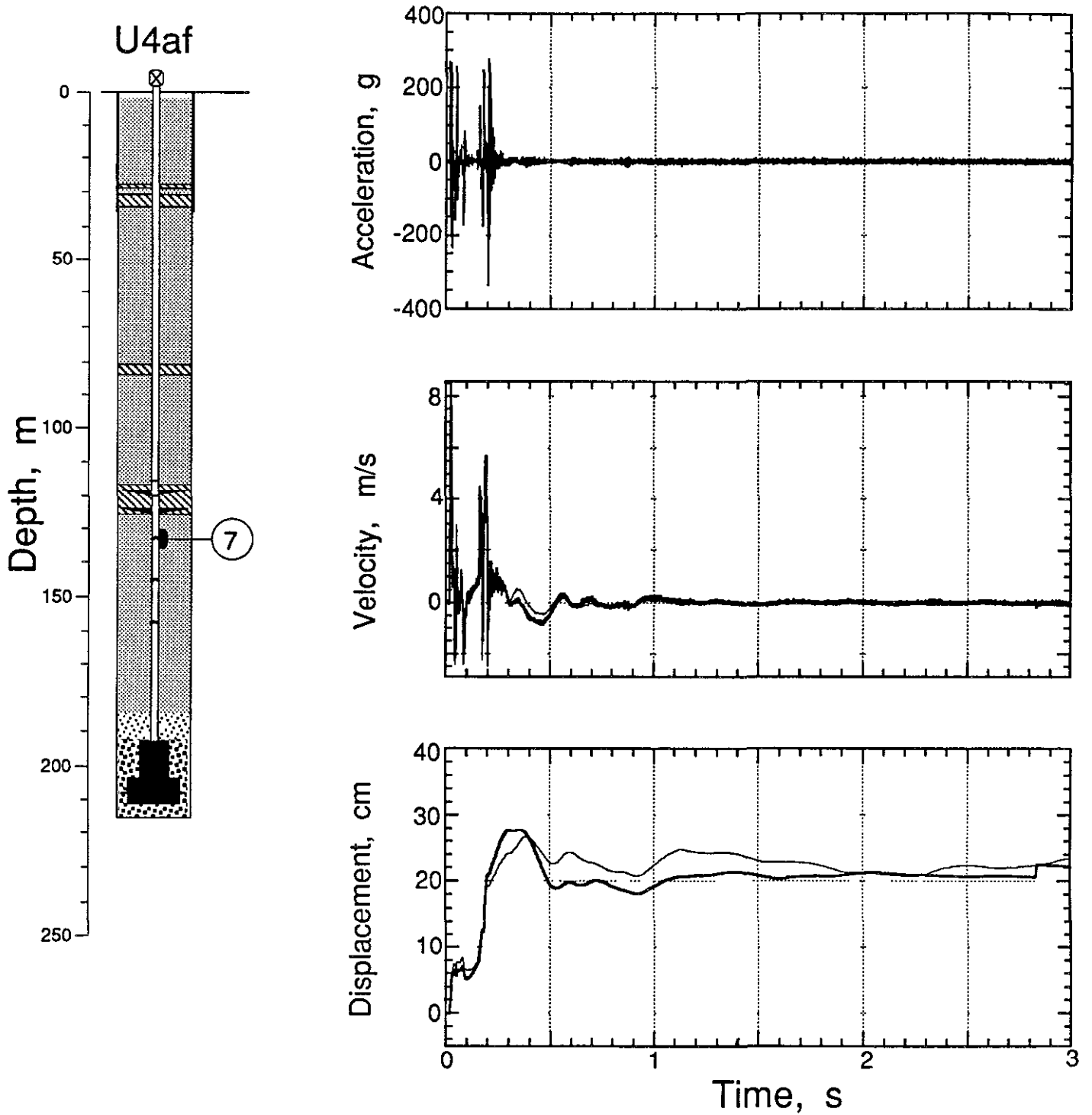


Figure 4.4 Explosion-induced vertical motion recorded on the emplacement pipe at the third pressure dome (station 7 at a depth of 132.9 m). When there is more than one trace in a plot, the lighter is derived from the accelerometer.

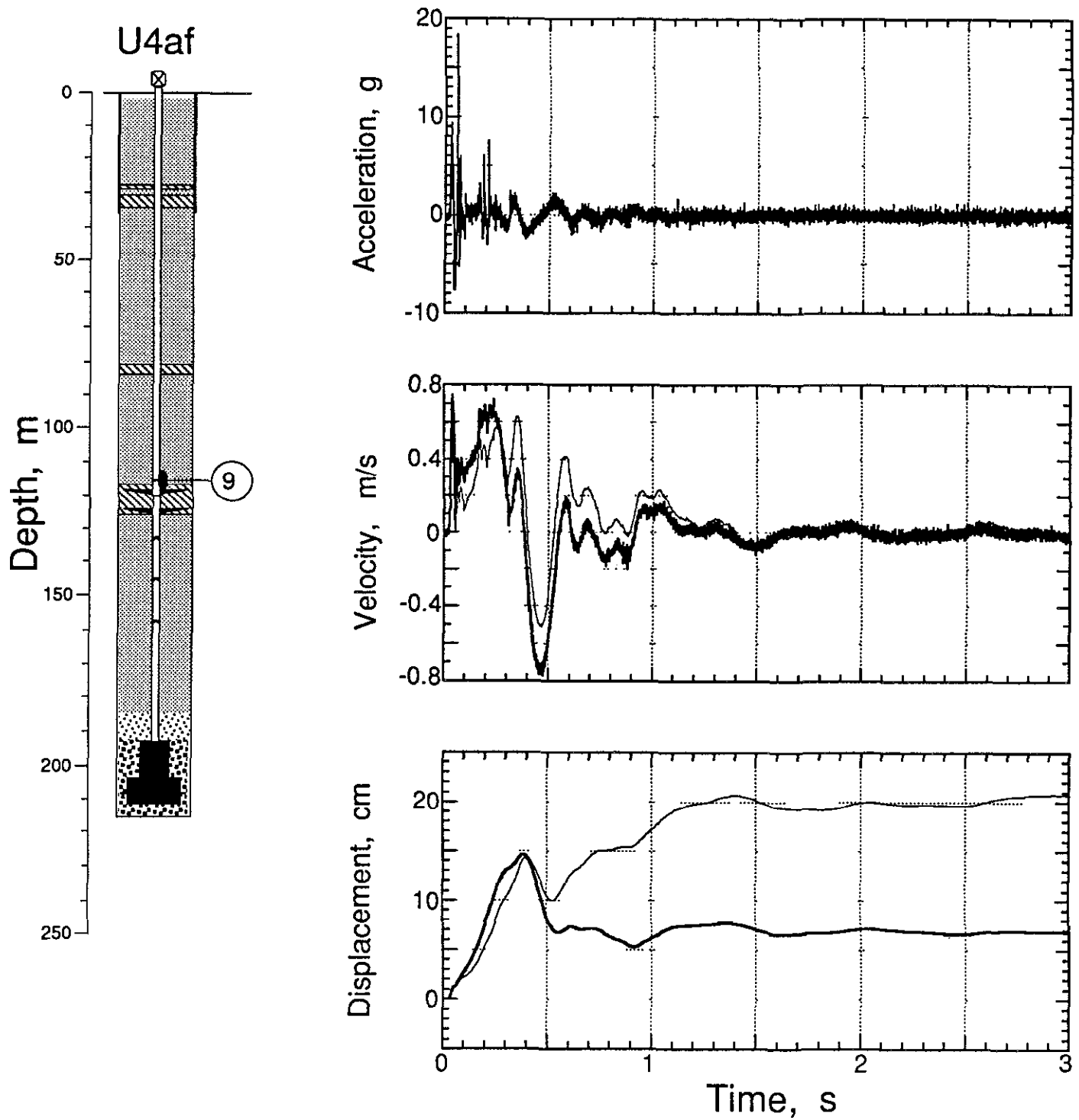


Figure 4 5 Explosion-induced vertical motion recorded on the emplacement pipe at the detector plate, 0.7 m above the formation coupling plug (station 9 at a depth of 115.2 m). When there is more than one trace in a plot, the lighter is derived from the accelerometer.

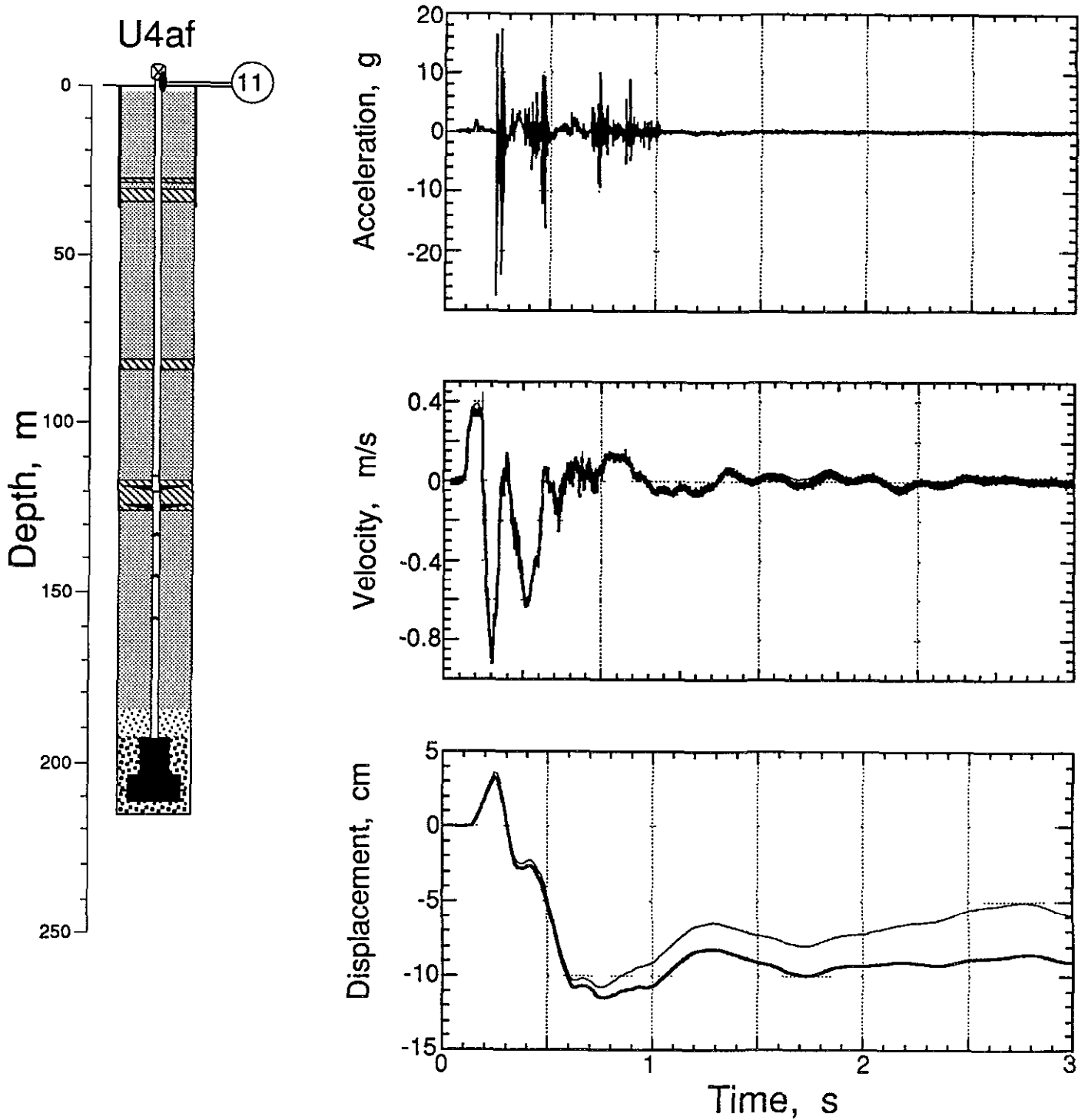


Figure 4.6 Explosion-induced vertical motion recorded on the emplacement pipe 0.6 m above ground and below the ball valve (station 11). When there is more than one trace in a plot, the lighter is derived from the accelerometer.

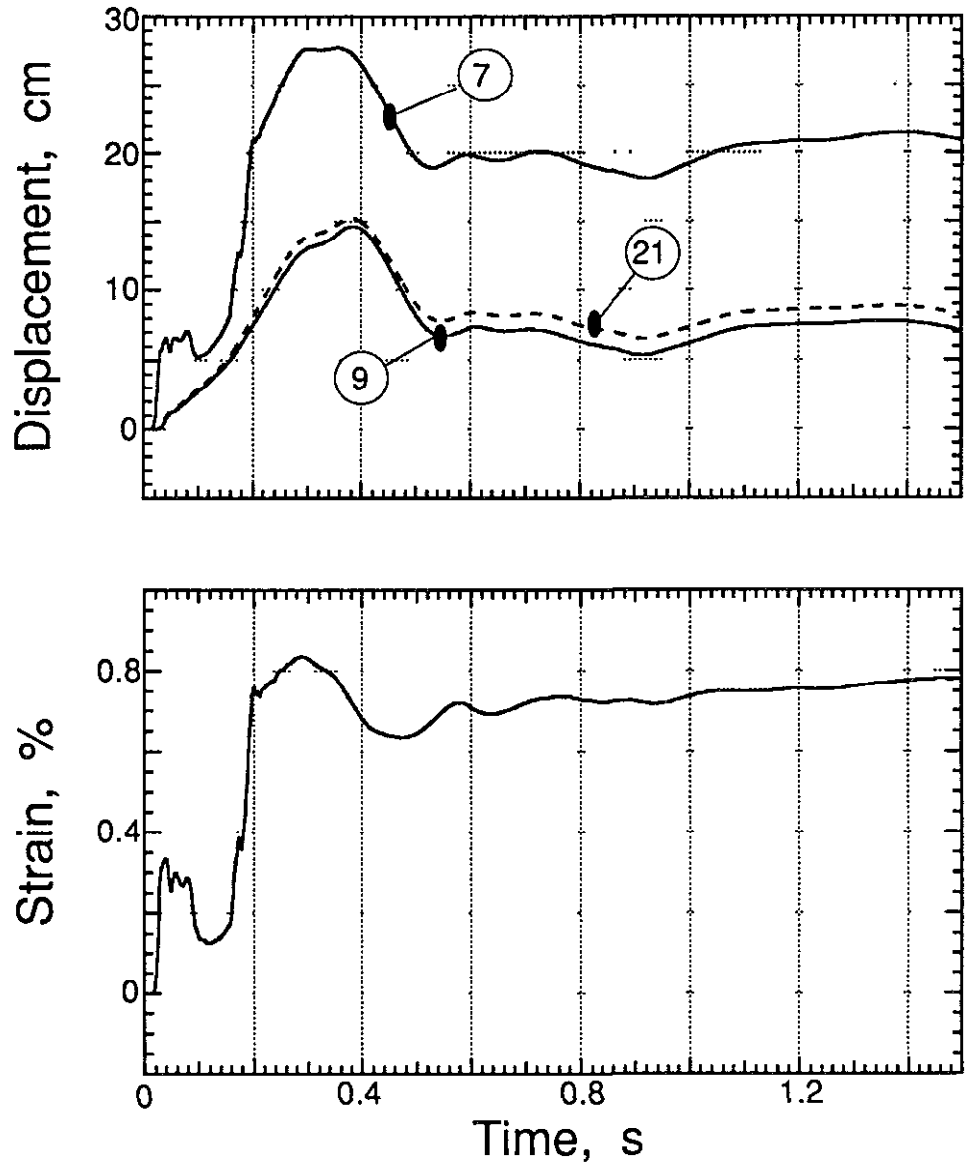
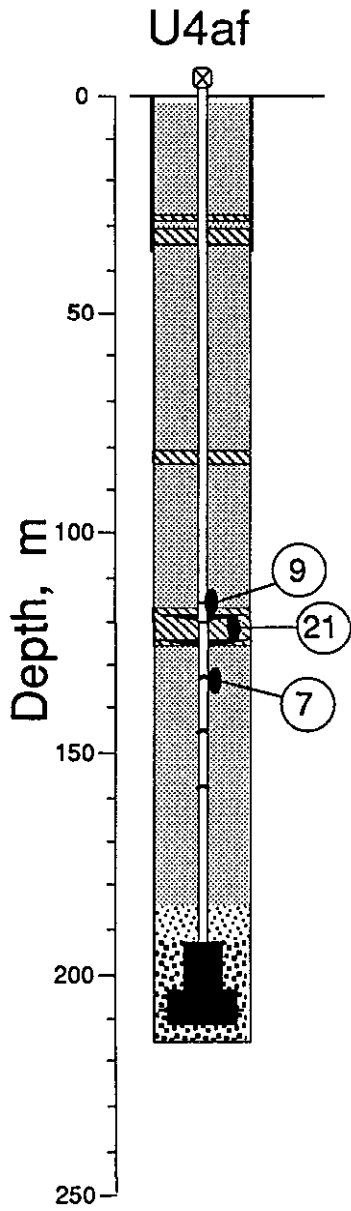
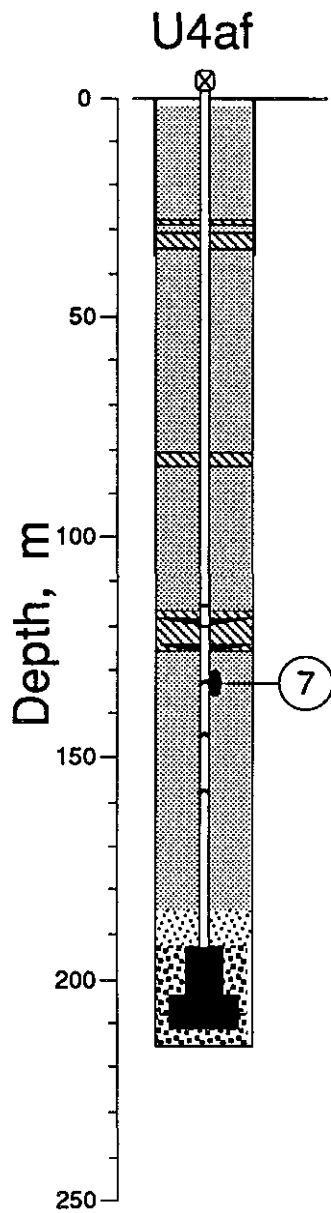


Figure 4 7 The upper plot shows the displacment histories of stations 7, 9 and 21 (dashed)  
 The lower plot is the mean strain history of the emplacement pipe between stations  
 7 and 9



The accelerometer channel was lost before collapse

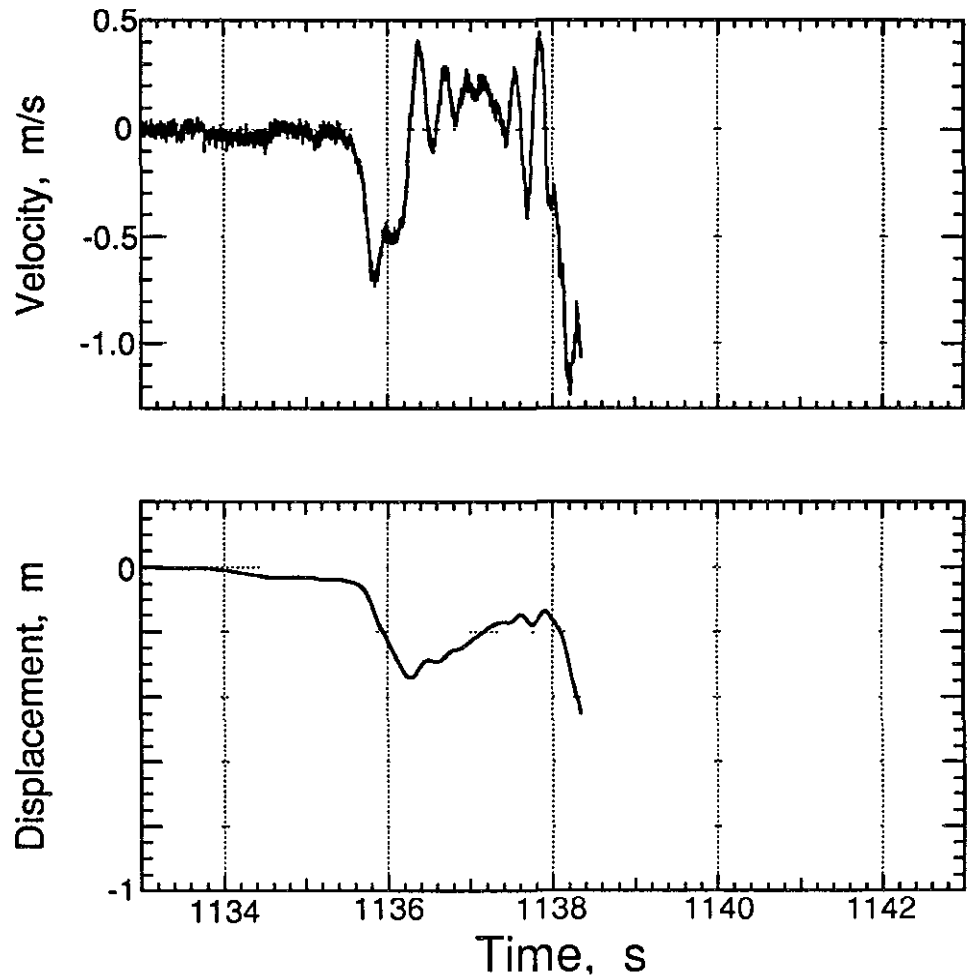


Figure 4 8 Collapse-induced vertical motion recorded on the emplacement pipe at the third pressure dome (station 7 at a depth of 132.9 m). Acceleration at collapse was not recorded.

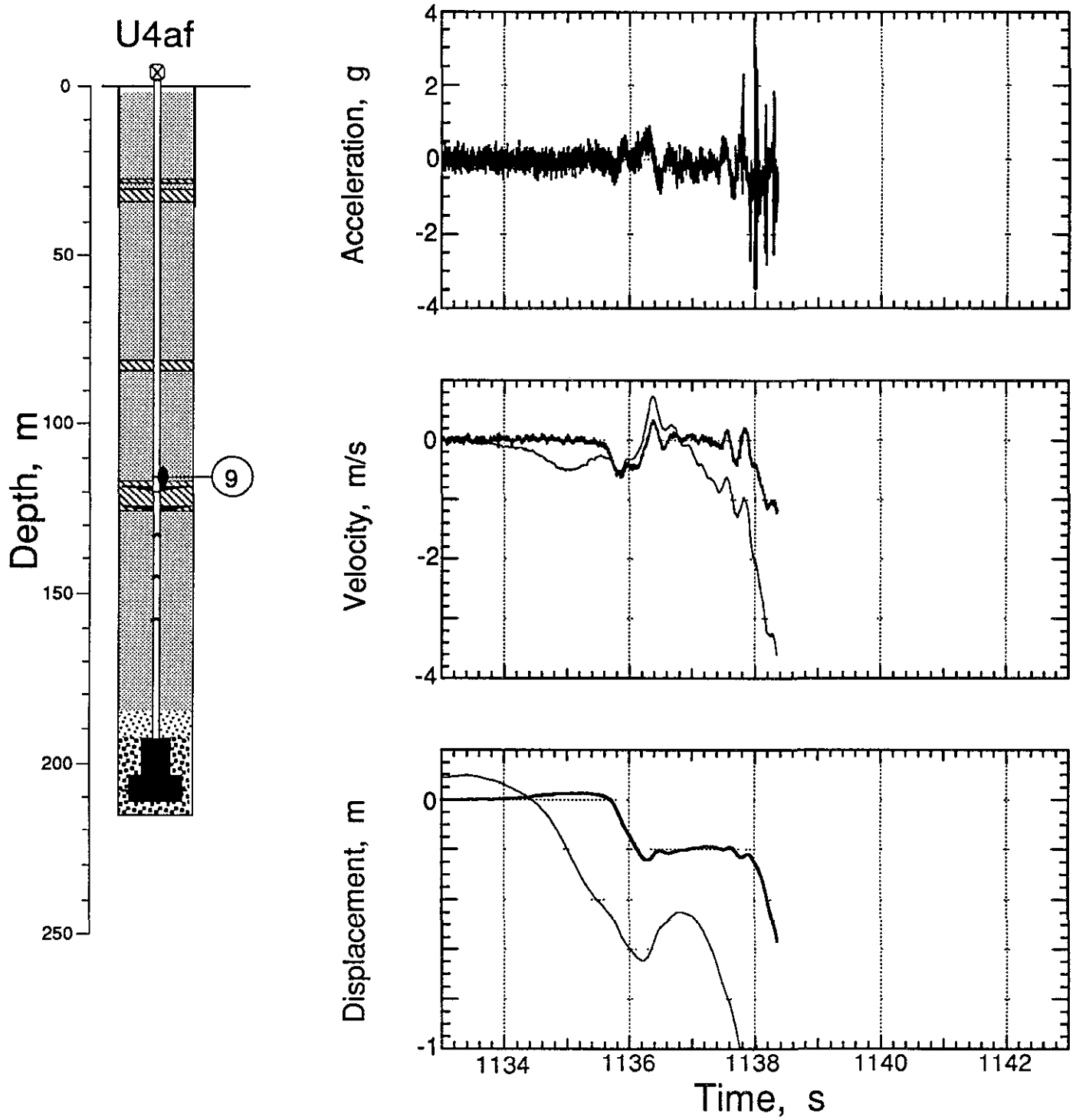


Figure 4.9 Collapse-induced vertical motion recorded on the emplacement pipe at the detector plate, 0.7 m above the formation coupling plug (station 9 at a depth of 115.2 m). When there is more than one trace in a plot, the lighter is derived from the accelerometer.

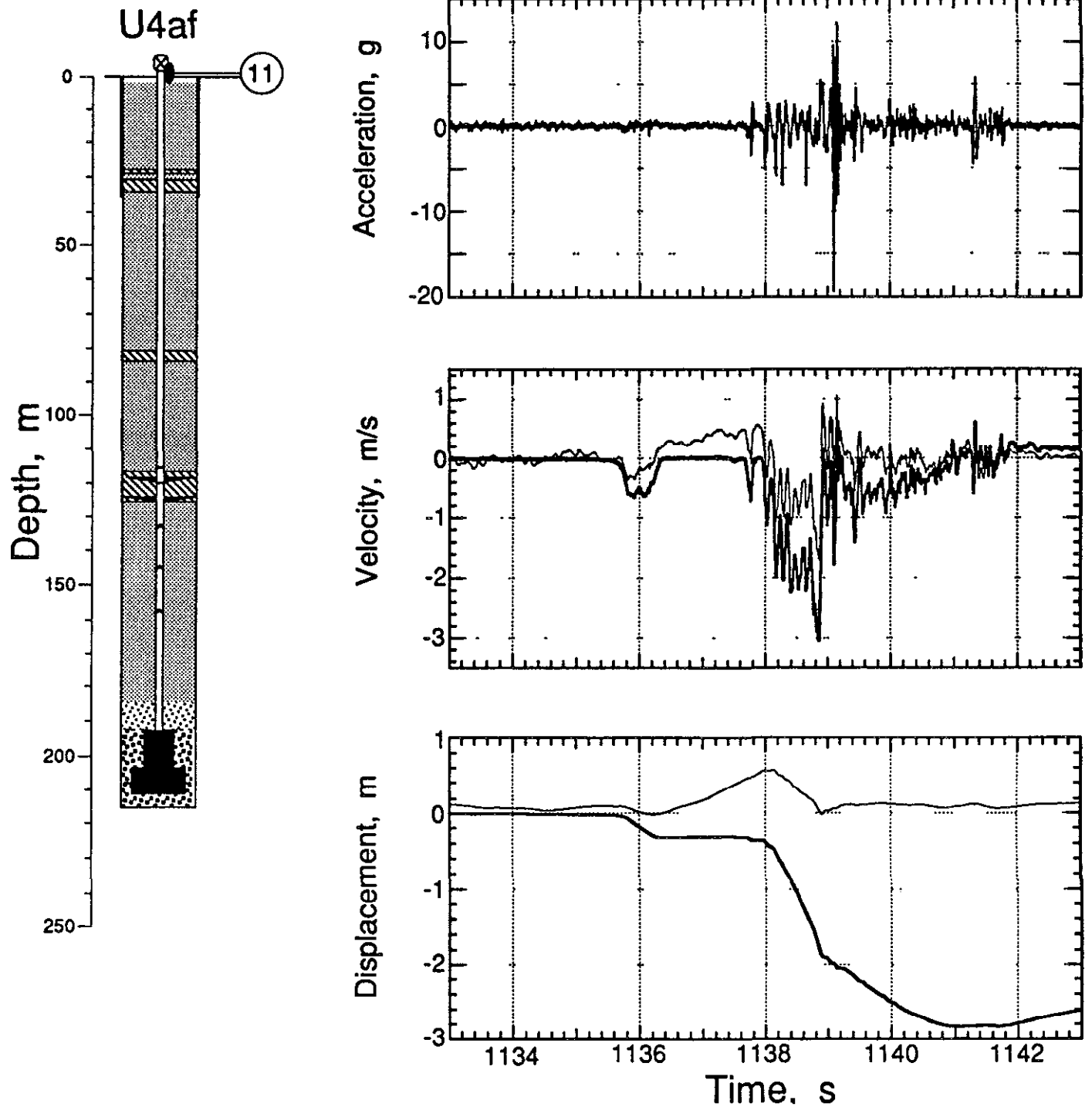


Figure 4 10 Collapse-induced vertical motion recorded on the emplacement pipe 0.6 m above ground and below the ball valve (station 11). When there is more than one trace in a plot, the lighter is derived from the accelerometer.

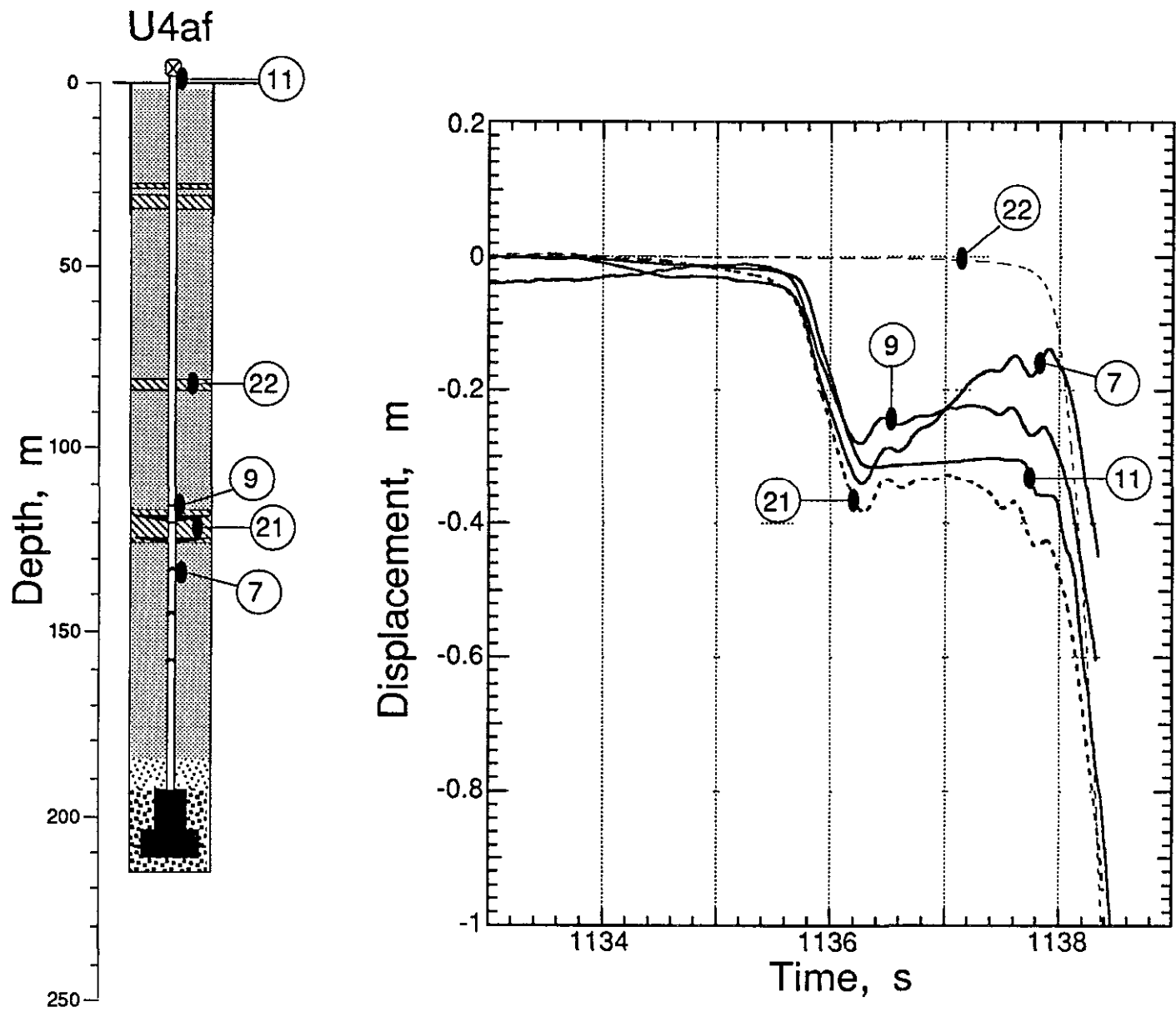


Figure 4.11 Overlay of all collapse-induced vertical displacements derived from measurements on the emplacement pipe. Also included are the displacements measured in the stemming plugs (dashed)

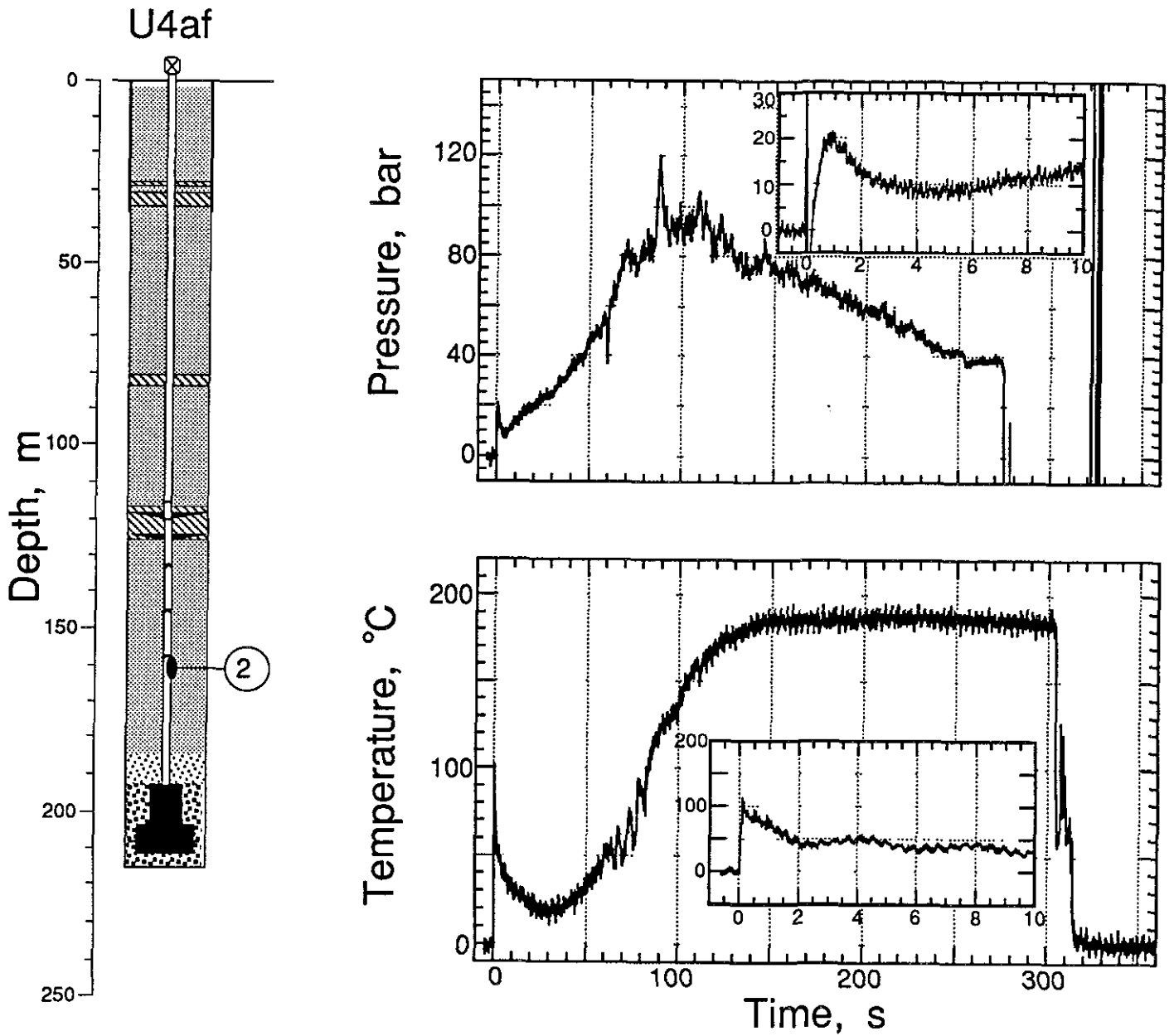


Figure 4.12 Pressure and temperature recorded in the emplacement pipe 2 4 m below the elevation of the pinhole (station 2 at a depth of 160.6 m). The inserts display the first 10 s of data.

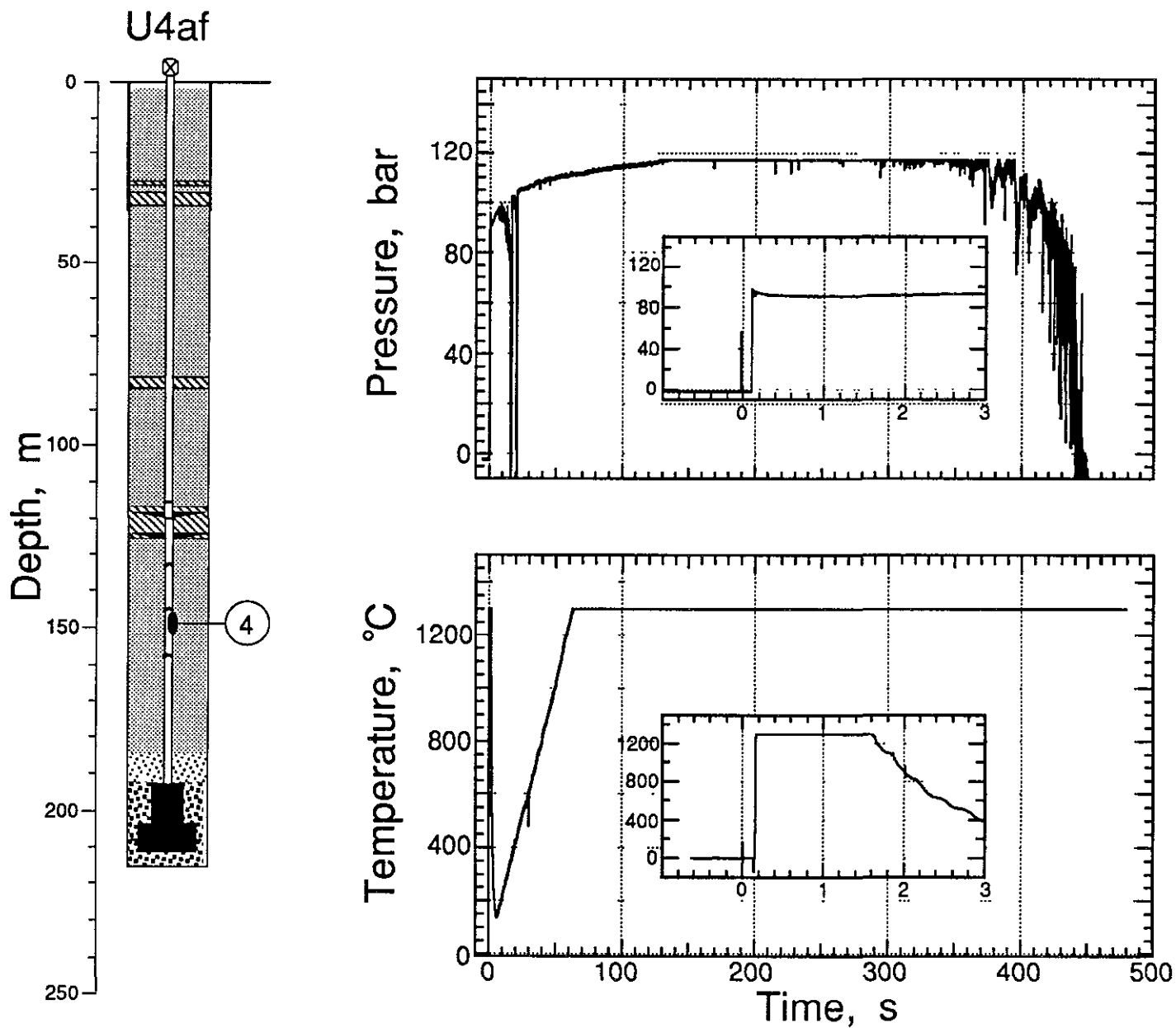


Figure 4.13 Pressure and temperature recorded in the emplacement pipe 3.3 m below the second pressure dome above the diagnostics canister (station 4 at a depth of 148.7 m). The inserts display the first 3 s of data.

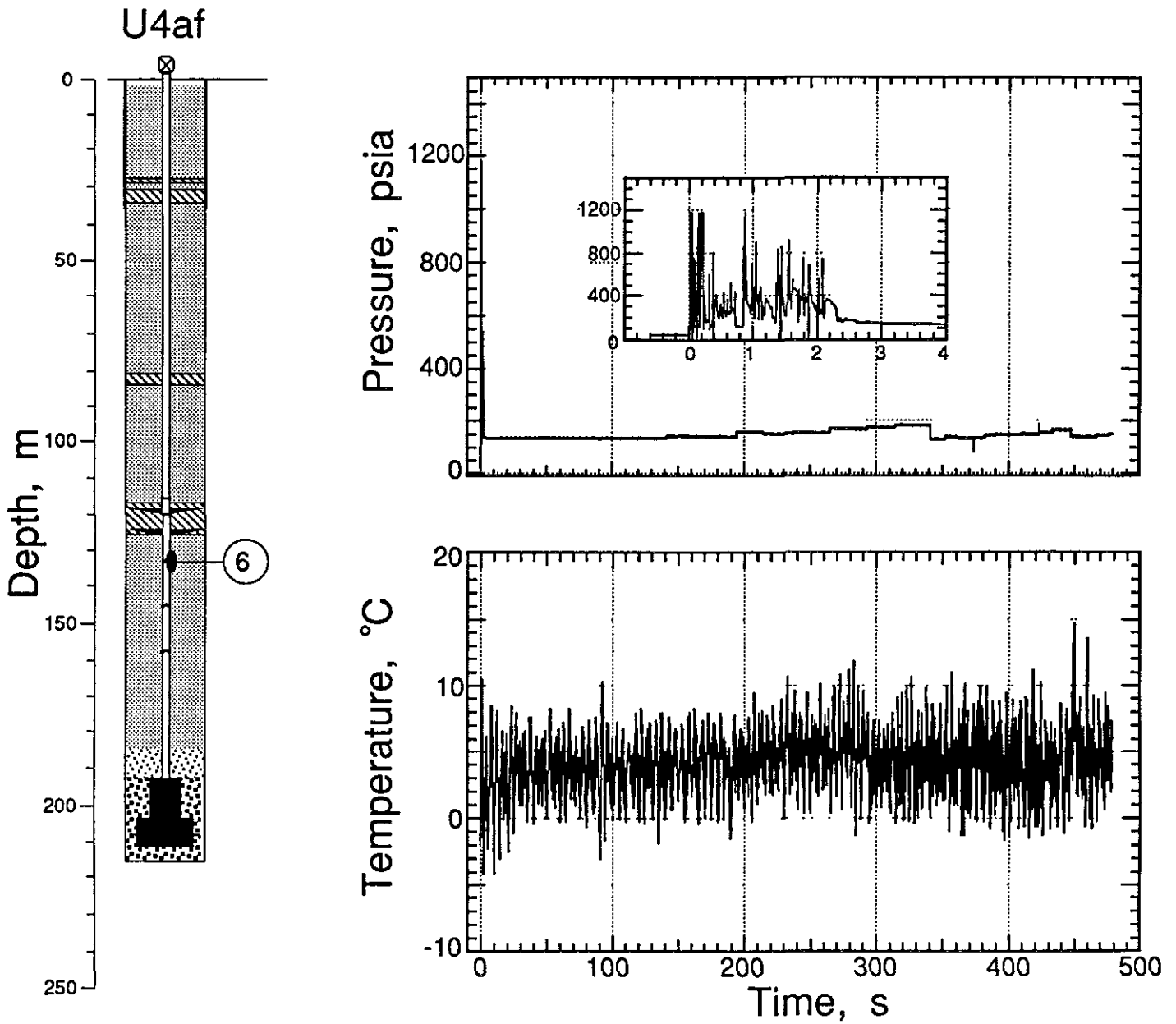


Figure 4 14 Pressure and temperature recorded in the emplacement pipe 3.2 m below the third pressure dome above the diagnostics canister (station 6 at a depth of 136.1 m). The insert displays the first 4 s of the pressure record.

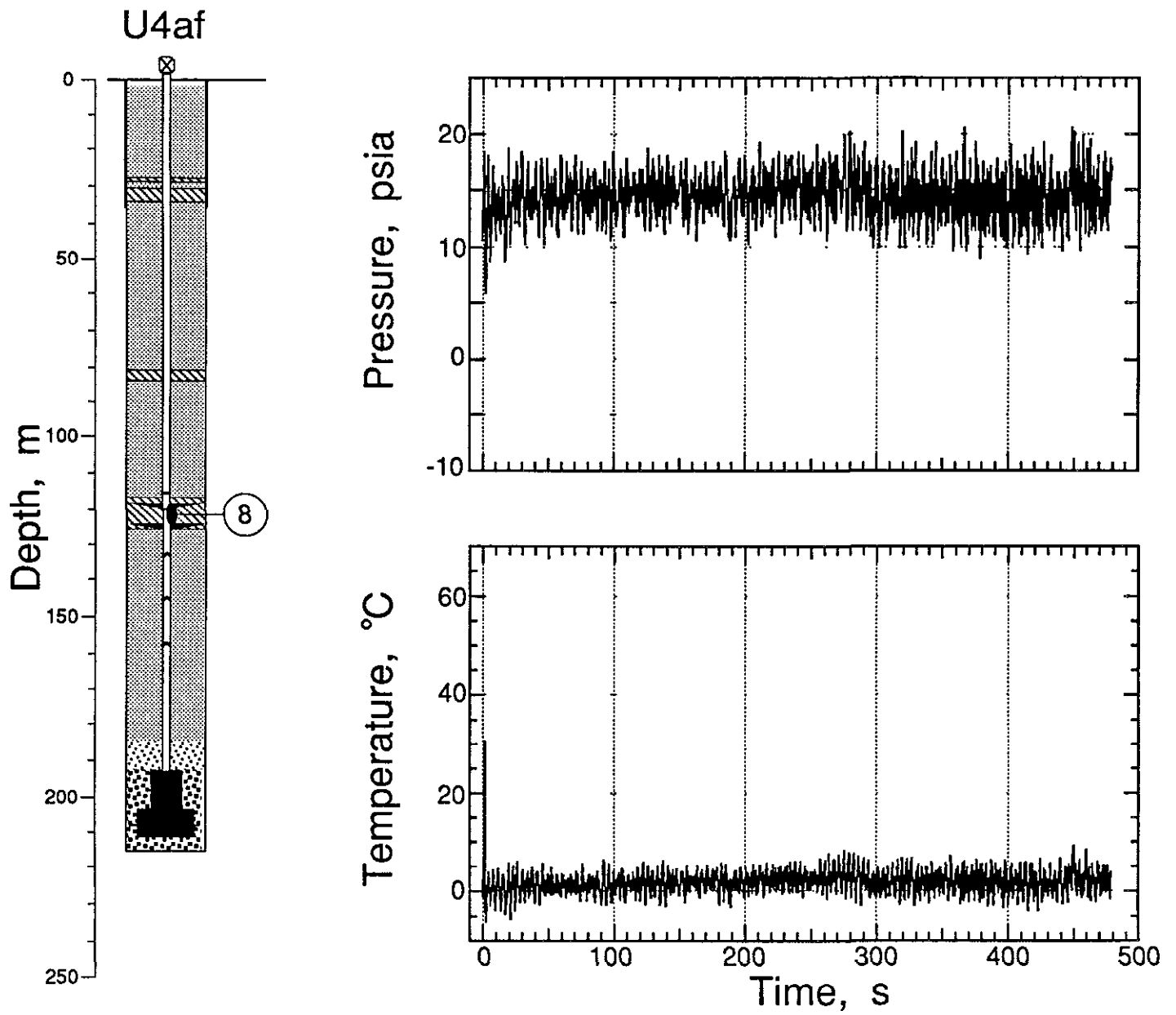


Figure 4 15 Pressure and temperature recorded in the emplacement pipe 1 2 m below the pressure plate (station 8 at a depth of 121.3 m)

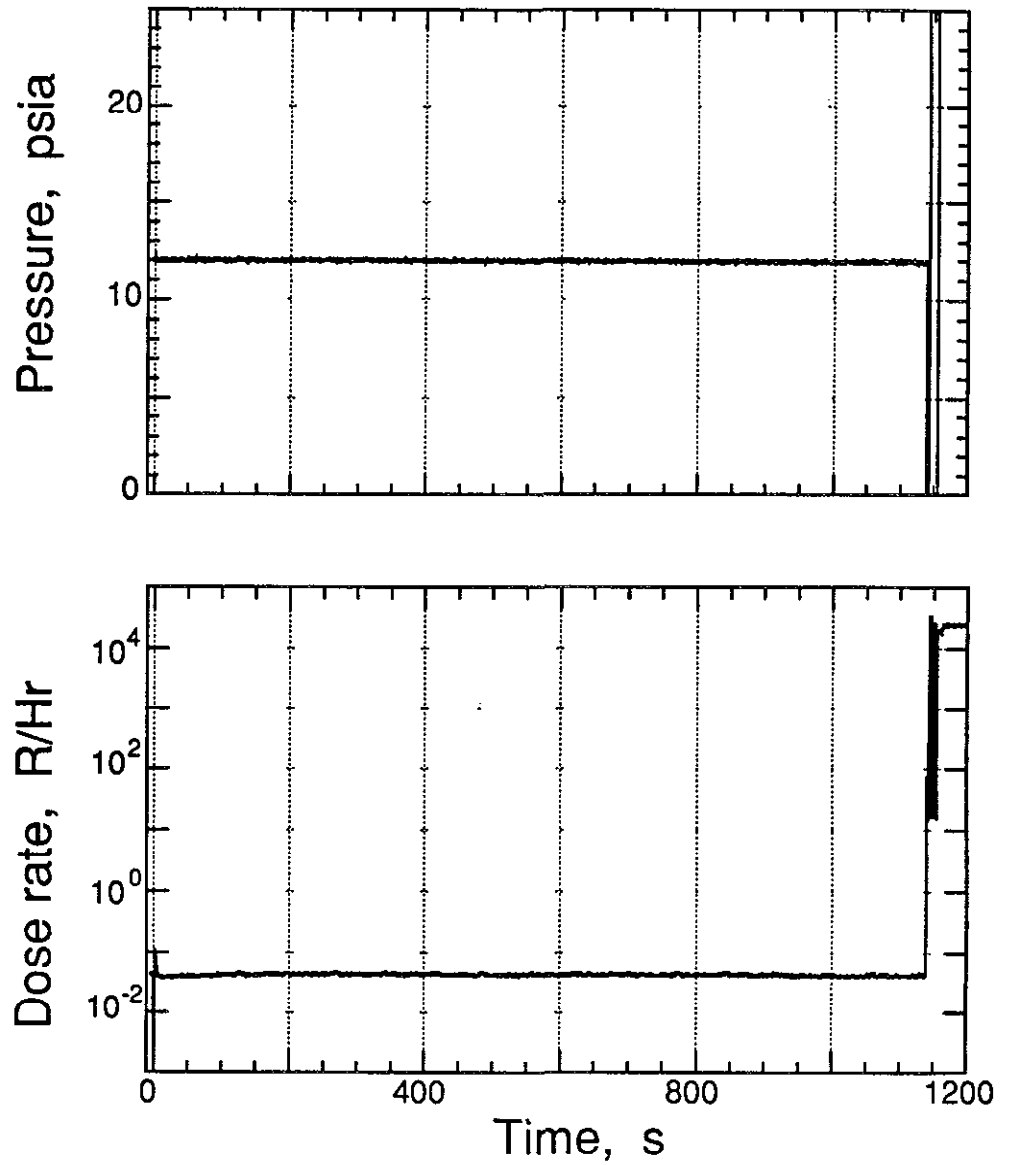
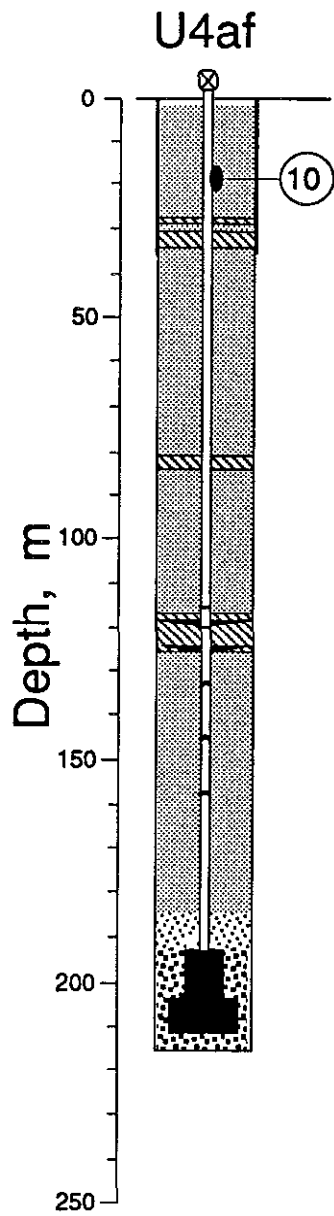


Figure 4 16 Pressure and radiation recorded in the emplacement pipe near its top (station 10 at a depth of 18.6 m).

## References

- 1 Nancy Howard, "U4af Preliminary Site Characteristics Summary, AGTG 77-31, Lawrence Livermore National Laboratory, Livermore, CA, April 4, 1977
2. William J. Mayer, "Containment Report for U4af," Holmes & Narver, NTS-A2 77-35, July 26, 1977.
- 3 LLNL contacts for additional information R A Heinle (CORTEX and SLIFER data)
- 4 Melvin E. Reed, "Special Measurements Final Engineering Report CARNELIAN, U4af", EG&G, Energy Measurements, Las Vegas, NV, SM 77E-51-51, 17 August 1977
- 5 Melvin E. Reed, "Special Measurements Physics/Instrumentation Package for CARNELIAN, U4af, Final Revision", EG&G, Energy Measurements, Las Vegas, NV, SM 77E-51-52, 23 August 1977

Distribution.

**LLNL**

TID/Brenda Staley (3)	L-053
Test Program Library	L-160
Containment Vault	L-221
Burkhard, N	L-221
Cooper, W	L-149
Denny, M	L-205
Goldwire, H.	L-221
Heinle, R (5)	L-221
Moran, M T	L-777
Moss, W	L-200
Pawloski, G	L-221
Rambo, J	L-200
Valk, T	L-154

**LANL**

Brunish, W	F-659
Kunkle, T.	F-665
Trent, B	F-664

**Sandia**

Bergstresser, T.	MS-1168
------------------	---------

**BNL/AVO**

Brown, T	A-5
Still, G	A-5
Stubbs, T.	A-5

**BNL/NVO**

Bellow, B	N 13-20
Davies, L	N 13-20
Moeller, A	N 13-20
Robinson, R	N 13-20

**Defense Special Weapons Agency**

Ristvet, B.

**Maxwell Technologies**

Peterson, E

**Eastman Cherrington Environment**

Keller, C.

